PART 1: INTRODUCTION TO THE GEOLOGY OF THE ROCHECHOUART IMPACT STRUCTURE

Philippe Lambert

Sciences et Applications,
33800 Bordeaux-France

lambertbdx@numericable.fr

Field Guide- Meteoritical Society 2009

SUMMARY

The 200 Ma old, 24 km diameter Rochechouart impact structure formed in granitic intrusive and metamorphic rocks of Variscan age (400-300 Ma) close to the margin of the Mesozoic sea. Fractured basement and autochthonous breccias form a several–decameter-thick semi-continuous zone over a 18-20 km diameter zone. Impact melt rocks, suevite and polymict lithic breccia spread over a ca 15 km inner zone forming a centro-symmetric deposit inclined 0.6° north. No topographic expression of the central uplift exists. The crater floor is at the same elevation (ca +/- 50 m) over a zone at least 20 km in diameter corresponding to the central part of the original crater. The pre-erosional diameter of the crater is probably larger than previously thought and possibly reached 40-50 km. Despite the patchy character of the remaining crater fill deposits, the structure is much less eroded than it looks, as the sequence of crater fill is complete as exposed near Chassenon. The suevite in Chassenon is capped by an ash-like horizontal deposit of very glass-poor, fine-grained, lithic debris derived from basement rocks. Material with similar grain size and composition is observed in centimeter- to meter-thick multi-layered glass-bearing intercalations (dikes) cutting through the suevite. The integrity of the Chassenon sequence strikingly contrasts with the age and morphology of the structure, implying a rapid and thick sedimentary deposit has covered the crater to protect it from erosion. The impactoclastic top deposit also firmly constrains the thickness and volume of the initial crater fill which appears extremely depleted (by a factor of 5 or more) compared with similar-sized impact structures and model based calculations. This anomaly remains unexplained. All the impactites including the glass-poor and glass-free impactites are characterized by a prominent K-metasomatism signifying pronounced post-impact hydrothermal activity. Exposed in isolated occurrences from the center to the periphery of the inner 15 km diameter zone, impact melt rocks are extremely unlikely to have formed a continuous sheet. They display a large variety of textures grading from pure melt rock into basal suevite distinct in composition texture and setting from the main suevite body forming the top of the impact deposit. Heterogeneity and relative inefficiency in mixing is characteristic of the whole impact deposit, resulting in heterogeneous melts at the scale of hand specimens but also at the kilometer scale, as suggested by close ties between the composition of melt-bearing rocks and the subjacent target rocks.

INTRODUCTION

From the geological point of view, the Rochechouart structure is located at the northwestern edge of the Massif Central (Figure 1), one of the largest pieces of the Variscan Belt, which formed as a result of a complex interplay of rifting, convergence, and collision between the continents of Laurentia, Baltica and Gondwana, and several microcontinental terranes (Matte, 2001).

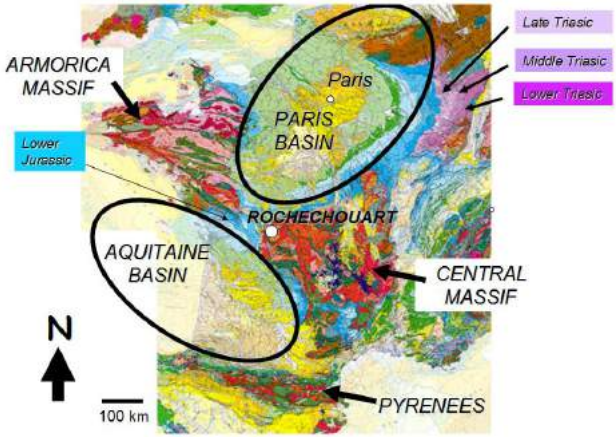

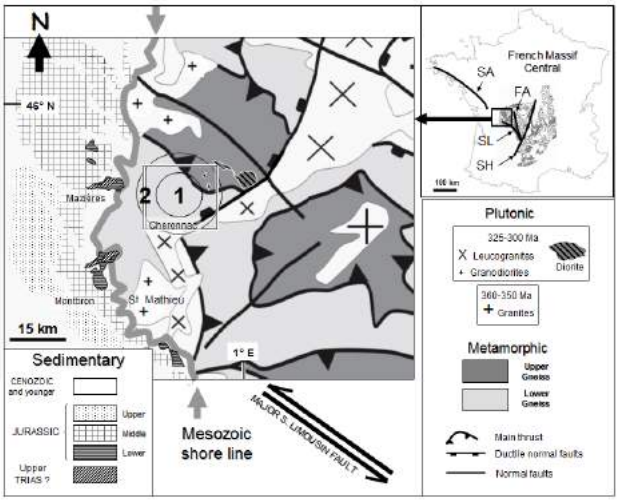

The 23 km diameter reported in the Impact Data Base (http://www.unb.ca/passc/ImpactDatabase) has no physical or phenomenological significance. It does not relate to the diameter of the initial crater. It corresponds to the diameter of the impact structure defined as the extent of damages in the target that are attributed to the impact and reported by Lambert (1977a-b).

The Rochechouart crater is eroded and has lost its original topographic expression (Figure 2). The size of the original crater is thus unknown. Its initial morphology is unknown too. But we know Rochechouart is not a central peak crater and thus departs from the model admitted for impact craters of its size range on Earth. The center of the crater is precisely what is exposed, and it is characterized by a large flat depression filled by impact deposits lying at the present day horizontal. Everything else (walls, inner rim?, annular depression?, outer rim) has been eroded away, implying it was standing higher in elevation. The size of the crater and its morphology thus count among the various enigmas of the Rochechouart impact.

Figure 3: Top: Geological map of France and position of the main sedimentary basins and Variscan massifs.

Bottom left: Regional geological setting of the Rochechouart impact structure showing the contact between sedimentary cover and Variscan basement at the western edge of the « Massif Central » and the setting of major units (adapted from Ledru et al., 1994). The inner circle (1) represents the extent of the impact deposit. The outer circle (2) indicates the outer limit of brecciation in the basement rock.

Frame intersecting the circles = area covered by Figures 2A-B. Right insert: Position of the French Massif Central and major Variscan faults (SH= Sillon houiller, SL= South Limousin fault, FA = Argentat fault, SA = South Armorica fault).

The age of the impact has long been a matter of debate. Previous studies, including K-Ar, Rb-Sr, apatite and glass fission track, as well as paleomagnetic dating (see Kelley and Spray, 1997, for a summary of ages), resulted in a broad (Middle Triassic to Late Jurassic) time window for the Rochechouart impact. More recently, $^{40}Ar/^{39}Ar$ laser dating of pseudotachylitic breccia from Champagnac yielded a 214 ± 8 Ma, Late Triassic, age (Kelley and Spray, 1997), which is currently accepted as the most robust age for the impact.

It has also been cited as supporting a theory that Rochechouart is a member of a ~214 Ma terrestrial impact crater chain (Spray et al., 1998). This hypothesis has, however, not been confirmed by the two most recent ages of 201 ± 2.3 Ma for the impact event obtained by Schmieder at al. (2009), which corresponds to the accepted age of the boundary between Trias and Jurassic (referred below as T-J boundary) (Verati et al., 2007; Schaltegger et al., 2008).

The evidence for geochemical contamination of Rochechouart impactites by the projectile was presented in the mid 1970's (Lambert, 1975). Since then, the identification of the projectile has been a matter of debate: interpretations have ranged from iron meteorite to chondrite projectiles (Janssens et al., 1977; Palme et al., 1980; Horn and El Goresy, 1980; Koeberl et al., 2007; Tagle et al., 2009).

The ordinary chondrite hypothesis is currently considered the most probable, based on Cr isotope studies by Koeberl et al. (2007). However, this hypothesis was recently contradicted by Tagle et al. (2009) based on platinum group element patterns and Ni/Cr/Ir inter-element ratios that were interpreted to favor a stony iron (non-magmatic iron) projectile.

Rochechouart impactites were first recognized by Kraut (1969) and the structure was studied in detail by Lambert (1974, 1977a). Ejecta deposits are widely exposed at Rochechouart; however, the knowledge of these rocks remains rudimentary compared to other terrestrial impact structures. Although the Rochechouart structure has been investigated continuously by the international scientific community since its impact origin was established, most studies have focused on specific issues such as dating the event or identifying the projectile (see references above). Full-scale field investigation remains limited to mainly French geological work by Kraut and French (1971), Lambert (1974, 1977a), and Chevremont et al. (1996).

ROCHECHOUART TARGET

Geological setting

The Rochechouart target rocks comprise a variety of metamorphic, plutonic and subvolcanic rocks (Figure 4). Two of the main metamorphic units associated with the Variscan orogeny are represented in the area, the Lower and the Upper Gneiss Unit (Floc'h, 1983). The Lower Gneiss Unit (LGU) is represented by para- and ortho-gneisses. Plagioclase-rich paragneisses with phyllosilicate contents of up to 8 vol% are the dominant rock type in the Rochechouart area.

Paragneisses tend to be dark gray or gray, contrasting with lighter-colored "orthogneisses" referred to here as "leptynites". Leptynites are the second most widely exposed metamorphic rock type in the target area, occurring in the southwestern region of the target (Figure 4).

They derive from pre-Variscan alkaline granitoid intrusions of mainly Early Ordovician (480 Ma) and Early Cambrian (550 Ma) ages (Faure et al., 2008). Small intercalations of paragneiss as well as lenses of migmatite are common in the leptynites. The migmatitisation is related to the first of the series of synmetamorphic ductile deformation events involved during the formation of the French Massif Central. This earliest deformation is developed coevally with an intermediate pressure/intermediate temperature metamorphism and anatexis dated around 385-380 Ma (Quenardel and Rolin, 1984; Costa, 1992; Roig and Faure, 2000).

A small unit of serpentinized peridotitic rocks intercalated with the gneisses of the lower part of the LGU occurs 12-15 km south of the center of the structure, at the eastern edge of the Cheronnac granite (Figure 4).

The primary structure of the rock is essentially lost. Antigorite is the major constituent. The Lower Gneiss Unit is interpreted as Proterozoic-Early Paleozoic remnants of the northern Gondwana margin that experienced crustal thinning and rifting in Ordovician times (Ledru et al., 1994).

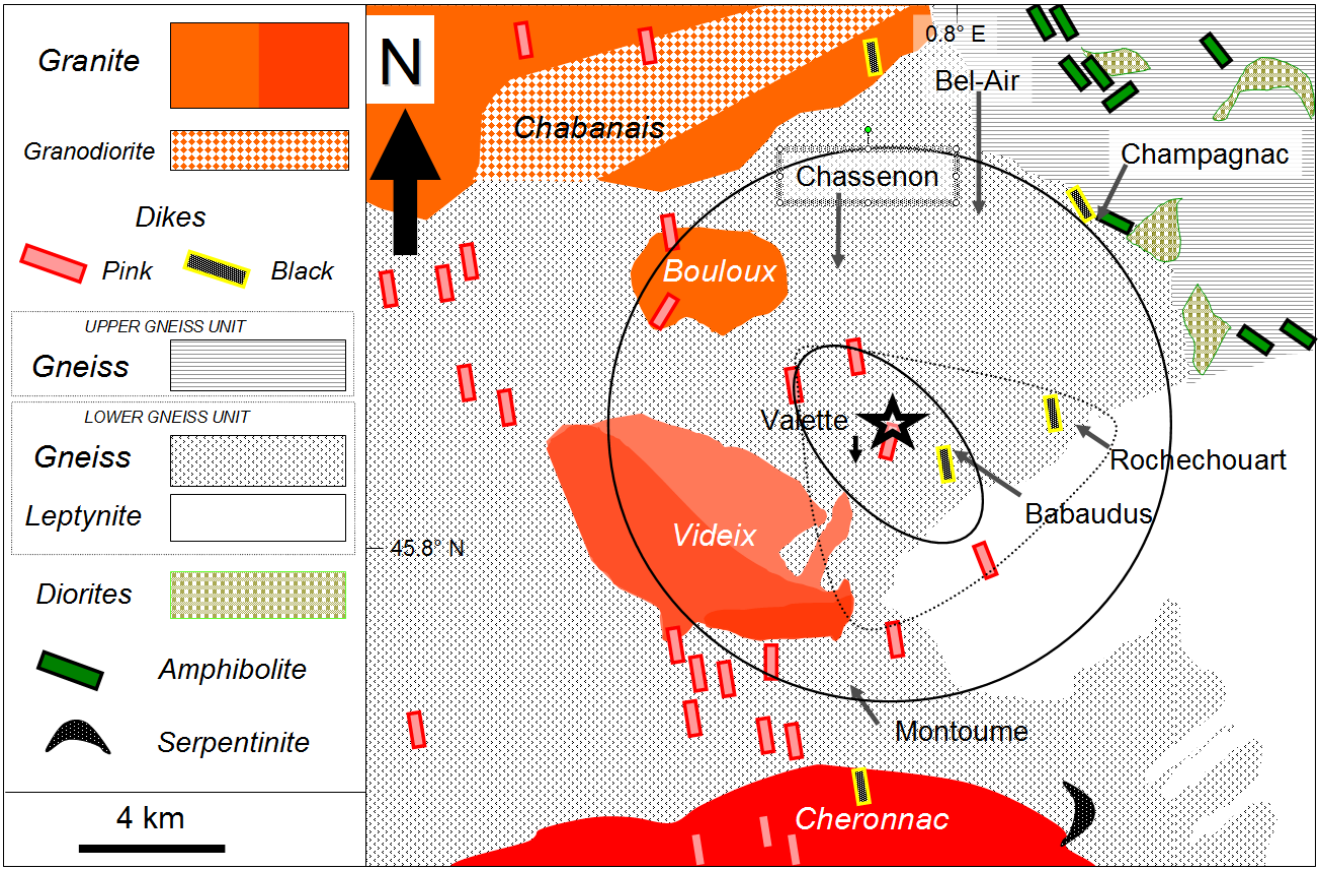

Figure 4: Schematic geologic map of the framed area of Figure 3 (after Lambert, 1974, 1977a and Chevremont et al., 1996). Target formations as exposed today at the level of the crater floor are represented. Impact deposits and surface deposits (including alluvial deposits) are omitted.

The Upper Gneiss Unit (UGU) crops out at the northern edge of the impact area (Figure 4). It is represented by gray gneisses consisting of quartz, plagioclase (oligoclase), and one or two mica minerals, and by a bimodal assemblage of more or less mafic gneisses, referred as the "leptynite-amphibolite sequence" (Floc'h, 1983; Faure et al., 2007). Such a sequence is exemplified at the large active quarry at Champagnac 7.5 km north of the center of the structure. Here, both darker amphibolite lenses and lighter orthogneisses are intercalated.

The amphibolite intercalations become significant in the northeastern quadrant of the area at a distance of 8 km from the center of the structure and beyond. Precursors of both the leptynites and the amphibolites are related to the above-mentioned Cambro-Ordovician intracrustal rifting episode predating the Variscan orogeny (Faure et al. 2008).

Both the LGU and the UGU experienced a Barrovian-type metamorphism dated around 360-350 Ma (Faure et al., 2007). This metamorphism is associated with the second major ductile deformation

event of the history of the Massif, characterized by a northwest-southeast trending lineation that is clearly expressed in the Rochechouart metamorphic rocks. The Late Visean time (ca 340 Ma) corresponds to the onset of syn-orogenic extension caracterized by huge crustal melting. The NW-SE spreading of the inner part of the Massif Central was partly accommodated by ductile wrench faulting along the SW edge of the Massif Central (South Limousin (SL) fault - Figure 3) and the SW edge of the Massif Armoricain (SA, on Figure 3) which is also part of the Variscan belt. The Rochechouart structure is located in the axis of this major fault system.

The metamorphic rocks of the Rochechouart area are crosscut by plutonic intrusions which occur predominantly in the western half of the impacted zone (Figure 2A). They correspond to the southern edge of the Chabanais intrusion and to the northern edge of the Cheronnac intrusions. Small granitoid bodies (Bouloux and Saint Gervais-Videix bodies) occur in-between (Figure 4). The Cheronnac granite is closely related to the main Saint Mathieu leucogranite intrusion outcropping further to the south (Figure 3). It is characterized by light color and bears orthoclase, muscovite and biotite, and only differs from the Saint Mathieu main intrusion by an oriented fabric. Both intrusions formed by crustal melting at 325-300 Ma.

The Chabanais intrusion is a gray-pink calc-alkaline granite-granodiorite with quartz, K-feldspar, plagioclase and biotite. The small, regionally-occurring granitoid bodies (Bouloux and Saint Gervais-Videix bodies) vary in composition between that of the Cheronnac and Chabanais intrusions. The eastern part of the Chabanais intrusion locally includes meter to decameter intercalations of dark gray biotite- and amphibole-bearing granodiorite and diorite (Figure 4). To the northeast and east of the structure, small diorite intrusions containing hornblende, biotite, plagioclase (An_{40-50}), and small xenomorphic quartz occur in the Saint Junien area (Figure 3). The largest body (ca 8 km^2) lies 12 to 20 km from the center of the structure.

Smaller bodies (ca 1 km^2 and less) crop out in the Champagnac area, 8-15 km from the center of the structure (Figure 4). Although the intrusive character of the diorite is ambiguous in places, the occurrence of amphibolite lenses supports their intrusion into the leptynite-amphibolite assemblage of the host UGU at most locations.

The former is seen in the northeastern corner of Figure 4 where meter to decameter thick intercalations of diorite and gneiss with graded contacts occur. In all the diorites, including those forming definite intrusions such as the largest body 20 km east of the center of the structure, plagioclase is more or less sericitized and locally calcitized. A complex array of fractures pervades the diorite, and these fractures are filled by secondary phases, especially adularia. Significant hydrothermal alteration is observed in the host diorite at the contact with these filled fractures with almost complete pseudomorphism of plagioclase by white mica and of biotite by chlorite (Chevremont et al., 1996).

The metamorphic units and the granites are transected by meter- to decameter-thick, fine-grained dikes of predominantly north-south orientation (Figure 4). These dikes account for less than 1% of the target material but contain most of the known shatter cone locations in the Rochechouart impact structure. Two main types - pink and black - are distinguished, both carrying millimeter- to centimeter-sized phenocrysts in a fine-grained groundmass. Pink dikes are granitic-granodioritic in composition and have been referred to as microgranites. These contain quartz and feldspar phenocrysts.

The black dikes have been referred to as “lamprophyres” and are more mafic (diorite/gabbro). In the Rochechouart structure they are referred as microdiorite (μdiorite). These dikes are relatively more abundant in the eastern part of the target, whereas microgranites occur more frequently on the western side (Figure 4). They have been dated at ca 300 Ma (Chevremont et al., 1996) and formed during the last stage of the Variscan orogeny and relate to the collapse of the whole belt.

Dikes are oriented mostly NS, in the same direction as major wrench faults (the Sillon Houiller (SH on Figure 3) and Argentat fault (FA on Figure 3)) appearing further east. These wrench faults are interpreted as transfer faults (Burg et al., 1991). An extensional regime is well recorded by the tectonic setting of intra-mountain Stephanian coal basins similarly oriented North-South in the French Massif Central among which the Saint-Étienne coal basin is the most famous (Faure et al., 2007 and references therein), as it corresponds to the para-stratotype of the Stephanian stage (304-299 Ma).

Apart from the recent (sub-contemporary) volcanism in the Auvergne region, no confirmed sign of magmatic activity is recorded in the French Massif Central after the Stephanian post-orogenic extension. A 265 Ma Rb/Sr age has been obtained by Reimold et al. (1987) on pegmatitic granitic rocks sampled near pseudotachylitic breccia veins in the Champagnac quarry. This suggests post-Variscan magmatic activity. But this age and a late post-Variscan magmatic episode in this part of France remain to be confirmed. The Rb/Sr method is known to yield too young ages as illustrated by recent measures in granites near the Rochechoaurt area (Alexandrov et al., 2000).

In the immediate vicinity of the impact deposits there are no traces of younger formations except for alluvial deposits and surface formations. The latter form a quasi-continuous cover over the whole area. Alluvial deposits overlie the northern part of the impact structure in a broad east-west zone centered on the Vienne River.

Several levels of alluvial deposits have been recognized as a function of their relative altitudes with respect to the level of the Vienne River. The lower age limit for the emplacement of the oldest alluvial deposit is poorly constrained to the Oligocene (ca 30 Ma). The upper boundary is constrained from the traces of flora typical of tropical climate which ended at ca 5-3 Ma in France (Chevremont et al., 1996).

Occurrence of large and highly rounded pebbles (up to 20 cm in diameter) has been tentatively interpreted as indirect evidence for a coastal conglomerate having covered the area during the Mesozoic (Chevremont et al., 1996).

Mesozoic sediments overlie the western margin of the Massif Central (Figure 3). The basal unit consists of a 5-30 meter thick sandstone deposited horizontally and exposed at Mazières and Montbron, only 16-17 km west and 24 km southwest of the center of the structure, respectively (Figure 3).

Similar fossil poor thin formation is known at various places in the Aquitaine Basin.

It occupies the same stratigraphic position directly above basement as near Rochechouart. Attributed to the Rhaetian on the basis of rare fossils by the 19th and early 20th field geologists (see for instance Glangeaud, 1901) it was appearing as such on the geological maps of Aquitaine Basin until the 1970's.

The latest editions of the geological maps of the area (released from 1980-1990) are now placing this sandstone unit at the base of Hettangian without justifying the change (comparison of the notices and sheets of the old 1/80000 geologic maps of Rochechouart with the recent 1/50000 maps of La Rochefoucault, Montbon, Mazières and Angoulême).

The age of the basal sandstones is in fact poorly constrained and no recent paleontological study has been found for the region. The Aquitaine Basin is essentially missing the Trias record and the absence of significant tracks of the material eroded away from the nearby Variscan Mountains remains puzzling. Close to Rochechouart (near Mazières and Montbron) the basal sandstone layer is covered by a 4-30 meter thick dolomitised limestone alternating with oolitic limestone. The latter delivers fossils attributed to Hettangian by Glangeaud (1910).

Geochemistry

Table 1 summarizes the major elements analyses of Lambert (1977b-c) for the three most important rock types of the Rochechouart target (gneiss, granite and leptynite) and for a selection of minor rock types. These datas set the basis for the correlation fields in a total alkali element-Fe-Mg ternary diagram and a Quartz-Albite-Orthoclase (Qz-Ab-Or) ternary diagram seen in Figure 5.

	SiO_2	Al_2O_3	Fe_2O_3	MgO	CaO	Na_2O_3	K_2O	TiO_2	P_2O_5
Gneiss (17)	66.19 (σ=3.0)	16.21 (σ=1.6)	5.79 (σ=0.9)	2.76 (σ=0.5)	1.84 (σ=0.9)	2.94 (σ=1.0)	3.28 (σ=1.6)	0.82 (σ=0.2)	0.16 (σ=0.02)
Leptynites (8)	75.18 (σ=3.5)	13.58 (σ=1.3)	2.09 (σ=0.6)	0.56 (σ=0.3)	1.28 (σ=0.9)	3.56 (σ=0.6)	3.56 (σ=1.3)	0.03 (σ=0.02)	0.03 (σ=0.02)
Granite (7)	72.94 (σ=3.0)	14.90 (σ=1.0)	1.40 (σ=1.1)	0.74 (σ=0.8)	0.79 (σ=0.5)	3.19 (σ=0.9)	5.65 (σ=1.4)	0.16 (σ=0.2)	0.22 (σ=0.12)
Diorite	59.37	18.57	6.86	4.08	1.79	3.01	5.23	0.83	0.27
Black microdiorite (3)	60.47	16.77	7.74	5.97	1.45	1.95	4.59	1.00	0.11
Amphibolite	44.50	18.68	12.82	8.71	9.55	1.95	1.88	1.75	0.16
Serpentinite	47.45	1.12	7.96	43.44	0.01	0.01	0.01	0.01	n.m.
Leptynite n°70	75.60	12.85	1.72	0.20	1.42	3.28	4.15	0.11	0.1
Monomict leptynite breccia (dyke n°70)	75.69	13.82	1.26	0.32	0.19	2.98	5.77	0.11	n.m.
Aphanitic core (dyke n°70)	75.46	14.12	0.63	0.30	0.14	1.82	7.44	0.10	n.m.
Impact melt rocks (45)	66.60 (σ=4.2)	16.24 (σ=2.4)	4.22 (σ=2.2)	1.29 (σ=1.1)	0.25 (σ=0.2)	0.34 (σ=0.3)	10.19 (σ=1.8)	0.76 (σ=0.1)	0.09 (σ=0.06)
Impactoclastite (3)	73.24	12.65	3.03	1,00	0.46	1.38	6.12	0.63	n.m.

Table 1: Chemical composition of the main Rochechouart lithologies. All data in wt%. (): Number of analyses. Leptynite, monomict breccia dike and aphanitic core of the breccia dike from locality n°70 (cf. Figure 7). MnO measured but not reported (all data below 0.1 wt%); n.m. = not measured. XRF and wet chemical analyses after Lambert (1977a); (Measurements performed in the mid 1970's by BRGM-French Geological Survey, Orléans, France. Uncertainty of individual analyses in % of the measured wt% oxide values as follows: Al-Fe: 0.5; Si-Mg-Ca: 1; Na-K: 2; Ti: 2.5; P: 5).

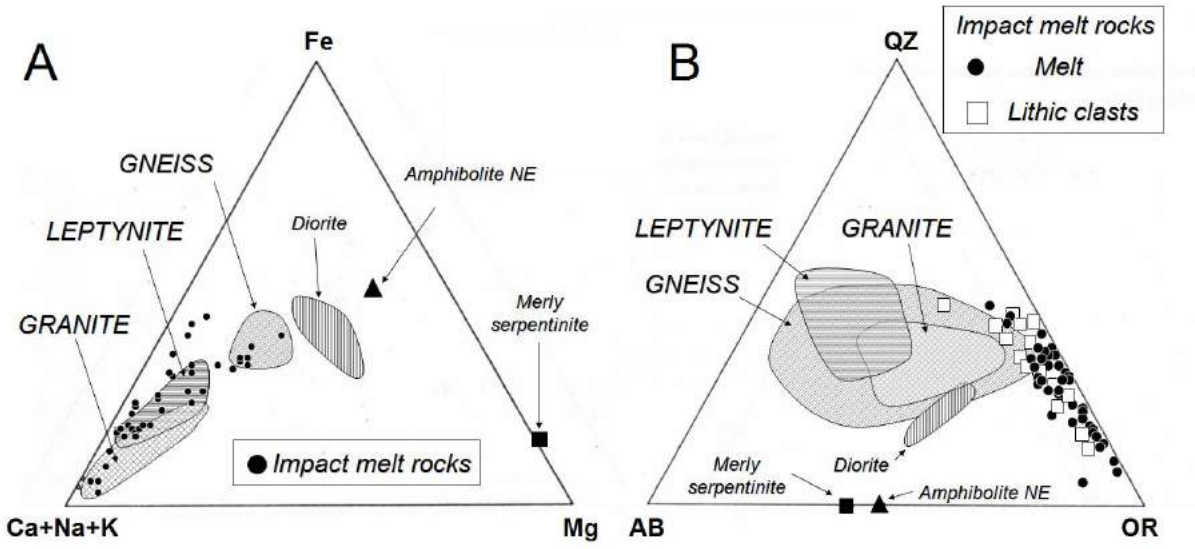

Figure 5: A: Plots of the composition of the main target formations and impact melt rocks in the total alkali elements-Fe-Mg ternary diagram. B: Plots of the composition of the main target formations, impact melt rocks, and lithic clasts in impact melt rocks in the Quartz-Orthoclase-Albite ternary diagram.

A larger set of chemical analyses has been obtained by atomic absorption spectrometry (AAS) for selected elements (Lambert 1977b). It covers the spectrum of lithologies observed in the Rochechouart basement. The complete set is shown on a Fe-Mg diagram as Figure 6A.

The results are summarized in Figure 6B which only shows correlation fields. The three main target formations plot together around the geometrical center of the Qz-Ab-Or diagram, which is

consistent with their common granitic character (Figure 5B).

Granites, leptynites and pink microgranite are characterized by high SiO_2 content and low Fe-Mg values, and plot together forming the granitic field represented next to the origin on the Fe-Mg diagram (Figure 6B). In detail, pink microgranites appear relatively more mafic than granite, as seen in Figure 6B. Leptynites are slightly richer in SiO_2 and FeO than granites as seen from the partial overlap of what in the ternary diagrams (Figure 5) and in the Fe-Mg diagram (Figure 6B).

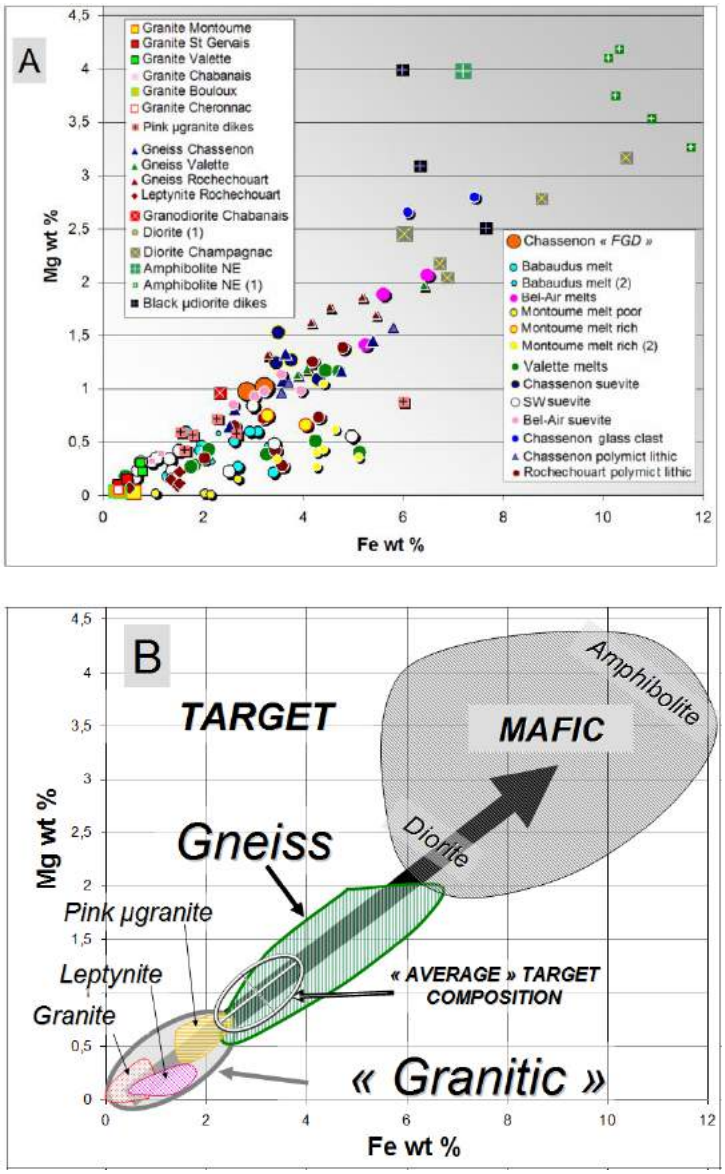

Figure 6: Fe-Mg plots for the target and impact deposits at Rochechouart after Lambert (1977a).
A: Data for 73 samples from the target and 243 impactites, impact deposits and selected clasts from suevite and impact melt rocks ((Measurements performed in the mid 1970's by BRGM-French Geological Survey, Orléans, France. Uncertainty of individual analyses: 1 to 5 % of the measured wt%). (1) Data from Chevremont et al., 1996. (2) Data from Tagle et al., 2009. « FGD » = Impactoclastites (fine-grained deposit); µgranite = microgranite; µdiorite = microdiorite.
B: Correlation plots for the main target formations. Ellipsoids represent the correlation fields for the various basement rocks exposed in the Rochechouart area. The "average" target composition field mixes the composition of the various basement rocks according to their relative proportion of exposure in the Rochechouart area (ca 50% granite + leptynite and 50% gneiss). Black solid arrow: symmetry axis of the correlation field common to all target formations

Ferromagnesian content in the granites increases from the Cheronnac granite and the Bouloux granitoid to the Saint Gervais granitoid, the granitoid of the Valette area and, finally, the Chabanais Granite. The Fe-Mg composition of the granite in the Montoume area is comparable to that of the nearby Saint Gervais granite, except for a slightly higher Fe content.

Gneisses plot separately from the granites in both the total alkali-Fe-Mg ternary (Figure 5A) and the Fe-Mg (Figure 4B) diagrams. The spread of gneiss compositions is larger than that for granites, as shown on Figures 5 and 6B. Differences of composition are also noted between gneisses from different localities. Gneiss near Rochechouart appears relatively more mafic than that near Chassenon. Gneisses near Valette tend to fall in between these groupings.

The granodiorite in the Chabanais granite gives a composition close to that of the nearby Chassenon gneiss.

Diorites plot separately from gneiss in both the total alkali-Fe-Mg ternary diagram (Figure 5A) and the Fe-Mg diagram (Figure 6B). Diorite spans from a composition close to that of the mafic gneisses of the area up to almost that of the amphibolites (Figures 5 and 6B) which crop out in the same area (in the northeast, Figure 4). The composition of the black dykes fits that of the diorites (Table 1). The amphibolites represent the mafic pole of the sequence of basement rocks exposed in the area of the impact deposits. Amphibolites are characterized by a low SiO_2 content and high Fe-Mg and CaO contents (Table 1).

Although the Merly serpentinite plots near the amphibolite on the Qz-Ab-Or diagram (Figure 5B), it forms a separate type characterized by very low CaO and Al_2O_3 contents and very high MgO content (Table 1). It is also characterized by high Ni-Cr contents (both in the 2000-2500 ppm range), contrasting with a relatively low abundance of Rare Earth Elements (all essentially below 2 ppm) (Chevremont et al., 1996).

Figure 7: Rochechouart church, characterized by unique octahedral and helocoïdal bell tower. Like the Nordlingen church in the Ries, the Rochechaourt church is made of impactite. Most of the building is made of polymict lithic breccia occurring immediately beneath the site. The porch and other architectonic items are made of Chassenon suevites.

Morphometry of the crater floor

One unique characteristic of the Rochechouart structure is the wide exposure of the crater floor/wall, i.e. the boundary between the impact breccia deposit and the more or less impact-damaged bedrock.

Although the contact is generally masked by vegetation and soil cover, it is cut by a dense network of small rivers over a ca 110 km^2 area corresponding to the extent of the crater deposits (Figures 8-9).

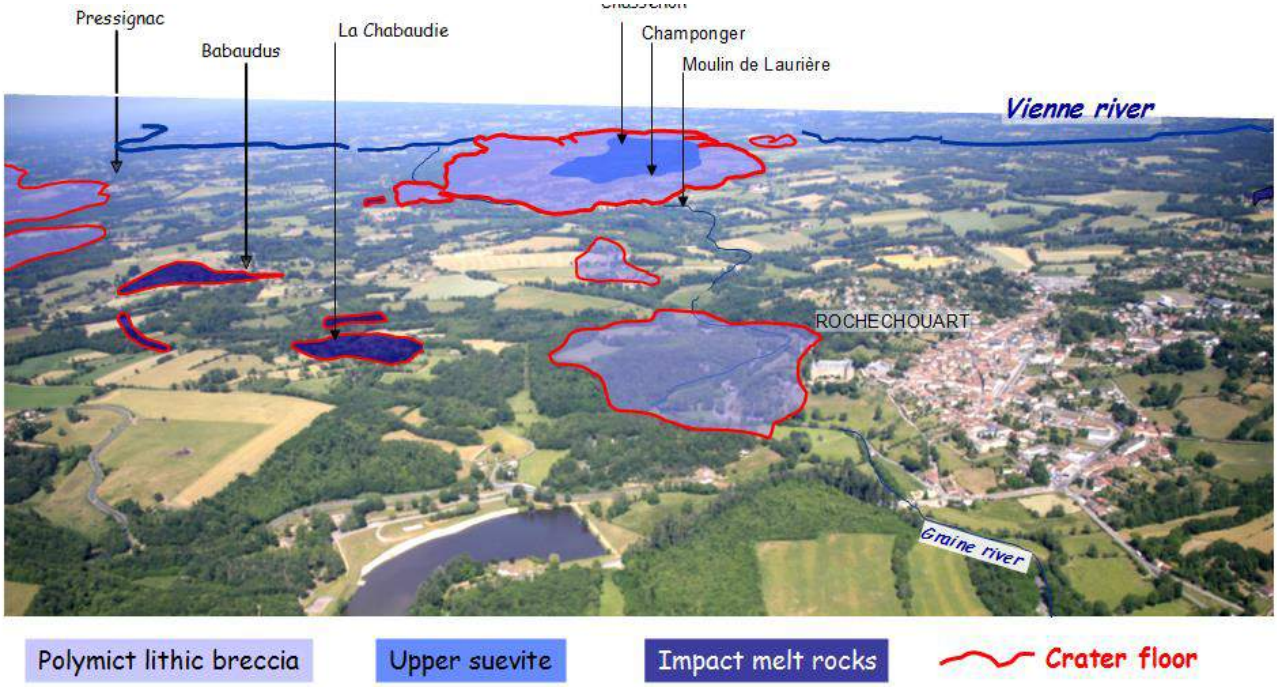

Figure 8: Aerial view of a W-NW traverse of the Rochechouart impact structure and approximate positioning of the main crater fill deposits. Note the abundant vegetation cover and the lack of topographic expression of the crater.

Where it is exposed, the boundary is complex, changing from horizontal to vertical attitudes at the decimeter to decameter scale (Figure 10). At the hectometer scale, the elevation of the crater floor displays variations up to 50 m, such as seen across the Graine River west of Rochechouart.

At the scale of the entire structure, these irregularities in the crater floor are smoothed out and the overall contact plane appears rather flat (Kraut and French, 1972, Lambert, 1974, 1977a–c). The contact on the eastern and western sectors of the structure lies at similar elevations of 200 to 250 m; at Montoume on the southern edge of the impact breccia deposits, it lies at ca 290 m elevation, whereas north of Chassenon it is at about 175 m (Figures 10-11). This indicates a marginal inclination of 0.6° north for the deposit. There is no marked raise of the crater floor elevation at the center of the structure. At most, specific traverses (Figure 11) reveal a 3-4 km wide central "high" in the vicinity of Babaudus rising up to ~ 50 m above a 4-5 km wide topographic "low" in the area of Chassenon.

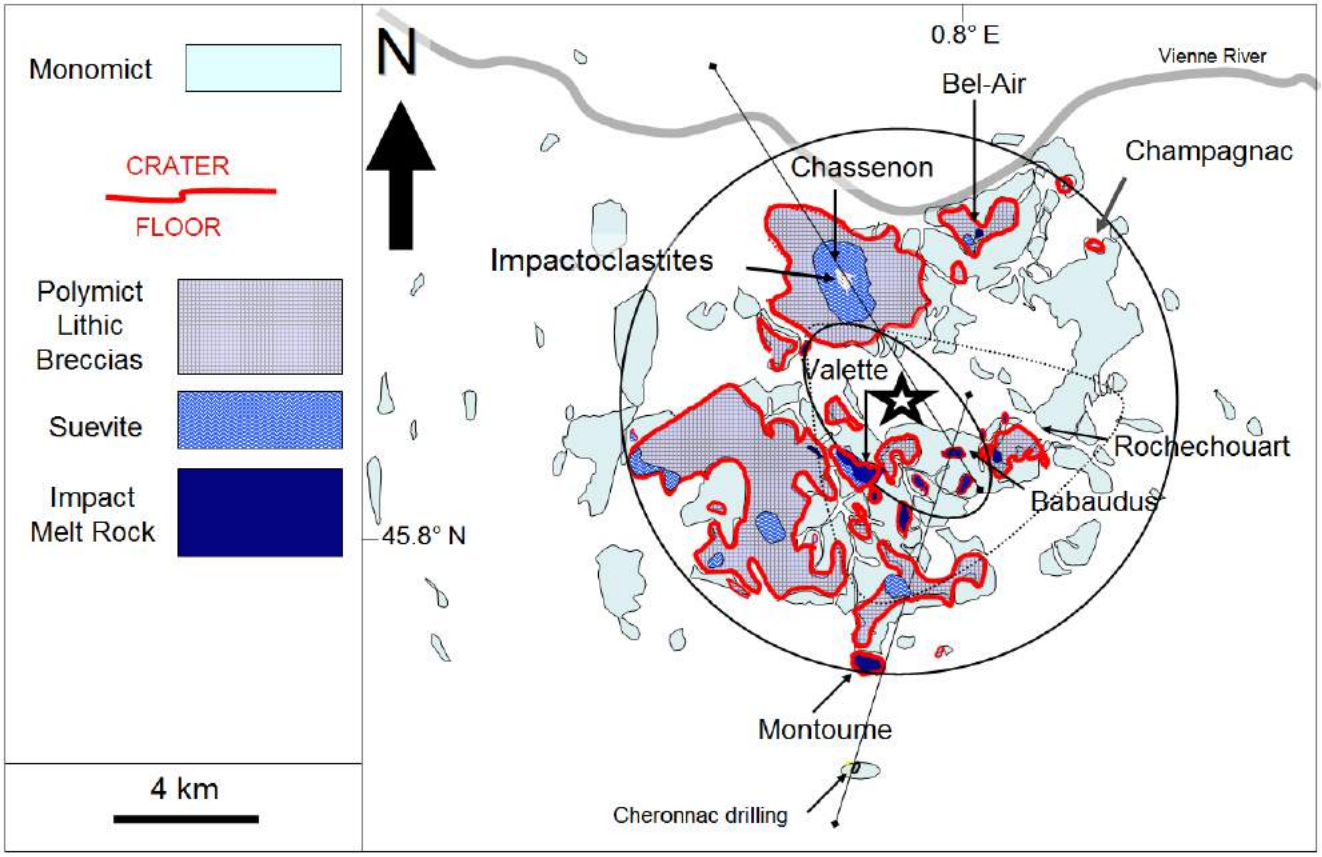

Figure 9: Schematic geologic map of the framed area of Figure 1 (after Lambert, 1974, 1977a and Chevremont et al., 1996). Rochechouart impactites. Target formations and surface deposits (including alluvial deposits) omitted. Dotted line: Spatial distribution of shatter cone localities (80% occurring within the ellipse). Lines: Positions of the two branches of the cross section shown in Figure 10. Impactoclastites: fine grained deposit and dikes (surface occupied on the map is exaggerated compared to reality in the field).

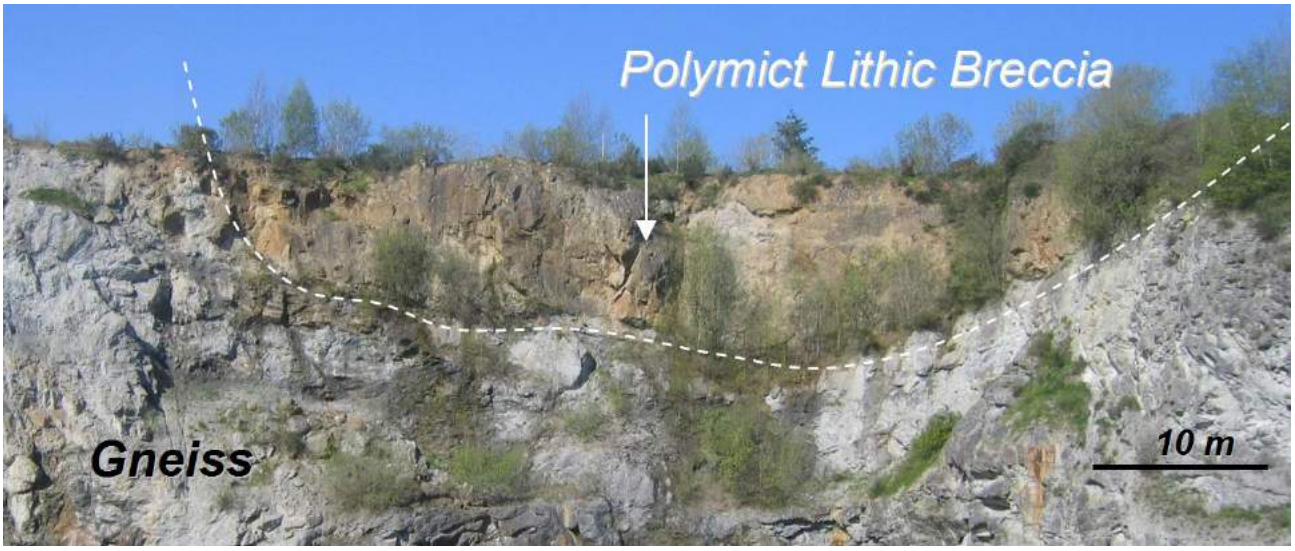

Figure 10: Field view showing the contact between a similar polymict lithic breccia and gneiss at Champagnac quarry 7.5 km NE of the center of the structure. Complex geometry of the boundary at the decameter scale. Fracturing and local brecciation of the target (photo courtesy of Claude Marchat, 2002).

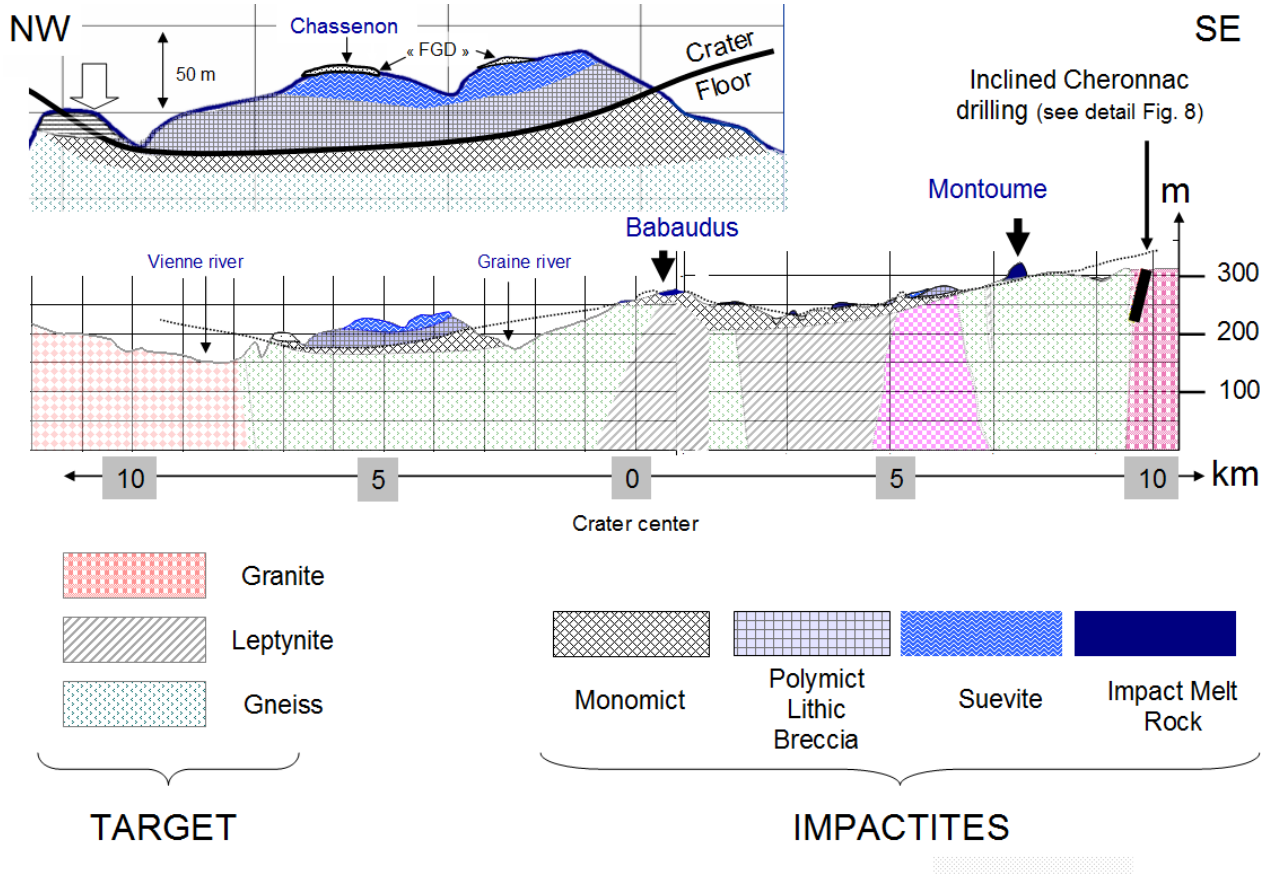

Figure 11: Schematic cross-section of the Rochechouart impact structure. Position of the cross-section shown in Figure 9. Top view: Close-up of the Chassenon deposit. Vertical exaggeration x10. FGD: Impactoclastites (fine-grained deposit and dikes: both vertical and lateral extent exaggerated for better visualisation) (after Lambert, 1974, 1977a and Chevremont et al., 1996). Open arrow: Alluvial terrace of the Vienne River.

Figure 12: Ground view from the east side of the structure, looking west showing the flat topography of the crater deposits which locally forms the top of the hills in the background.

AUTOCHTHONOUS AND sub-AUTOCHTHONOUS IMPACTITES

The close correlation between the topographic surface and the original crater floor ensures that abundant exposures of the impactite-to-basement transition are exposed. Several types of impactite are distinguished according to macroscopic texture and/or petrological characteristics:

Shocked rocks with no macroscopic fracturing or fragmentation

Basement rocks near the center of the structure in the Valette area and at significant distances from the center of the structure such as near Bel-Air, or near Videix, respectively 4.5 km north-northeast and 6 km south-southwest of the center (Figure 9) lack extensive fracturing or brecciation at the macroscopic scale but display evidence of severe shock metamorphism under the microscope.

Most feldspars recrystallized after in situ melting, micas are thermally decomposed and/or melted, and quartz is more or less completely recrystallized from diaplectic glass and in patches shows remnants of multiple sets of planar deformation features (PDF). Chemical analysis (Lambert, 1977a) indicates a strong enrichment in K_2O and a strong depletion in Na_2O and CaO of these highly shocked autochthonous or parautochthonous basement rocks.

Precise mapping of these impactites is prevented by limited outcrop. Yet they are likely to be local and limited in lateral extent (“pockets”).

Shatter cones

Shatter cones are best displayed in the fine grained and massive microgranite dikes. Conversely they are poorly represented in the granite. They are also rare in gneiss, where striated irregular surfaces are more common (Lambert, 1974, 1977a). Petrographic study indicates that shatter coned rocks essentially bear no or little shock metamorphic evidence at the mineral scale, with at most some PDF in quartz and more generally only fracturing (Lambert, 1977a). The 30 sites reported by Lambert (1977a) lie in a ca 60° arc extending up to 7 km from the center towards the southeast (dashed line in Figure 4). Some 80 % of these sites fall into an elliptical area within the northwest corner of the aforementioned sector and extending in the same southeasterly orientation. This elliptical zone, ca 6 km long and 3 km wide, is centered near Valette (Figure 4). Two sites reported by Kraut and Becker (1975) at ca 7 km from the center of the structure (one in the east and the other in the west) have been searched but no shatter cones were found. Out of the 30 sites only 4 yielded a significant population of striated surfaces of sufficient quality to enable statistical measurement of cone orientation (Sorel et al., 1977).

These localities are all situated near the center of the structure. At each location both striated surfaces and striations fit onto the same virtual master cone. Master cone orientations are different from site to site. At the two closest locations ca 1.5 km from the center of the structure the measured master cones plunge steeply toward the center of the structure at 73-76 ° (Sorel et al., 1977). At the two outermost locations (ca 3 km from the center) the master cones point up near-vertically (Sorel et al., 1977).

Figure 13: Shatter cones at Champonger quarry, below the Chassenon deposit. View field ca 1.5 meter wide. Picture taken in the early 1990. Photo courtesy of Association Pierre de Lune.

Monomict lithic impact breccias

These breccias comprise highly fractured and fragmented bedrock (Figure 13) in which fragments are rotated and displaced and lie in a fine-grained clastic matrix usually representing less than ca 20 vol% of the rock.

Fragment sizes are generally between 1 and 100 millimeters. The clasts are highly irregular and angular. Most of the minerals in these rocks display no or only weak shock metamorphism, corresponding to stages 0 and 1a in the IUGS nomenclature (Stöffler and Grieve (2007).

It is missing in the central part of the structure, over a 1 to 3 km wide - 8 km long zone oriented east-west (Figure 2B) where the basement shows only local occurrences of monomict ltihic breccia dikes and more rarely polymict lithic breccia dike and pseudotachylite-like dikes (see next section).

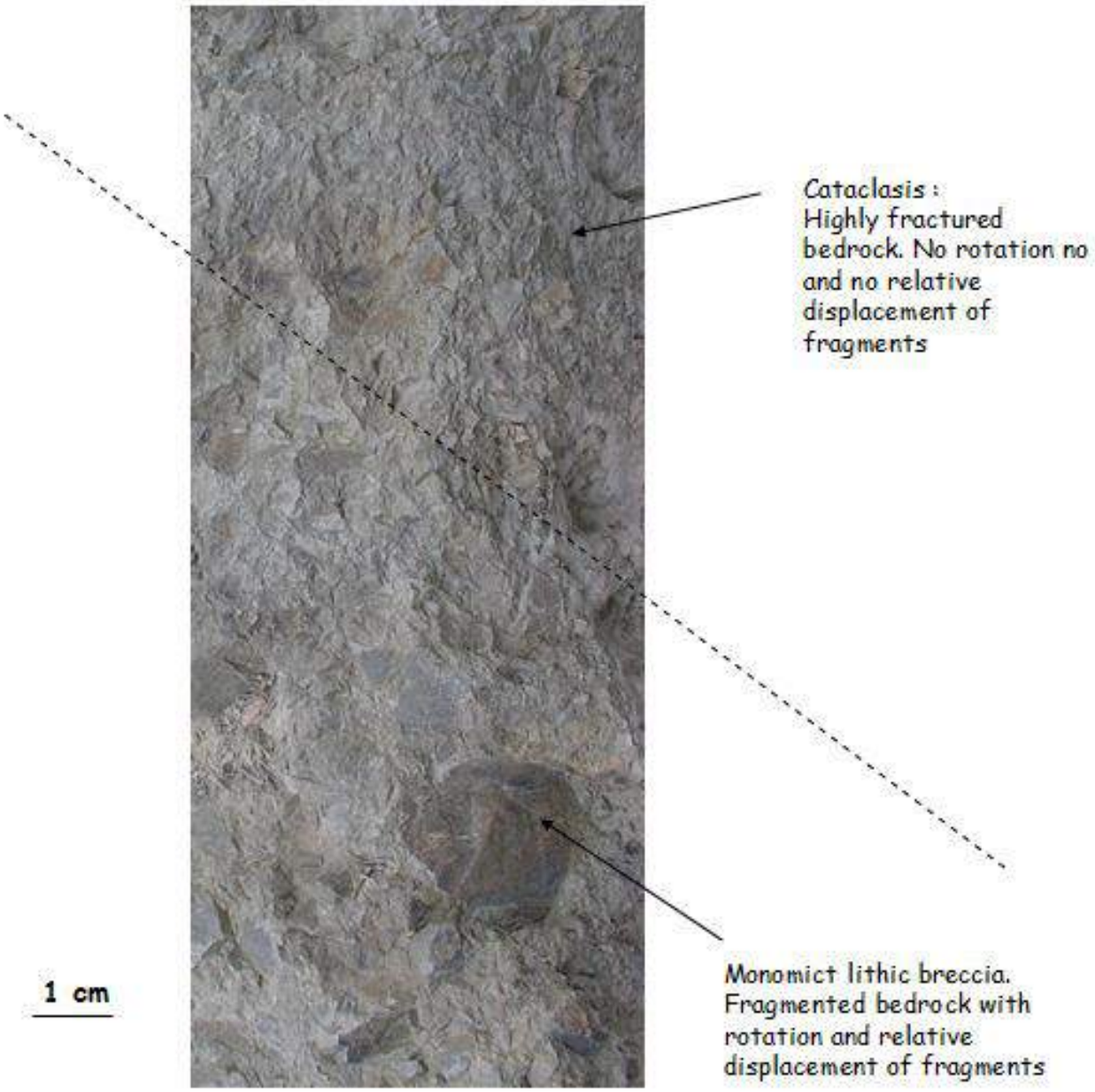

Figure 13: Highly fractured orthogneiss at Champgnac quarry. Cataclasis and progressive grading into a monomict lithic breccia.

Field observations indicate a close relationship between monomict lithic impact breccias and fragmented rock lacking displacement of the fragments (Figure 13). These are mapped as a single monomict impactite unit in Figures 9 and 11.

As shown in Figure 9, the monomict impactite is better exposed in the 15 km diameter inner zone (zone of the ejecta deposits). The maximum thickness of this monomict impactite unit is ca 90-100 meters, recorded at Champagnac 7.5 km from the center of the structure.

Elsewhere is usually thin (meter to a few decameter) and very variable at the hectometer scale.

The monomict lithic impact breccia is also exposed outside the inner 15 km diameter zone (Figure 9), but it is not as extensive or abundant as the large patches that occur in the inner zone. The most remote occurrences are found ca. 12 km west of the center of the structure (Figure 9).

Geochemical analysis of granitic and gneissic monomict lithic impact breccias shows a significant difference in composition compared to the undeformed target material (Table 2). The monomict lithic impact breccias are systematically depleted in Na_2O and enriched in K_2O (Table 2). On average, there is an increase by a factor of 2 in the K_2O/Na_2O ratio in the monomict breccias compared to non-brecciated basement.

			K_2O/Na_2O	K_2O/CaO
BEDROCKS (unshocked)		Gneiss (42)	1.2	1.8
		Leptynite (26)	1.3	2.8
		Granite (21)	1.6	7.2
IMPACTITES	MONOMICT BRECCIAS	Gneiss (17)	3.4	n.m.
		Leptynite (2)	4.0	n.m.
		Granite (10)	3.0	n.m.
	POLYMICT BRECCIAS	Lithic (86)	6.9	n.m.
		Suevite (99)	9.1	n.m.
		Impact melt rocks (95)	21.6	40.7
		Lithic in melt (18)	15.8	n.m.
	IMPACTOCLASTIC DEPOSIT		18	40.8

Table 2: Summary of the K_2O/Na_2O and K_2O/CaO ratios of the main Rochechouart lithologies (including the distinction between unshocked basement rocks and brecciated ones). (): Number of analyses. n.m. = not measured. AAS, XRF and wet chemical analyses after Lambert (1977a).

Breccia dikes

A variety of breccia dikes is exposed in the Rochechouart basement. It includes i) monomict lithic impact breccias resembling the monomict lithic breccia forming the monomict unit described above, ii) polymict lithic breccias (examples at Figures 14-15) resembling the polymict lithic breccia observed above the crater floor in the crater deposits (see allochthonous impactite section next) and iii) impact pseudotachylite and impact pseudotachylite-like breccias forming complex networks of millimeter- to decimeter-sized veins characterized by a prominent fine-grained matrix unresolved under the optical microscope, where evidence of a glass origin for the matrix is verified in the former type (such as at Champagnac site, Reimold et al., 1987) and is not in the latter (various sites reported in Lambert, 1977a, 1981).

Materials matching the textural characteristics of the suevite, the impact melt rocks and the impactoclastites (see description in the next section) in the crater deposit are not observed in the dikes and veins cross-cutting the Rochechouart basement formations.

Shock features are observed in rock and mineral clasts of all the types of breccia dikes (Lambert, 1981). On average, the level of shock recorded by the lithic fragments in the various types of dikes in the Rochechouart target remains low - stage 1b at most (in reference to IUGS nomenclature of Stöffler and Grieve, 2007) - and most clasts do not display shock deformation. The basement rocks crosscut by these dikes commonly lack any other macroscopic evidence of shock damage but can display a fractured-fragmented texture. Another noticeable and common characteristic of these breccia dikes is the lithologic compositions of the clast populations that match the wall rock lithologies. No clasts of sedimentary material have been observed so far in any of the Rochechouart breccia dikes.

The width of the monomict and polymict lithic impact breccia dikes at Rochechouart varies from ca 10 cm to several meters (as exemplified in the Champagnac quarry). Like the massive monomict and polymict lithic impact breccias found, respectively, below and above the crater floor, these dikes display a large proportion of more or less angular rock clasts embedded in a matrix of fine debris.

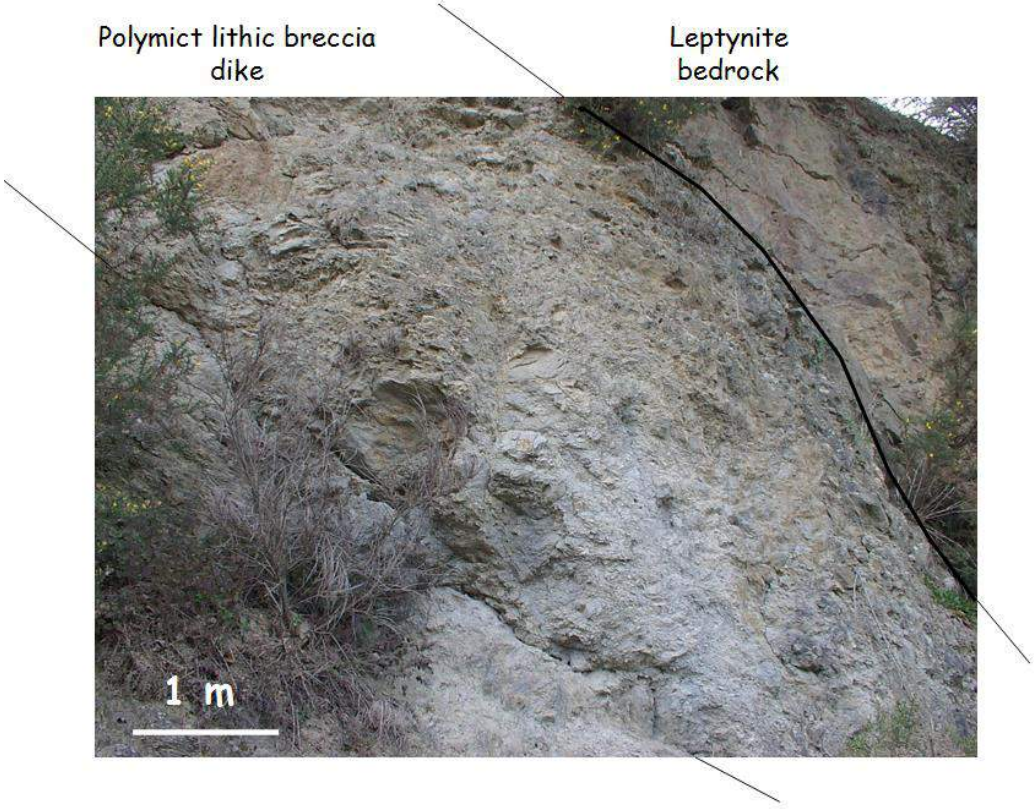

Figure 14: Polymic lithic breccia dike at Champgnac quarry. Vertical distance to the crater floor is estimated < 100 m

The only difference between the monomict and polymict lithic impact breccias in the dikes and those forming massive units concerns the grain size and the shape of the clasts. The average diameter of clasts obtained by image analysis of sections of polymict lithic breccia occurring as a dike in the bedrock at Cheronnac is ca 3 millimeters, whereas it is 12 millimeters for a massive polymict lithic breccia deposited near Rochechouart (Table 3). The difference in the aspect ratio of clasts is not as marked as the difference of grain size (1.5 in the breccia dike, against 1.6 in the massive deposit measured by image analysis on the material in Table 3) yet it

indicates clasts in the dikes tend to be more spherical than in the massive deposit. A similar trend, but more pronounced (aspect ratio at 1.4), characterizes the clasts of the impact pseudotachylite/impact pseudotachylite-like material (measured by image analysis of a micrographs from Puyjoyeux and Cheronnac samples. The latter are characterized by an average grain size of clasts 2-3 orders of magnitude below that measured for the clasts of the polymict lithic breccia and suevite in the crater deposits (Table 3).

CLASTS	AREA FRACTION > 1 mm	AREA FRACTION 1< <5 mm
Pseudotachylitic	2.34%	0,00%
Microgranite	0.36%	0.21%
Gneiss	3.53%	0.82%
Granite	25.06%	7.56%
Total	31.29%	8.59%

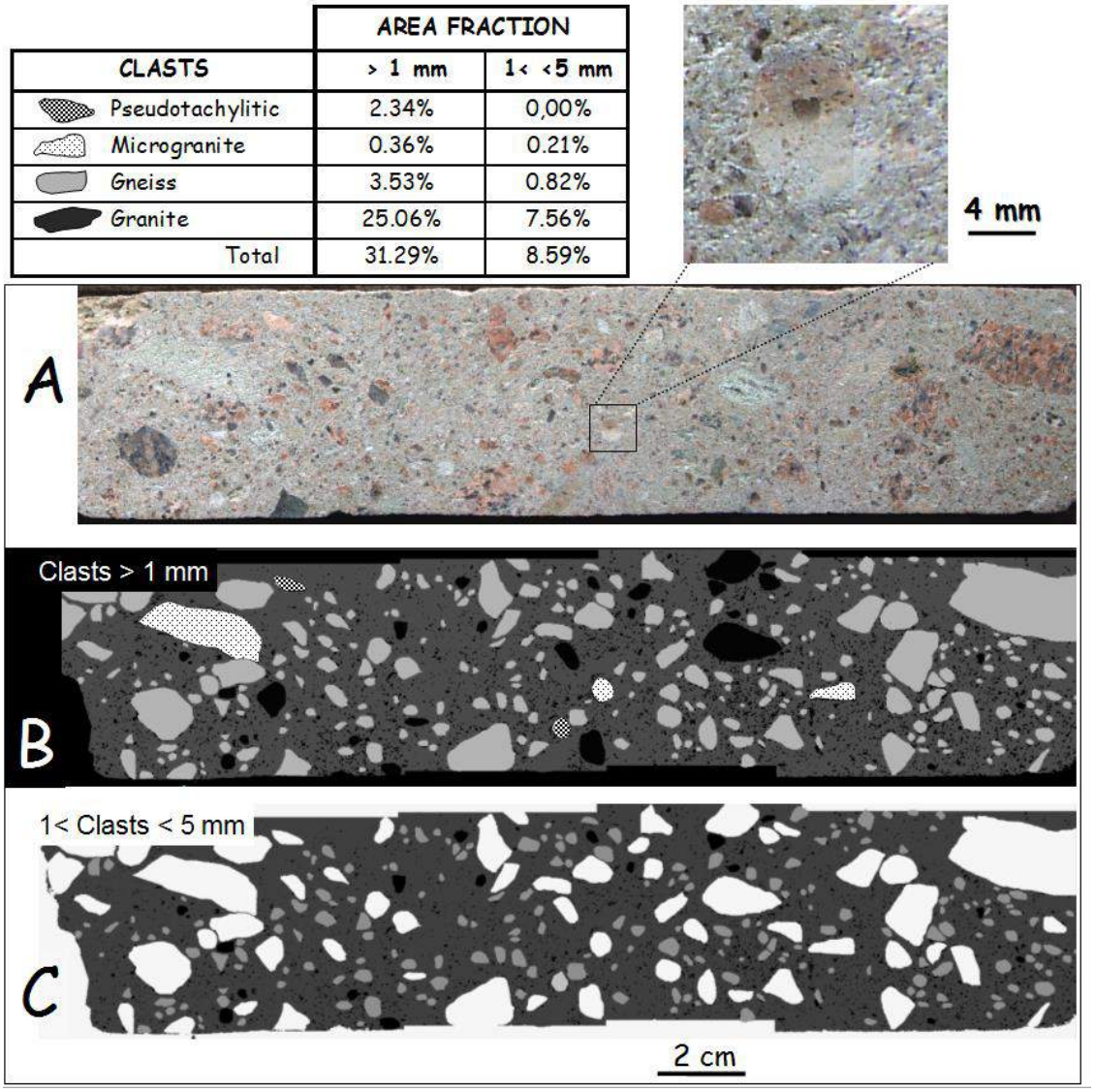

Figure 15: Polymict lithic breccia at 93 m in the 5 cm diameter drill core at Cheronnac, 10 km south of the center of the structure (see location on the map at Figure 9 and location on the drill core log at Figure 18). A- Macroscopic view of the axial cross section plane showing a large contribution form local granite with a mix of very rounded and isometric clasts significant of abrasion related to friction during transportation and very angular clasts indicating no or very limited transportation. Insert on the upper right corresponding to a close up view of a light colored banded and fined grained clast of pseudotachylite. B- Segmented false color images of the Figure 7a distinguishing different phases in the clasts population > 1 mm in length. Phases identified at the table on the upper left corner giving the proportion of the phase according to relative surface area measured by image analysis. C- Idem B fort clasts comprised between 1 and 5 mm in length. Larger clasts (not measured at the table) appear in white.

			Volume %			
	Diameter in mm	**Average**	**> 5**	**>1**	**>0.3**	**>0.05**
Massive Deposit	Lithic breccia and suevite	>10	29	>50	n.d.	n.d.
	Impactoclastite	<0.05	0	0	0.2	5
Dike	Lithic breccia	3	29	32	n.d.	n.d.
	Impact pseudotachylite	<0.05	0	<1	<1	8
	Impactoclastite layer 1	<0.05	0	0	0.4	12
	Impactoclastite layer 2	0.9	0	4	13	n.d.
	Impactoclastite layer 3	0.8	0	4	6	n.d.

Table 3:. Average diameter of particles and volume% as function of particle size, from statistical measurements by image analysis on polished macro- and micro-sections. n.d. = not determined. (Sample locations: Cheronnac drill core for lithic breccia dikes, Rochechouart and Chassenon for the massive breccia deposit; Chassenon for the impactoclastic deposit and dikes (layers detailed in Figure 19 and 20)).

The best exposure of various types of breccia dikes and their complex time-space relationships is in the active quarry of Champagnac (Figures 4 and 10). Both impact-generated lithologies and basement are exposed at a quarry-face that is currently ca 1500 m long and 80 m high (Figure 16).

The basement rock displays a complex network of breccia dykes. Multiple sets of fractures intersect each other, including low-angle faults, which have been studied in detail by Kenkmann and Ivanov (1999) and Kenkmann et al. (2000) (Figure 16).

Although not as spectacular as those at Champagnac, breccia dikes are common in all basement rock types at other sites as well. Examples of breccia dikes in gneiss are exposed at the center of the structure in small, old quarries along the Graine River.

Figure 17 illustrates an interesting example, now lost, as the site was utilized for landfill in the late 1970s. Located near Puyjoyeux 5 km from the center of the structure, 2 km southeast of Rochechouart, the site displays a 20-50 cm thick dike characterized by a complex dike-in-dike breccia texture. The centimeter-thick core (denoted 3 in Figure 17A) displays a distinct white color and is made of an optically unresolved very fine-grained material embedding a few small sized rounded clasts.

Flow features, vortex-like features and crude sorting are observed. The core grades into a highly fractured-brecciated leptynite (denoted 2 in Figure 17A). At the edge of the dike, the contact with the leptynite wall displays millimeter-thick breccia veins bearing the same very fine-grained matrix material as that in the core. A few thin veins also branch into the wall (denoted 4 in Figure 17B).

Table 1 reports the major element compositions of the leptynite wallrock and the core and margin of the monomict breccia. SiO_2 contents are exactly the same for the three samples, but the breccia is relatively depleted in Na, more significantly depleted in Ca, and strongly enriched in K. The same trend is observed for the core but the differences of compositions compared to that of the host rock are more pronounced in the core sample than in the peripheral monomict breccia (Table 1).

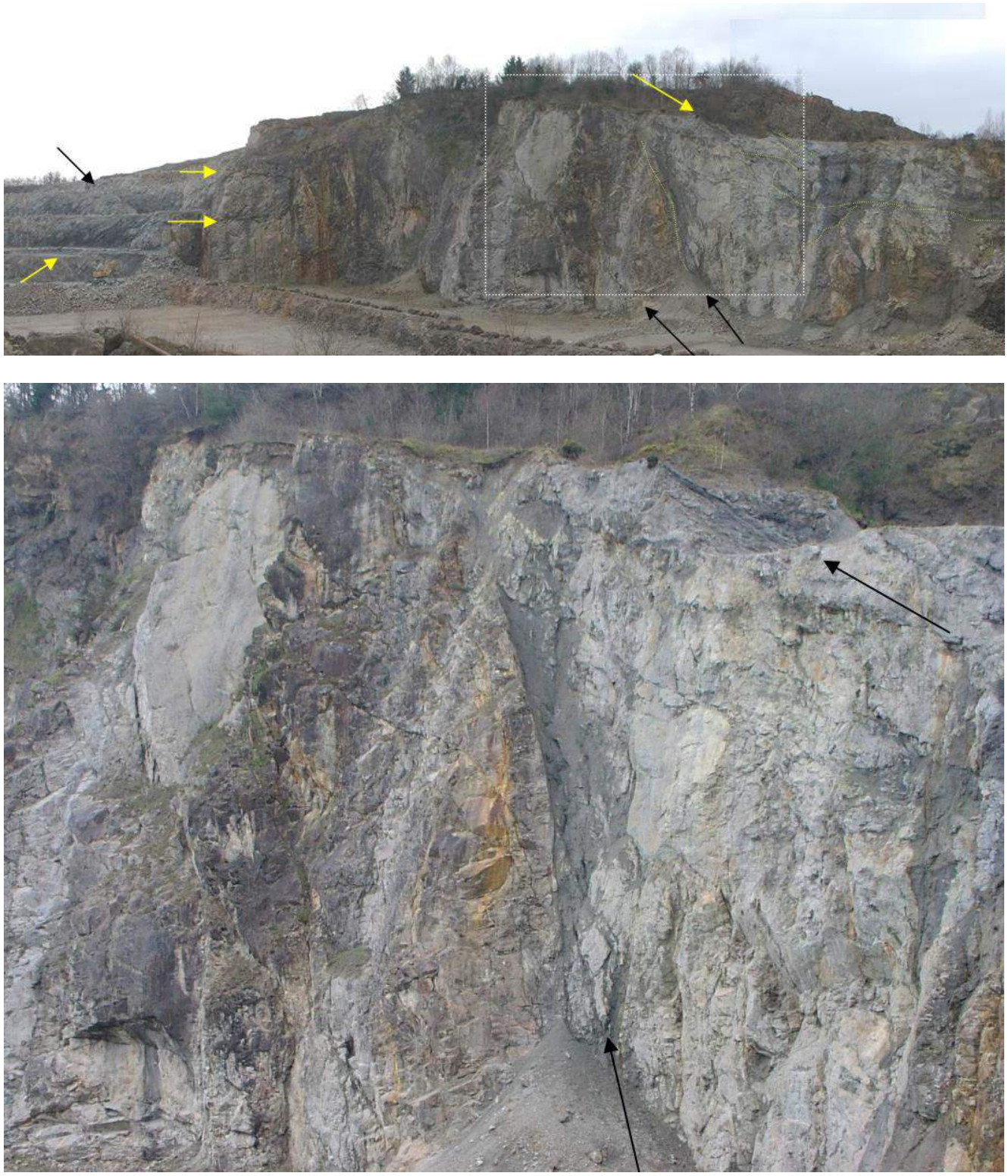

Figure 16: Top: General overview of part of the Champagnac quarry located 7.5 km NE of the center of the structure. Bottom: Detail of the framed zone showing the complex network of fractures and dikes crosscutting the bedrock. Arrows: major faults and breccia dikes.

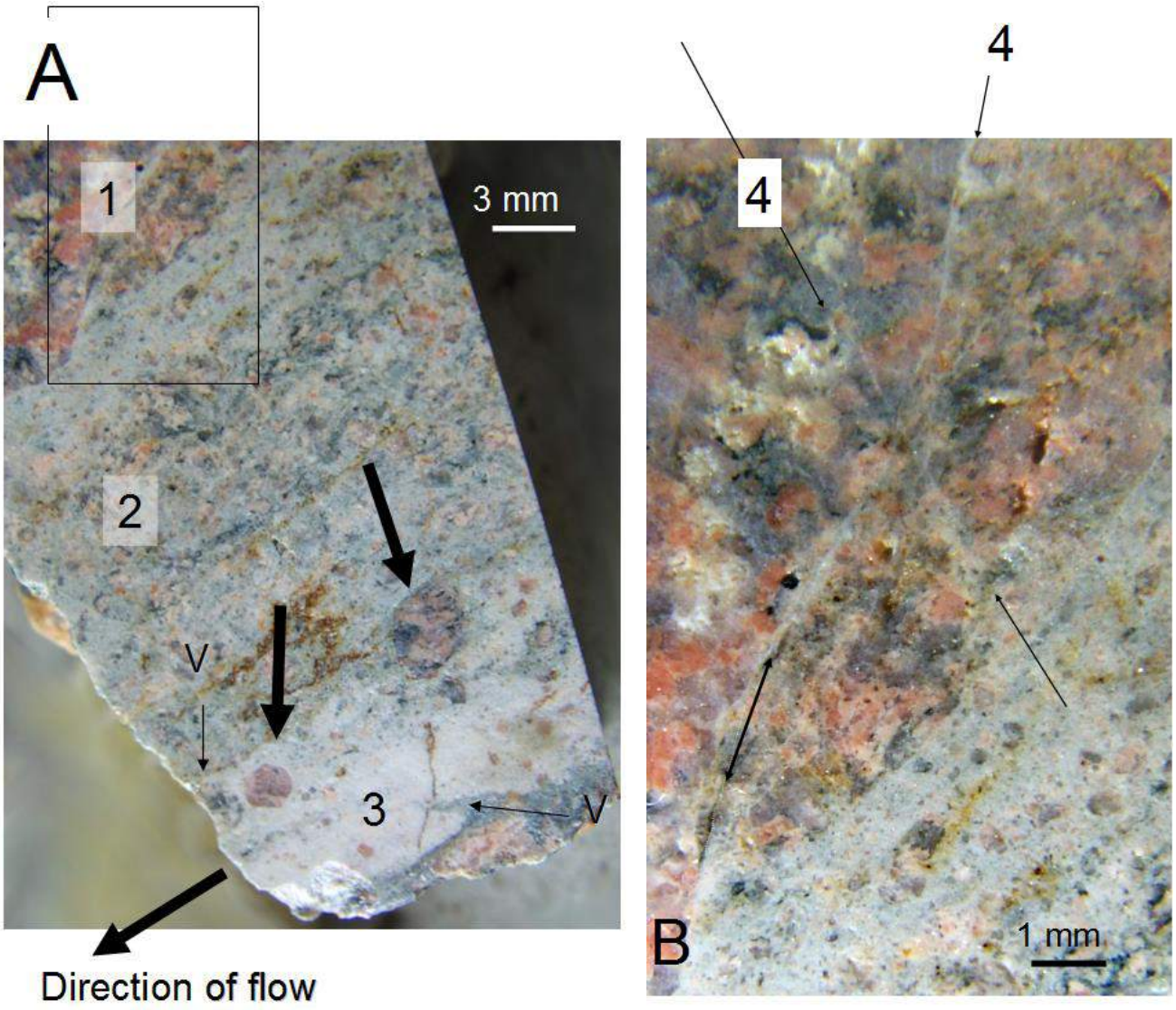

Figure 17:. Complex breccia dike crosscutting leptynite at « Puyjoyeux » quarry, 2 km SE of Rochechouart, ca 6 km from the center of the structure. A-Detail of the zone at the contact of the dike and the leptynite displaying a progressive passage from bedrock (denoted 1) to monomict lithic breccia (denoted 2), and then to a very fine-grained material forming the core of the dike (denoted 3). The latter is characterized by flow features and a few small, rounded clasts (black arrows). Chemical analyses for the 3 materials given in Table 1. The zone at the contact with the bedrock (plain white arrow) displays millimeter thick breccia veins bearing the same very fine-grained matrix material as that in the core. B: Close up view of the leptynite wall and the contact with the breccia dike (framed zone in A). Note the thin intersecting veins branching in the wall (denoted 4).

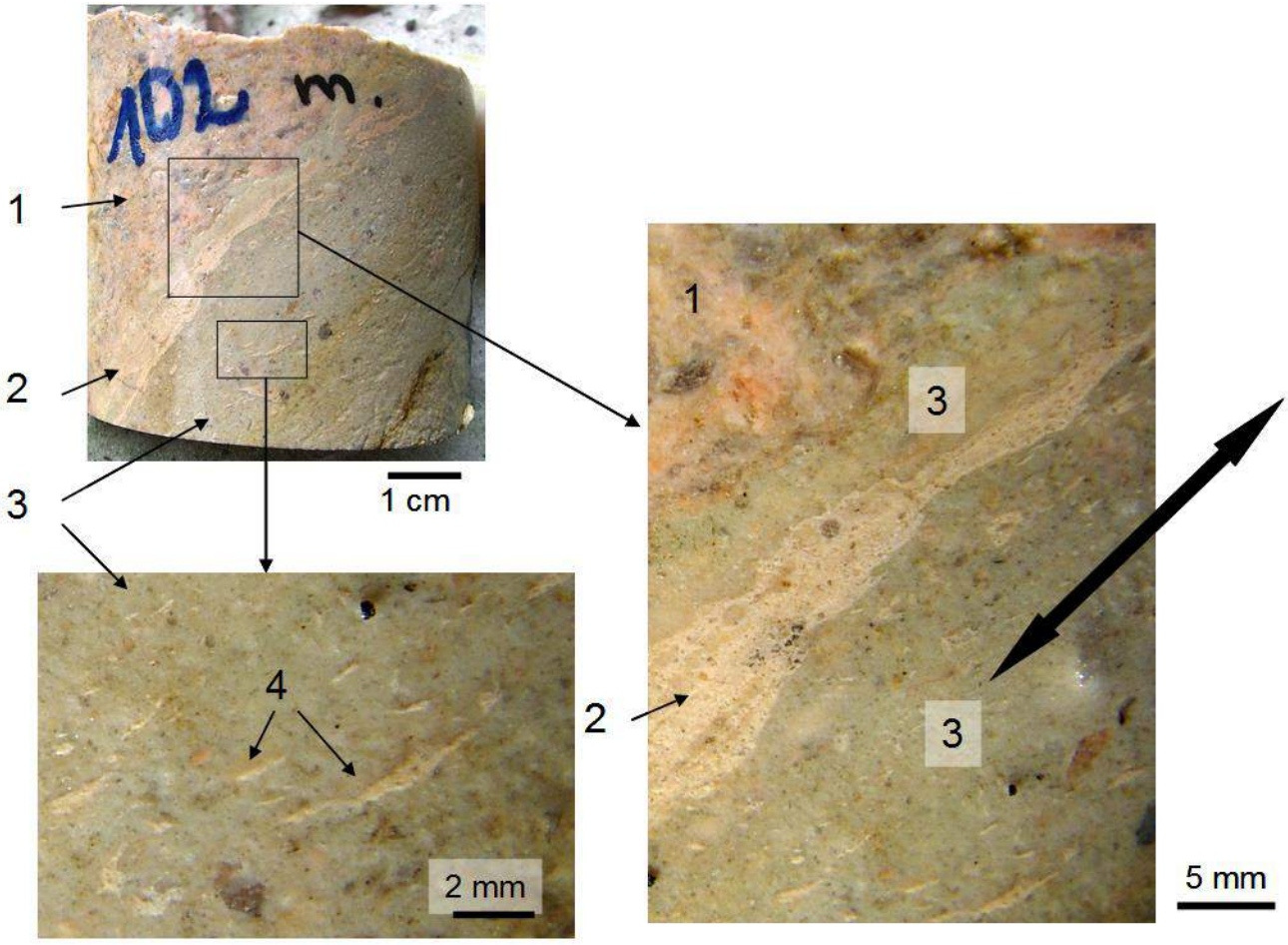

Figure 18: Complex breccia dike at 102 m depth in the Cheronnac drill core, 10 km S of the center of the structure. 1: Brecciated granite belonging to a 4 meter wide monomict breccia dike. 2: Centimeter thick vein forming the core of the dyke displaying an aphanitic and locally fluidal texture, surrounded by 3: a different color breccia also characterized by the prominence of an optically unresolved very fine-grained matrix embedding clast of the core material. 4: Close up view showing elongated and schlierig debris of the aphanitic core breccia in the aphanitic peripheral breccia. Black double arrow: Preferred orientation of clasts in the aphanitic peripheral breccia and direction of flow features in the aphanitic core breccia.

Another example of a multi-layered breccia dike is illustrated at Figure 18. It is observed in the 131 m long, 45° inclined drill core near Cheronnac, 10 km south of the center of the structure (Figure 18). The section cuts through ca. 90 m of granite and 40 m of gneiss. The granite is intersected by 1 to 5 m thick microgranite dikes (Figure 19). Two impact pseudotachylite-like dikes each about 10 cm thick are found at 56 and 102 m depth.

Figure 18 shows the particular multi-layered texture of a complex dike-in-dike breccia dike centered at 102 m in the drill core. As at Puyjoyeux the core of the dike is formed by an optically unresolved very fine-grained translucent material (denoted 2 at Figure 18) embedding a few small sized clasts. Some clasts are rounded and some are strongly elongated and schlieric in the direction of the dike, suggesting near-melting conditions. This core material is interpreted as the remnant of an impact pseudotachylite which has been reprocessed by a second generation of fracturing along the dike as it is surrounded by a darker material (denoted 3 at Figure 18), also characterized by an optically unresolved very fine-grained material, where clasts (still rare) are dominated by elongated and schlierig debris of the

layer 1 material (denoted 4 at Figure 18). This complex dike forms the core of a 4 m wide monomict breccia dike (Figure 19).

Two relatively thick (up to 4.3 m) intercalations of polymict lithic breccia are also encountered in the Cheronnac drill core respectively at 60 and 93 m depth. Their clast fraction is dominated by fragments derived from the local granite (Figure 19), with minor contributions from gneiss, microgranite and pseudotachylitic material similar to that encountered at 102 m.

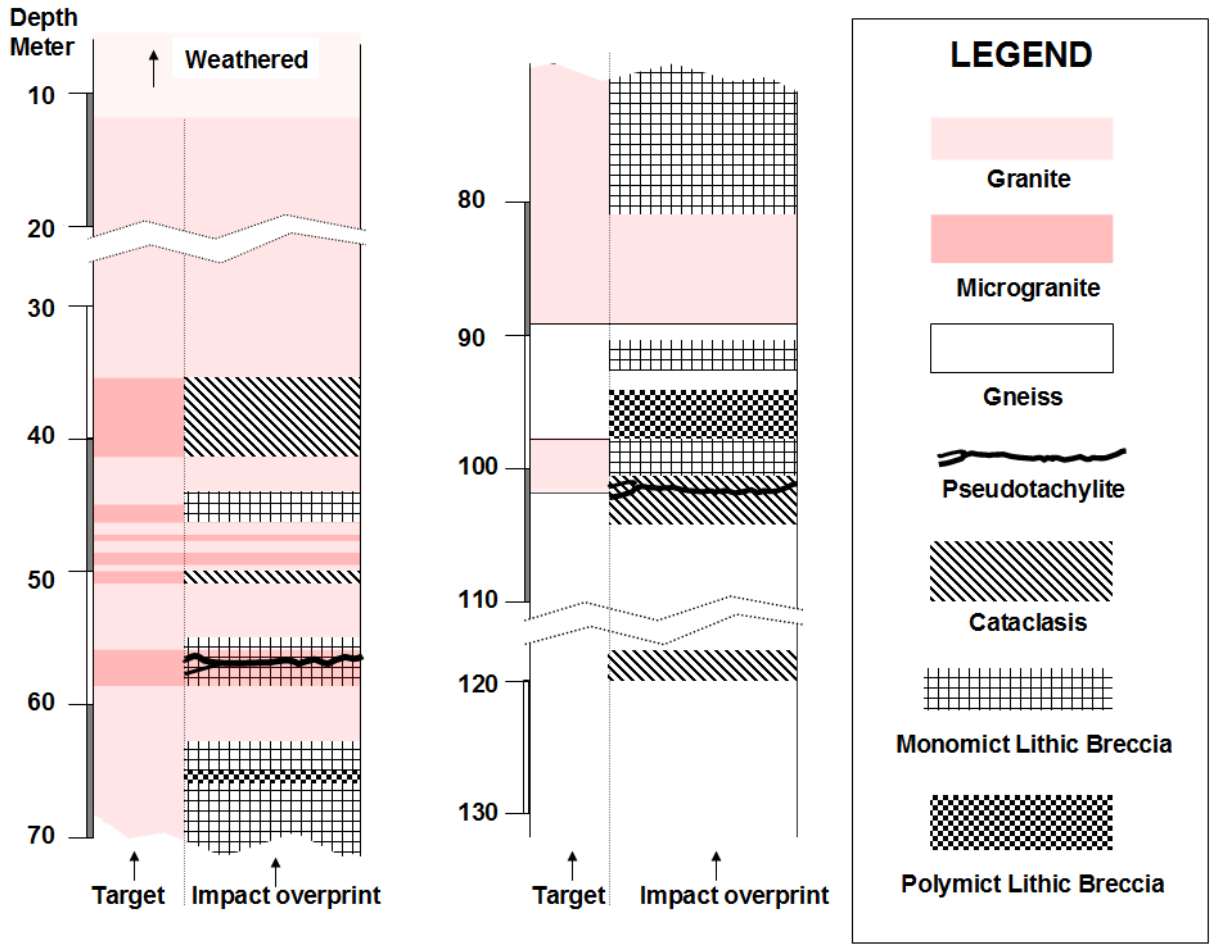

Figure 19: Schematic log of the 45° inclined- 5 cm diameter drill core from Cheronnac 10 km south of the center of the structure (see location on Figure 2B). Target lithologies are represented with the impact overprint indicated on the right side (20-30 m and 110-120 m intervals interrupted for graphic purposes).

Eight monomict lithic breccia dikes were intersected by drilling at Cheronnac (Figure 19). The largest dike is 13 m thick and developed in granite. The deepest dike is 2.3 m thick and occurs in gneiss at ca. 120 m (Figure 19).

Breccia dikes similar to those encountered in the Rochechouart bedrocks are known from direct exposures and from drilling below the crater floor at many other terrestrial impact structures.

The various breccia intercalations found in the inclined drilling at Cheronnac compare to those encountered in the basement of the Ries crater below the suevite deposit, as exposed by the Nördlingen 1973 deep drilling (Engelhardt and Graup, 1977; Stöffler et al., 1977).

The Nördlingen 1973 deep drilling record shows that up to c.a. 8 m wide polymict lithic breccia dikes below the suevite deposit are constrained to the upper section (the first 100 m) below the floor of the crater (Engelhardt and Graup, 1977). The emplacement of these dikes is related to the movement of large blocks of basement rock mobilized during crater floor readjustment (Stöffler et al., 1977). The thick polymict breccia dikes cut by the inclined Cheronnac drilling down compare in both position and texture to those at Ries and their origin is interpreted in a similar way. The Cheronnac breccia dikes delimit large blocks of basement rock mobilized during crater floor readjustment and landmark the upper section of the bedrock just below the crater floor level.

Ries and Rochechouart structures being comparable in size, it is deduced from the position of the 4.3 m thick polymict lithic breccia dike found at 70 m below the surface at Cheronnac (positioned at 93-98 m on the inclined drilling: see Figure 8) that the level of the crater floor is less than a few ten's of meters above the present ground surface at this particular site (10 km away from the center). As the crater deposits is dipping 0.6 ° N and the presumed elevation of the floor at Cheronnac is at the same level as observed in the field at Montoume located 2 km north of Cheronnac (see Figures 9 and 11) once the whole structure is tilted back to a horizontal position.

The cross-section through the upper section of the crater floor at Champagnac active quarry is currently (and temporarily) displaying a double set of low-angle over thrust faults marking the limit of two highly fractured locally brecciated gneiss megablocks overlapping each other and overlapping a non brecciated diorite (see further detail at stop 19 in part 2).

ALLOCHTHONOUS IMPACTITES

Allochthonous rocks in the Rochechouart area are polymict breccias that display variable degrees of alteration. All display definite evidence of shock metamorphic effects. Together, these breccias appear to have once represented a single, continuous, horizontal stratigraphic unit over the entire extent of the 15 km diameter inner zone of the structure. However, the present topographic effects have imparted a patchy character (Figure 9), with the current remnants of the impact deposits being exposed in the topographic "highs" of the area.

The highest local high of the Rochechouart area is 323 m in elevation, at the position of the Montoume impact melt body at the southern edge of the 15 km diameter inner zone (Figures 9 and 11).

The thickest occurrence of what remains of the initial impact deposits is generally less than 70 m thick. It forms a ca 14 km^2 patch at Chassenon (Figures 9, 11). The deposits are better preserved in the western and southern parts of the structure than in the eastern and northern parts (Figure 9). In the north, the deposits have been strongly eroded by the west-flowing Vienne River (Figures 9, 11) resulting in low topography (150 m elevation).

The Rochechouart structure displays the three classical lithologies of impact deposits encountered at terrestrial impact structures, namely polymict lithic breccia, suevite, and impact melt rocks. In addition, however, a distinct, fine-grained material is found, which is characterized here separately from the other impact breccia types.

Rochechouart allochthonous impact breccia deposits.

The largest clasts observed in polymict lithic breccia, suevite, and impact melt rock are a few decimeters in size and nowhere do they exceed one meter. The overwhelming proportion of clasts is less than 10 centimeter in size, and a large proportion is of centimeter size, or smaller. No sorting or preferred orientation of clasts is observed in any of these impactites.

So far, only fragments of the same metamorphic and plutonic rocks that are currently exposed in the Rochechouart basement have been found in the impactites. This includes diorite and amphibolite in the northernmost part of the impact area, however, no clasts of serpentinite have been observed. With the exception of a single carbonate clast recently reported in a thin section of lithic impact breccia (Sapers et al., 2009), no other sedimentary rock fragments have been found.

The level of shock metamorphism recorded by clasts in these breccias is highly variable and covers the full range of shock metamorphic effects known for granitic material (see classification of Stöffler, 1971 and Stöffler and Grieve, 2007), with the exception, so far, of high-pressure polymorphs of quartz which have not been observed despite an extensive search (Lambert, 1977a).

Shock damage ranges from brittle deformation (fracture), plastic deformation (deformation bands and kinks), phase transition (planar deformation features related to plastic deformation of the low pressure phase), to phase change (partial meltíng, decomposition, recrystallization). More details on shock metamorphism at Rochechouart have been given in Kraut and French (1971), Lambert (1977a-b), Ferrière and Koeberl (2007), and Trepmann (2008).

Despite the abovementioned variability of shock levels of clasts for all types of Rochechouart impactite, statistical measurement of shock degrees in individual clasts shows that, on average, the shock recorded by lithic clasts in impact melt rock is higher than that in clasts in the suevite, which is in turn higher than that in clasts in polymict lithic breccia (Lambert, 1977a).

All Rochechouart allochthonous impact breccias display evidence of post-impact alteration. Melts and glasses are devitrified, recrystallized, chloritized and/or sericitized (Kraut and French, 1971; Lambert, 1974; 1977a-b; Reimold et al., 1987; Sapers et al., 2009) (Figures 20-21).

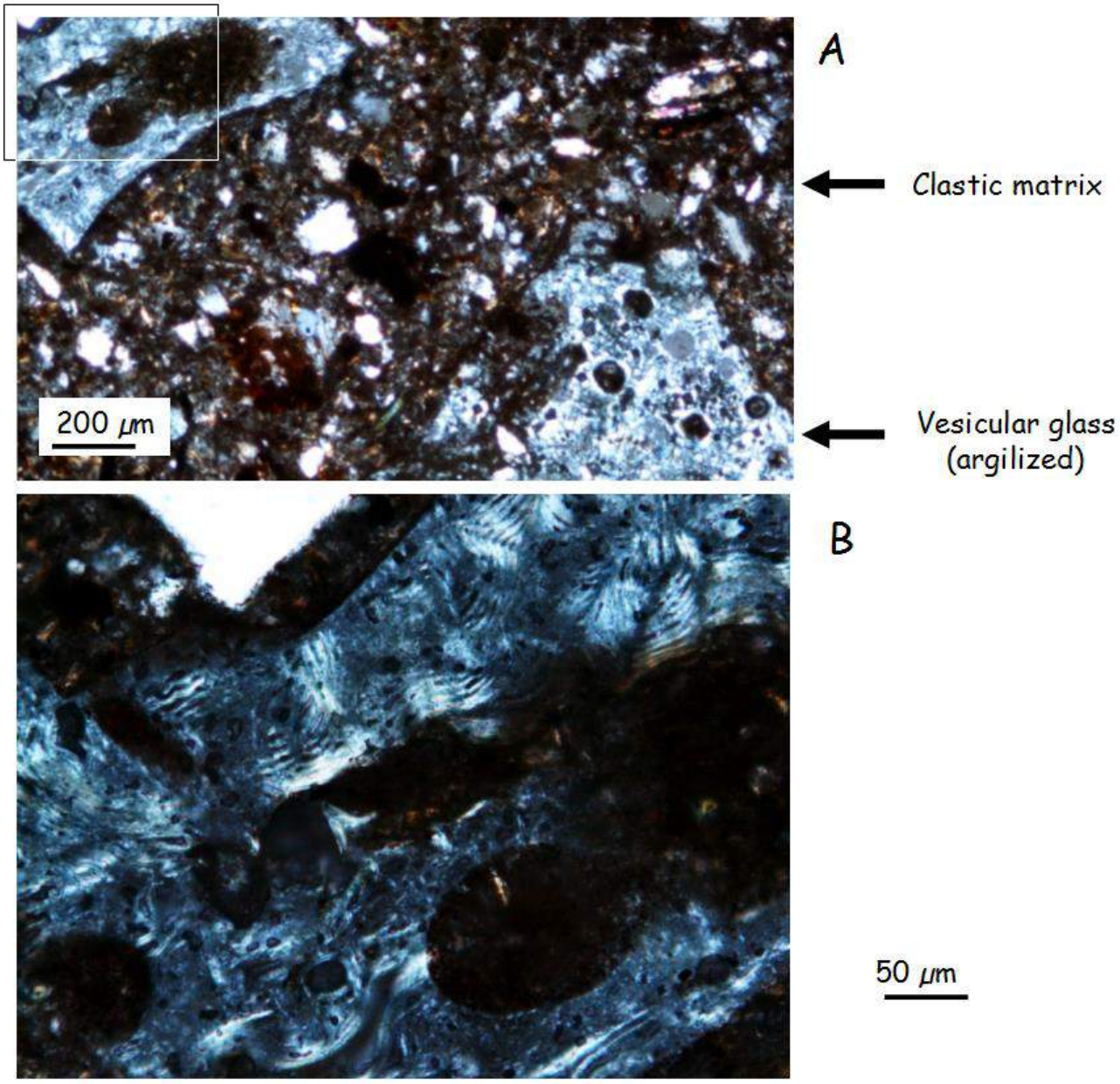

Figure 20: Petrographic details seen by optical microscope in plane polarized light of a double-polished thin section of a sample of the Chassenon suevite. Clastic matrix and vesicular glass clast (arigilised).

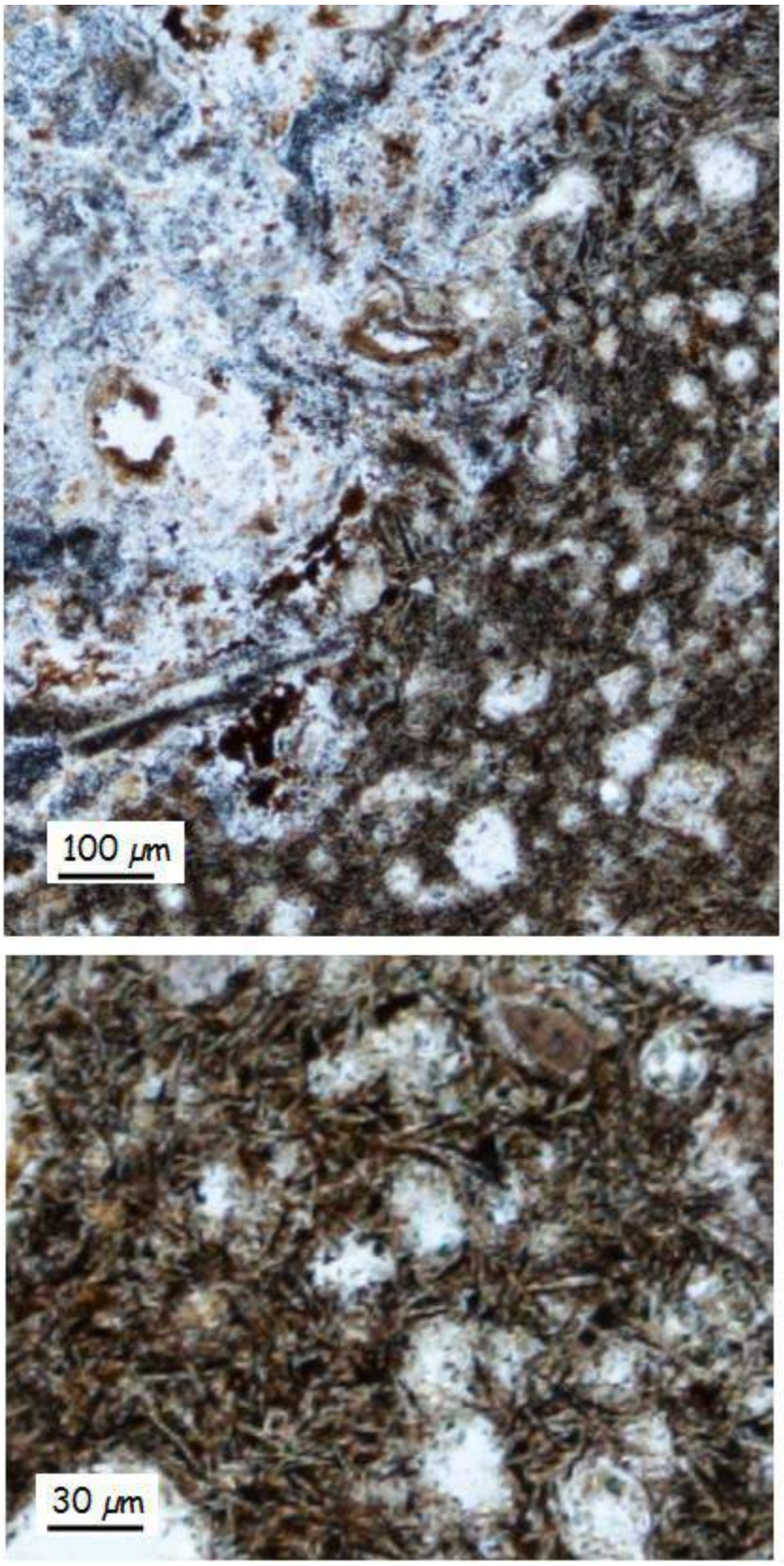

Figure 21: Optical microscope view in plane polarized light of a thin section of a clast-poor, vesicular impact melt rock from Babaudus. Boundary between the vesicular melt matrix (entirely recrystallised: detail in B) and a vesicle-free melt clast (also entirely recrystallised) of quartzofeldspathic composition.

More generally there there is no (or only trace) of glass left as glass in any of the melt bearing impactites at Rochechouart. All tectosilicates shocked to stage 1b and higher in the lithic clasts of all the Rochechouart allochthonous impact breccias are altered and/or recrystallized (Lambert, 1977a). PDFs in quartz and feldspars are systematically decorated by fluid inclusions (Lambert, 1977 a).

Figure 22: Optical microscope view in plane polarized light of a thin section of polymict lithic breccia near Rochechouart. Quartz with PDFdecorated by fluid inclusions

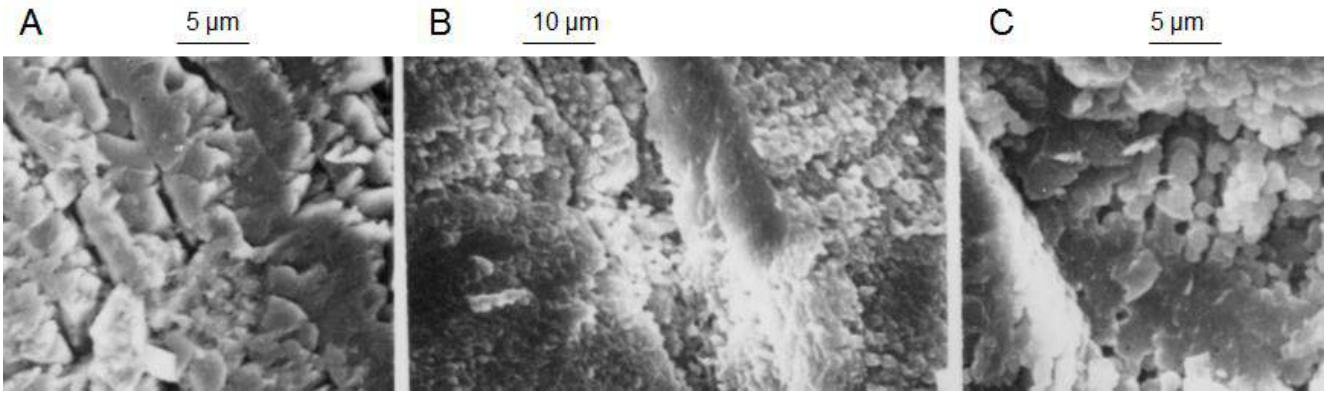

Figure 23: SEM view of quartz with PDF in A: shocked gneiss near Le Bouchet near the center of the structure. B-C: Lithic clasts in polymict lithic breccia from the same locality as A. Note the micro-cristaline character of the quartz. All the crystallites are sharing the same orientation and the quartz grain appears monocristaline under the optical microscope.

Feldspars in the highly shocked lithic clasts are largely replaced by argillic assemblages. These argillic assemblages are also developed in the clastic matrix of the polymict lithic breccias and the suevite. The size of these phases and their intricate relationship with the fine debris in the matrix make mineral identification difficult and sometimes hampers the identification of impactite type.

The following review of the specific features of the various types of Rochechouart allochthonous impact breccias deposit distinguishes between polymict lithic impact breccias, suevite, and impact melt rocks according to the nomenclature proposed by Stöffler and Grieve (2007).

Polymict Lithic Impact Breccias

Polymict lithic breccia is by far the most abundant impactite unit preserved in the Rochechouart structure. It covers ca 41 km^2 and is found near the center of the structure between Babaudus and Valette and up ca 7 km away near La Chassagne and Videix (Figure 9). Polymict lithic breccia typically occurs directly above the target bedrock. The maximum thickness of the currently exposed unit is ca 40 m, recorded in Rochechouart town and measures (Figure 9). Based on the lateral extension and thickness of the polymic lithic breccias at the various locations as observed in the field, the total volume of polymict lithic breccia remaining in the Rochechouart crater is calculated at about 1 km^3 (Table 4).

EXPOSED TODAY	Area km^2	Thickness (m)		Vol. km^3	Melt	
		Average	Max		Fraction	Vol. km^3
Polymict lithic breccias	40.9	26	40	1.1	0%	0
Suevite	4.9	15	20	0.07	1-38%	0.01
Impact melt rocks	1.9	7	20	0.01	50-95%	0.01

Table 4: Field based estimates of the area, thickness and volume for the main impactite deposits in the Rochechouart crater as exposed today.

Despite its clearly polymict character, there is evidence for a relatively local origin for the clasts in the polymict lithic breccia. Clasts are characterized by angular to sub-rounded shapes and are embedded in a fine-grained clastic matrix. Morphometric measurements by image analysis on thin sections indicate that 30 % of the clasts are 5 mm and larger, and 50 % are > 1 mm (Table 3).

Locally, slight apparent stratification is observed in the polymict lithic breccia unit, for example in the cliff below Rochechouart castle. The faint bedding extends parallel to the exposed crater floor, which here dips 20-30° to the south (Figure 24).

As seen in Figure 25, geochemical analysis for the Rochechouart and Chassenon polymict lithic breccia gives elongated data fields that only partially overlap. The Chassenon polymict lithic breccia is more mafic than the “average” target and plots into the area of the gneiss field (Figure 25). The Rochechouart polymict lithic breccia is centered on the “average target” and extends over the lower portion of the gneiss field and the upper portion of the granite field. As seen in Figure 4B, the long axis of the Fe-Mg field for both the Chassenon and Rochechouart polymict lithic breccias is parallel to that of the target (granite+gneiss) but it is slightly shifted towards higher Fe.

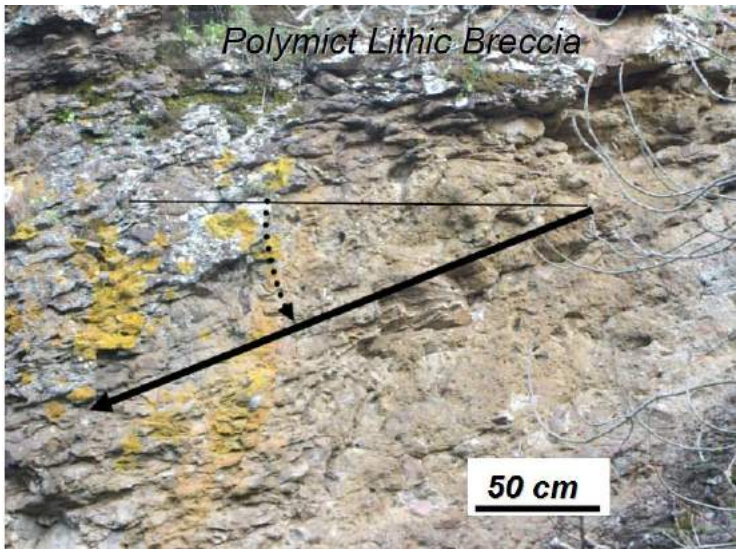

Figure 24: Field view of polymict lithic breccia at Rochechouart. Faint apparent inclined stratification

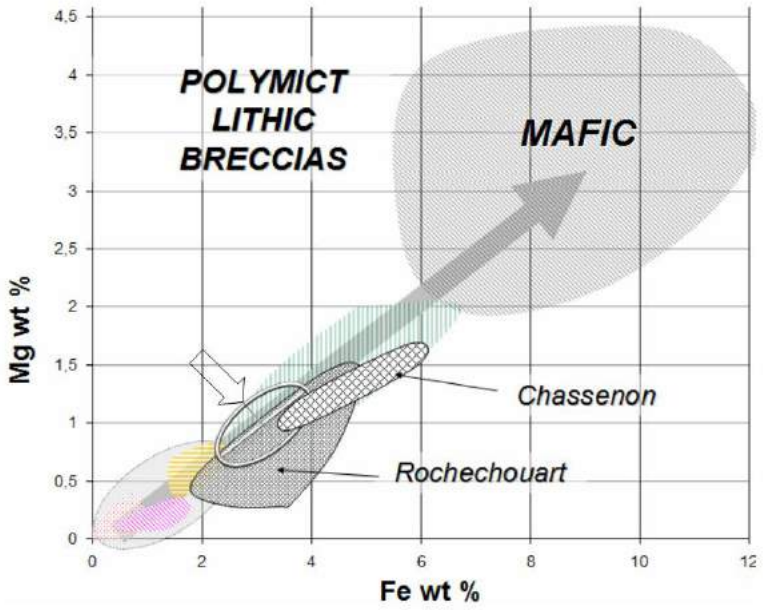

Figure 25: Fe-Mg plots for the main polymict lithic breccias exposed in the Rochechouart structure, near Rochechouart and near Chassenon respectively. Background: plots of the granite (lower left) and gneiss (Figure 6B). Ellipsoid (open arrow):"average" target composition field mixes the composition of the various basement rocks according to their relative proportion of exposure in the Rochechouart area (ca 50% granite + leptynite and 50% gneiss).

Suevites

The material termed suevite in the Rochechouart structure is granulometrically and texturally very similar to the polymict lithic impact breccia. The only difference is the occurrence of melt (altered and/or crystallized) fragments in the suevites. Melt is observed both in the matrix and in the clast fractions of suevite (Figure 26). Quantitative analysis of the melted fraction in suevite by combined macroscopic and microscopic image analysis on polished sections (Lambert 1977a) indicates that the majority of

melt occurs as particles >5 mm in size, especially where the overall proportion of melt is high (> 15 vol%). The total amount of melt in the suevite is highly variable, from 0.1 to 38 vol%. On average, it is 12 vol% or less (Lambert 1977a).

The maximum thickness of the suevite is ca 20 m as deduced from field data at Chassenon. The area of exposure of suevite comprises approximately 4.9 km^2, 12% of that of the polymict lithic breccia. According to lateral extent and thickness of the patches, the total volume of suevite left in the structure is estimated at ca. 0.07 km^3 (Table 4), or about 5% of that of the polymict lithic breccia.

From estimates of the melt fraction at the various suevite localities from Lambert (1977a) and the volumetric estimates for the various suevites, the total volume of melt in the suevite actually exposed in the Rochechouart structure is estimated at about 0.01 km^3 (Table 4).

Two main types of suevites are reported, which are distinct in setting and texture, namely, the upper suevite forming the largest suevite unit and corresponding to the usual definition of suevite and the bottom melt-rich suevites.

Upper Suevite (or suevite sensu stricto): This suevite occurs directly overlying polymict lithic breccia. It forms small isolated patches close to the periphery of the impactite deposits in the southwestern part of the structure (Figure 9); however, it is absent from the center of the structure. As in the case of polymict lithic breccia, a faint ondulose to sub planar stratification is observed locally in the suevite (Figures 9-10).

The largest and most famous suevite occurrence is in the Chassenon area. It forms a continuous horizontal sheet up to 20-30 m thick, 2 km long, and 1.2 km wide (Figures 9 and 11). It accounts for 90 % of the total volume of suevite left in the crater structure.

The Chassenon suevite is deposited on top of 30-40 m of polymict lithic breccia (Figure 11) as deduced from stratigraphy accessible in the field and confirmed by shallow seismic profiling done in the context of ongoing archaeological investigation of the Chassenon site (Bobee et al., 2005).

Referred to for over 15 decades as volcanic material in the French geological literature (Manes, 1833; Kraut, 1935), the Chassenon suevite was actively quarried for building purposes up to the early 20th century (Figures 27-28). It was used extensively from the 1st to 4th centuries for Roman constructions, including baths, a temple, an arena, and villas at "Cassinomagnus," which was more important in Roman times than today's village of Chassenon.

The Chassenon suevite has been instrumental in the recognition of the Rochechouart impact structure, after delegates of the international scientific community were taken by F. Kraut in the late 1960s to the remnant of the last active quarry in Chassenon village. This quarry and its unique, finely stratified deposit have unfortunately disappeared in the 1980s after local municipalities used the quarry for landfill purposes and then covered it.

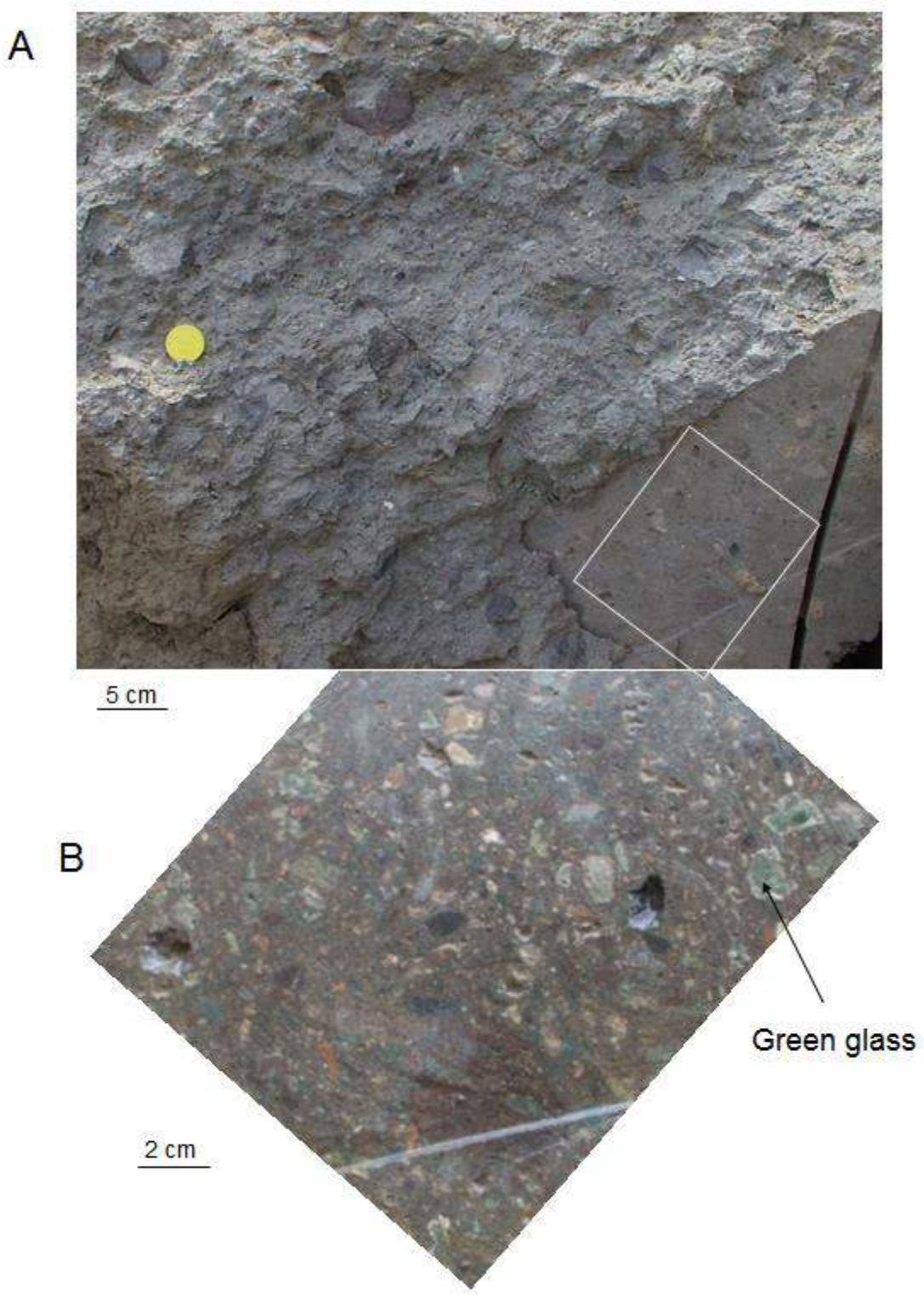

Figure 26: Field view of the upper suevite (suevite sensu stricto) at "Grosse Piece" quarry near Chassenon.

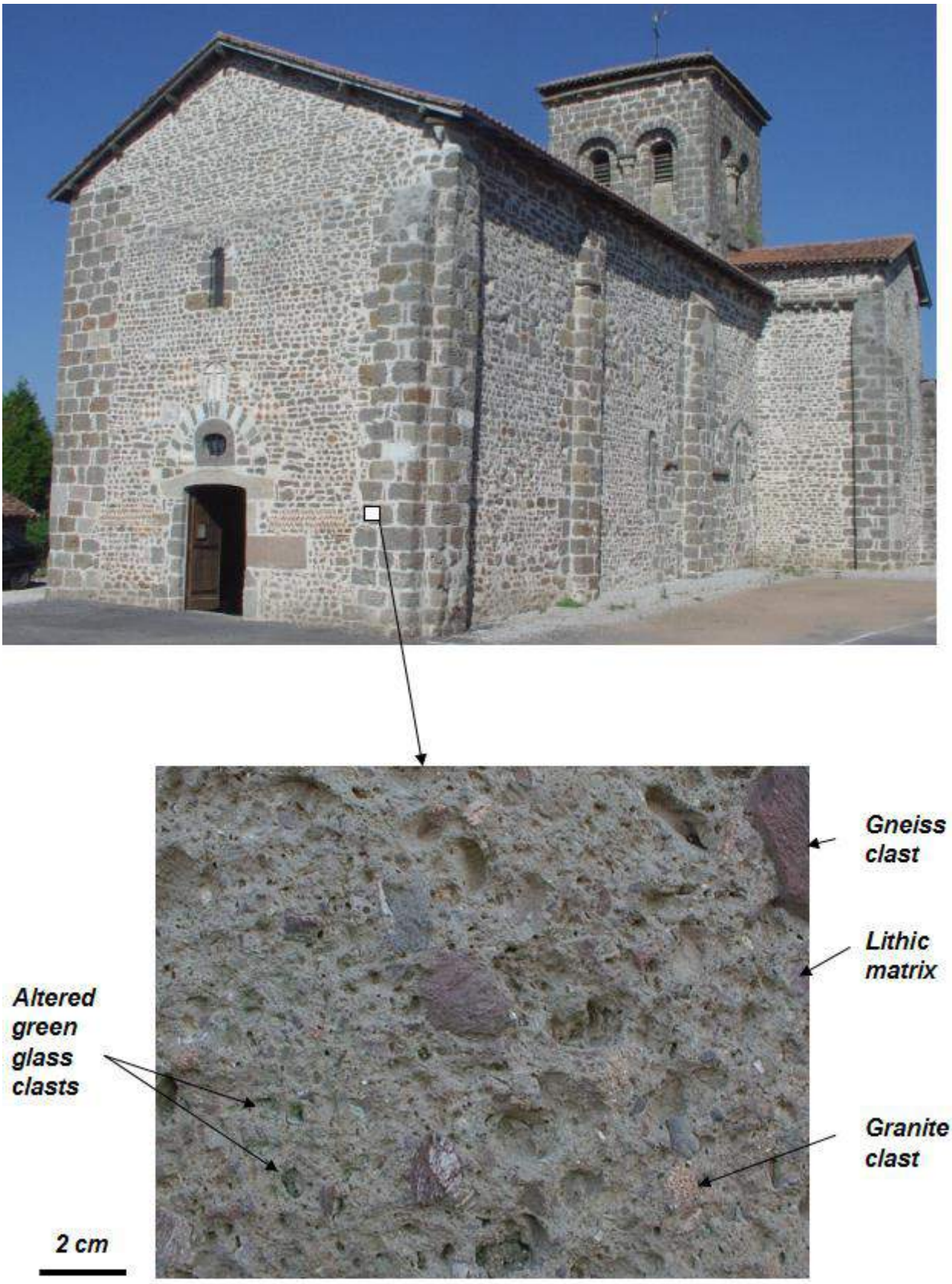

Figure 27: Chassenon Roman church builted in suevite (suevite sensu stricto) and close up view of the wall

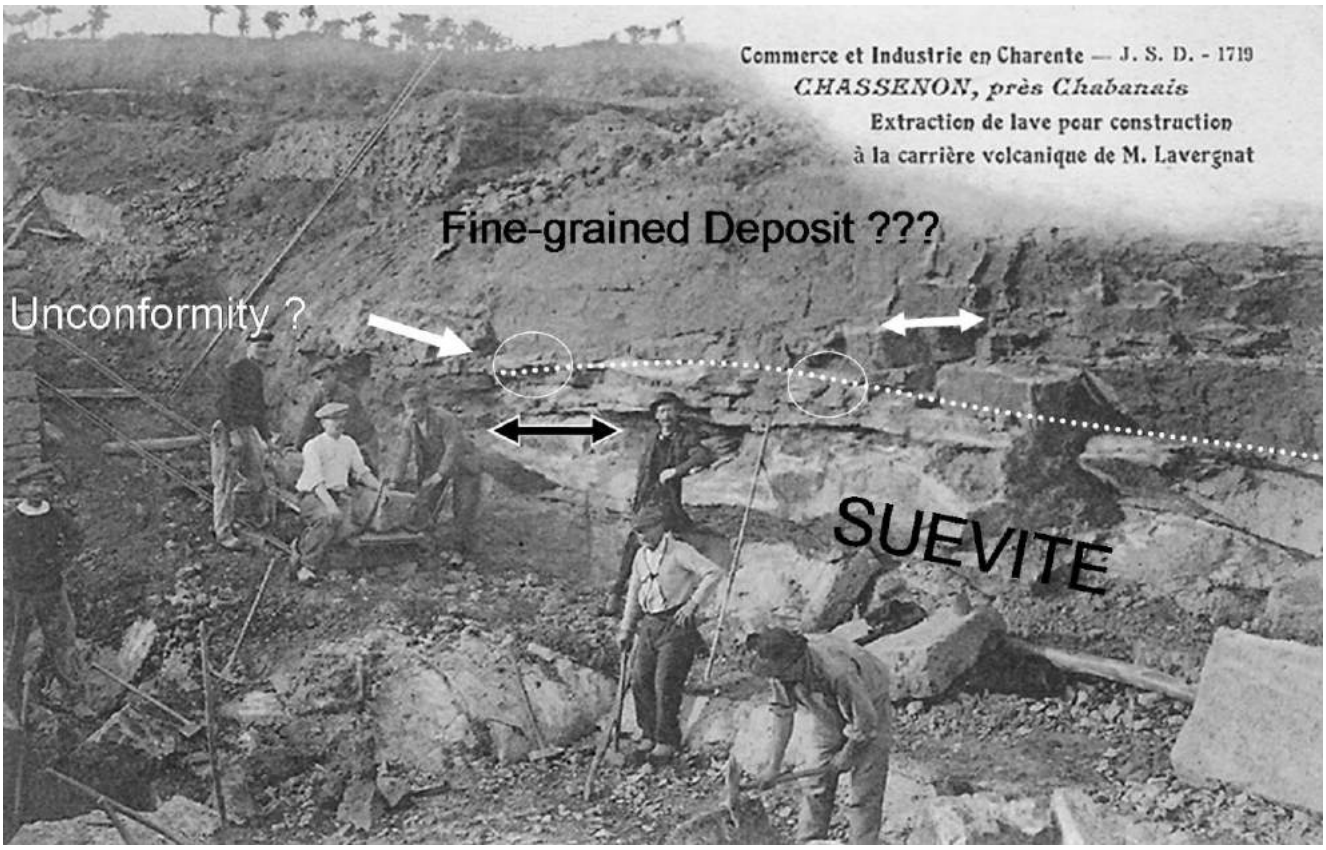

Figure 28: Top of the suevite at the « Volcanic » quarry of Chassenon as seen on a postcard dated to the early 1900's (also known as Carrière des Arènes). The quarry's exploitation for construction material ended in the 1930's and the remnant of the quarry finally disappeared in the early 1980's after having been filled in. The top deposit seen on the picture appears massive. It displays a slightly curved stratification (white double arrow) resembling cross-bedding that seems to intersect the underlying suevite at low angle (unconformity ?: dotted line). This top unit is supposed to correspond to the impactoclastic deposit which was sampled at the remnant of this quarry in the early 1970's (see text). The underlying suevite displays a faint stratification roughly parallel to the horizontal (black double arrow).

Smaller outcrops of the same suevite deposit are still exposed along road cuts and at various remnants of Roman quarries in the nearby woods. The typical Chassenon suevite is a polymict breccia with angular to subrounded clasts typically of mm to cm size (Figures 26-27). Clasts are formed by target rock fragments and glass (altered glass) particles, including highly vesicular debris resulting from partial shock melting of lithic material. Shape and size of glass particles essentially compare to that of lithic clasts. Contorted, twisted shapes are rare among the Chassenon glass particles (Figure 26).

The suevites in the Chassenon area are characterized by a uniform texture and color (gray-green). They also display a narrow field of compositional variations compared to the other impactites as seen on the Fe-Mg diagram (Figure 29). Chassenon suevites plot close to the "average" target and generally match the composition of the local gneiss (comparing Figures 6B and 29).

Melt-rich suevite (melt-poor impact breccias): These breccias are characterized by highly variable colors and textures. They are only found directly overlying the bedrock. They are observed in the vicinity of impact melt rocks. They bear a clastic matrix, which incorporates a relatively large proportion (20-50 vol%) of melt clasts (example at Figure 30).

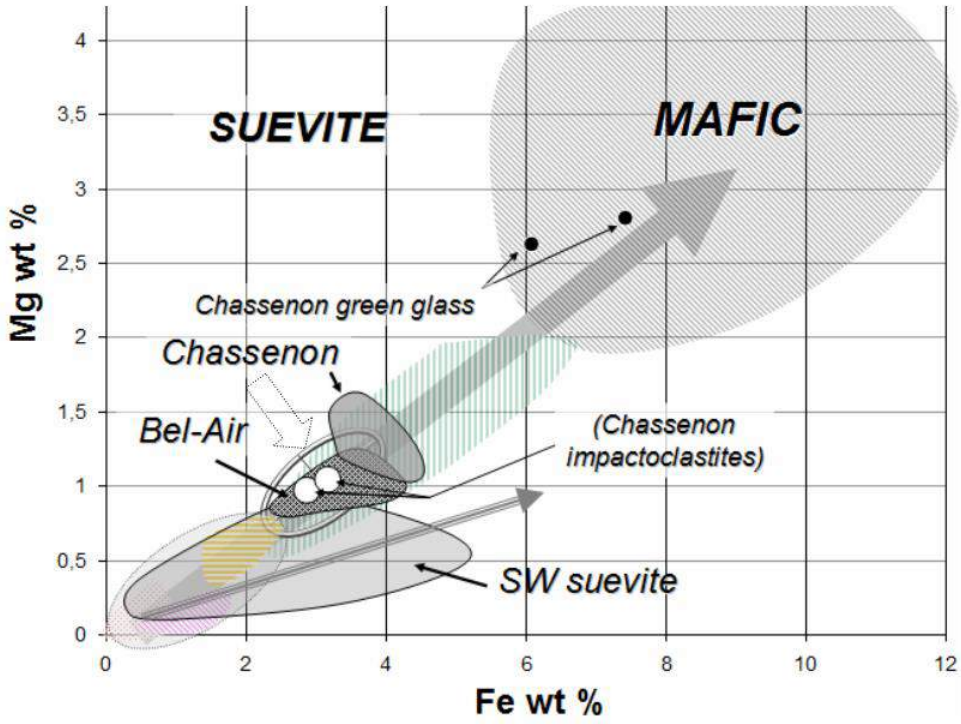

Figure 29: Fe-Mg plots for the suevites. Background: plots of the granite (lower left) and gneiss (Figure 6B). Ellipsoïd (open arrow):"average" target composition field mixes the composition of the various basement rocks according to their relative proportion of exposure in the Rochechouart area (ca 50% granite + leptynite and 50% gneiss).

Unlike melts in the Chassenon suevite which usually displays a homogeneous texture (glass (altered) + vesicles), melt bearing clasts in the melt rich suevite are characterized by a complex and heterogeneous texture where lithic debris clasts and/or clast of partially melted lithic debris are incorporated in the melt (Figures 30-31).

This material is not observed around the center of the structure, only from a distance of 2-3 km from the center. A small patch occurs in the Bel-Air area, here it is characterized by a yellow color. Most melt-rich suevites are observed in the south-southwest part of the impact deposit (between Valette-Montoume-Videix), where the breccias are predominantly pink, maroon, and red. These melt-rich suevites plots separately on the Fe-Mg diagram (Figure 29), and their Fe-Mg content is also distinct from that of the Chassenon suevite.

The southwestern melt-rich suevites show the broadest variations, the compositions of which spread over the granitic field, whereas the Bel-Air melt-rich suevite plots at higher Fe-Mg values in the lower part of the gneiss field (Figure 29). The southwestern melt rich suevites crop out in a region of the target where granites are dominant (Figures 4 and 9), whereas the Bel-Air suevites overlie gneisses.

The Fe-Mg plot for the southwestern suevite compositions matches that of the impact melts occurring in the same region (from Valette to Montoume: see Figure 40 next section). As seen in Figure 29, the long axis of the Fe-Mg correlation field for the southwestern suevites is not parallel to that of the target (granite+gneiss). It is shifted towards higher Fe, as observed also for Babaudus, the Montoume and the Valette impact melt rocks (see Figure 40 next section).

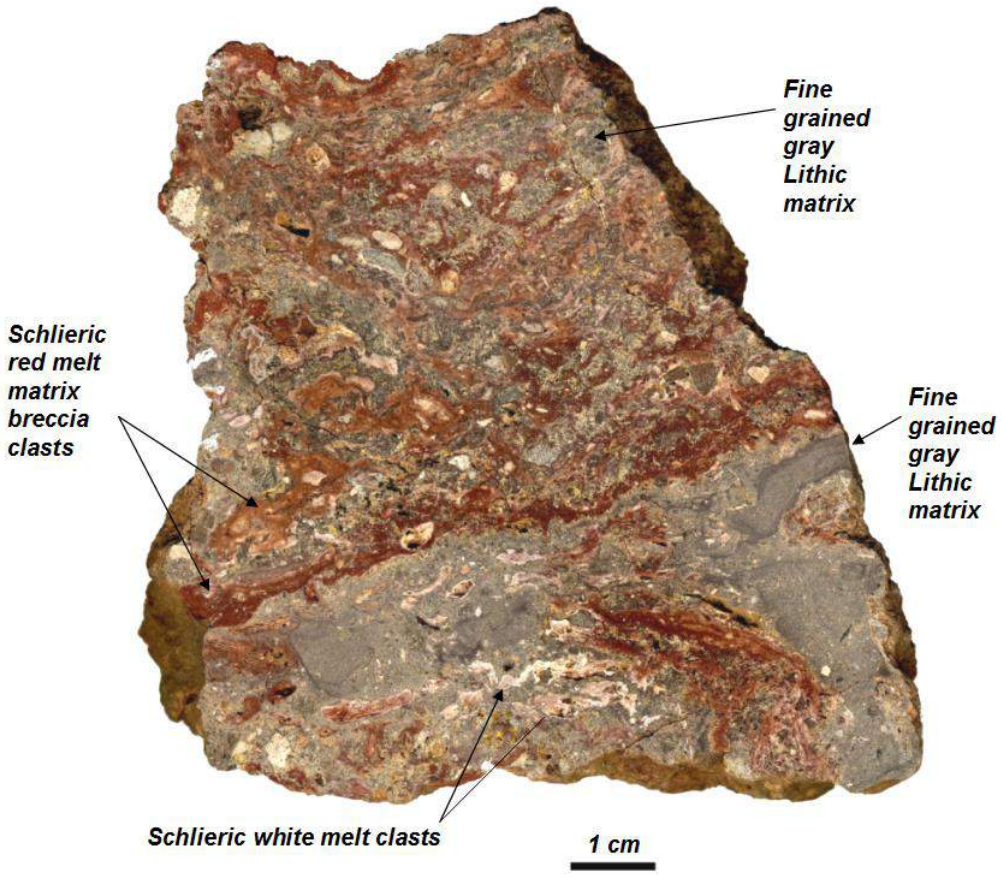

Figure 30: Melt rich basal suevite near Valette 2 km SW of the center of the structure (photo courtesy of Martin Schmieder).

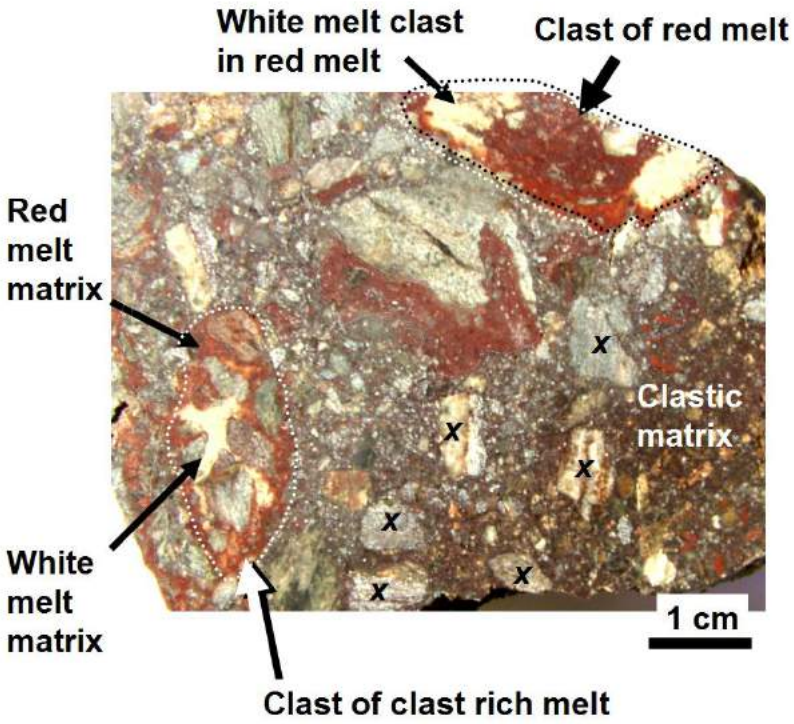

Figure 31: Cross-sections of a basal suevite occurring at the immediate contact with bedrock and outcropping at the edge of the Valette impact melt sheet 2.5 km SW of the center of the structure. Lithic clasts are essentially all derived from the same gneiss (« x »: gneissic fabrics clearly preserved and sharp edges of lithic clasts). Note large rounded « clasts » of red melt matrix breccia including- either as clasts or as matrix- a white melt matrix material. Note the diffuse contour between the two melts.

The variability of textures and the compositional differences observed in the Rochechouart suevite, together with their specific settings, suggest different origin. The upper suevite layer, forming most of the suevite at Rochechouart and lying on top of the polymict lithic breccia, is apparently distinct from the melt rich suevite observed at the contact with the basement. The latter is clearly tied to the presence of impact melt rocks. The narrow field of Fe-Mg composition for the upper suevite (Chassenon suevite) (Figure 29) seems to indicate greater homogenization of the upper suevite relative to the basal suevites and impact melts rocks, which are much more varied in composition. This may also reflects the relative importance of "slow and late" conduction melting mechanisms (as opposed to rapid and early shock melting) of more or less shocked but unmelted clast introduced and mixed in a hot environment. This mechanism requires the proximity a significant heat source i.e. the proximity of an impact melt body as observed in the field. This mechanism probably accounts for a significant part of the melt observed in the melt rich basal suevite.

The relative abundance of homogenized glass and the relative lack of heterogeneous melts in the top suevite compared to the basal suevite may not only reflect their variation from different shock regimes in the crater but also different post-depositional metamorphic processes mechanism. The top suevite is interpreted as the product of thorough dispersion and mixing of melt and cold lithic debris during ejection and fall back, resulting in a rapid cooling of the melts to glass and preventing late thermal melting of lithic clasts in contact and or in the vicinity of the impact melt sheet. The basal suevite on the other hand is the result of heterogeneous and local mixing conditions between the impact melt and ground-surge deposits at the contact with bedrock near the center of the structure. The relatively high shock level recorded on average by the lithic clasts originating at the bottom of the crater in the center of the crater, plus the heat provided by the overlying melt sheet would have aided further partial melting and incomplete assimilation of melted lithic clasts in the basal suevite.

Impact melt rocks

The currently exposed Rochechouart impact melt rocks are all in direct contact with bedrock. They display a large variety of textures related to the nature, proportion, orientation and granulometry of clasts that may even vary at the hand specimen scale (Figures 32-33). These rocks are characterized by a matrix made entirely of melt which is recrystallised (see detail at Figure 33).

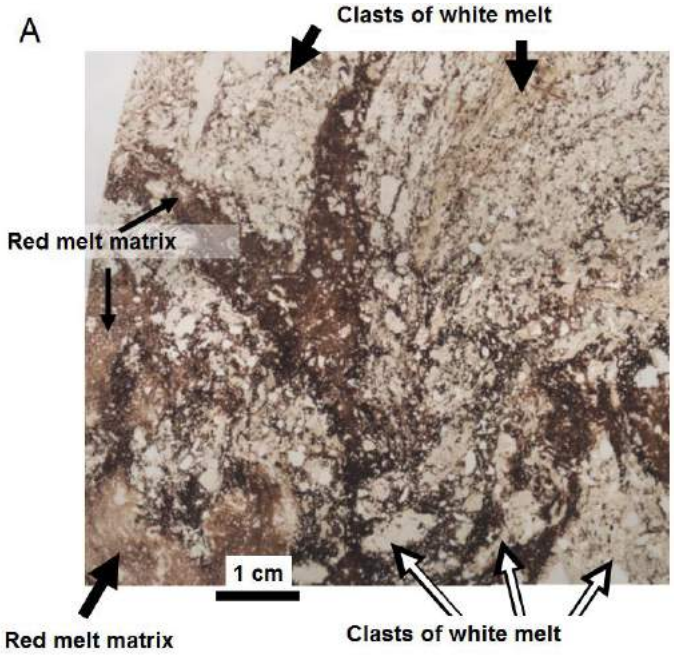

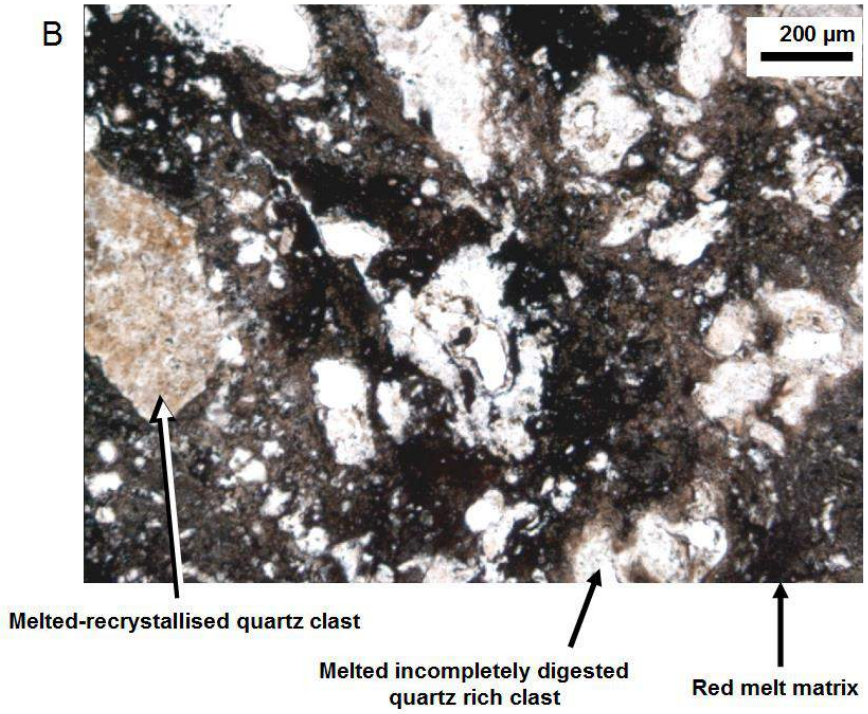

Figure 32: A: Optical view of a thin section under plane polarized light of a massive and vesicle-free 99 vol % melt impact melt rock near Valette (2km SW of the center of the structure) with equal proportion of two different melts (both recrystallised) showing both contorted flow features. The white melt bears the remnant of the original lithic fabric (trace of the gneiss foliation) and reflects incomplete assimilation by the red melt. B: Close up view of A under plane polarized light.

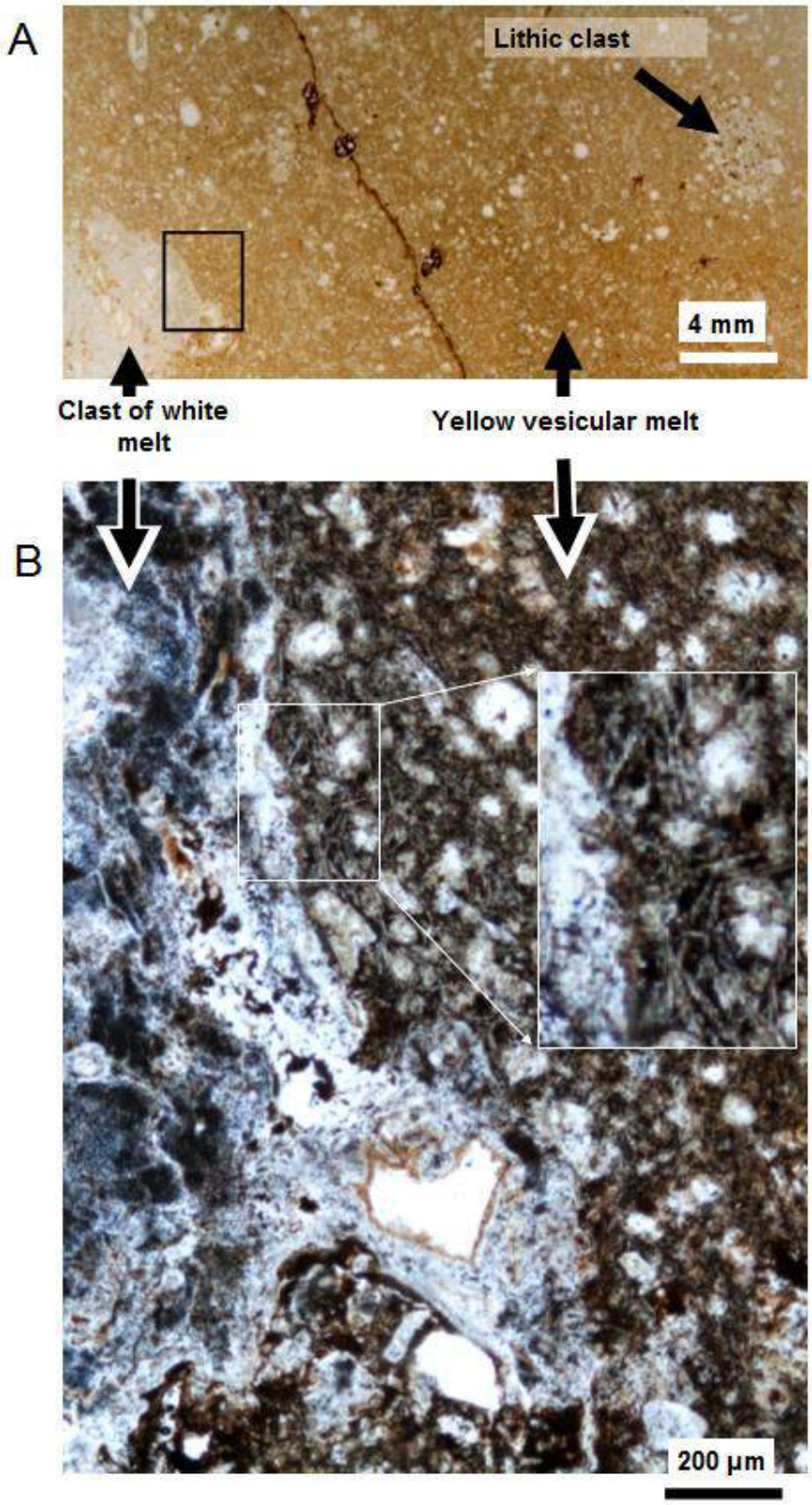

Figure 33: A: Optical microscope view in plane polarized light of a thin section of a clast-poor, vesicular impact melt rock from Babaudus (1.5 km from the center of the structure). (Black rectangle: field of the micrograph shown in B). B: Detail of the boundary between the vesicular melt matrix (entirely recrystallised) and a vesicle-free melt clast (also entirely recrystallised) of quartzofeldspathic composition. Enlarged block: detail showing the crystalline state of the melt matrix.

Quantitative analysis by combined macroscopic and microscopic image analysis on polished sections indicates a variable amount of melt ranging from 47 to 99 vol% (Lambert 1977a).

Proportions of melt over 90 vol% are rare. About 75% of the studied Rochechouart impact melt rocks contain more than 10 vol% lithic clasts. Clasts generally display fluidal textures indicative of plastic deformation – likely due to thermal softening. They show complex contacts with the matrix, indicating partial assimilation and digestion in the matrix (Figures 32-33).

Rochechouart impact melt rocks form small isolated patches mostly limited to the central 4 km diameter region of the structure. However, small patches of impact melt rocks have been reported up to 7.5 km from the center of the structure (Figure 9). Vesicular impact melt rocks are observed mainly in the central part of the structure at distances of 2-3 km from the center and less (Figure 34). Vesicles are commonly non-symmetrical. They are elongated horizontally at Babaudus and Fontceverane (Figure 35). The impact melt rocks occurring at distances of 4 km or more from the center of the structure do not contain vesicles.

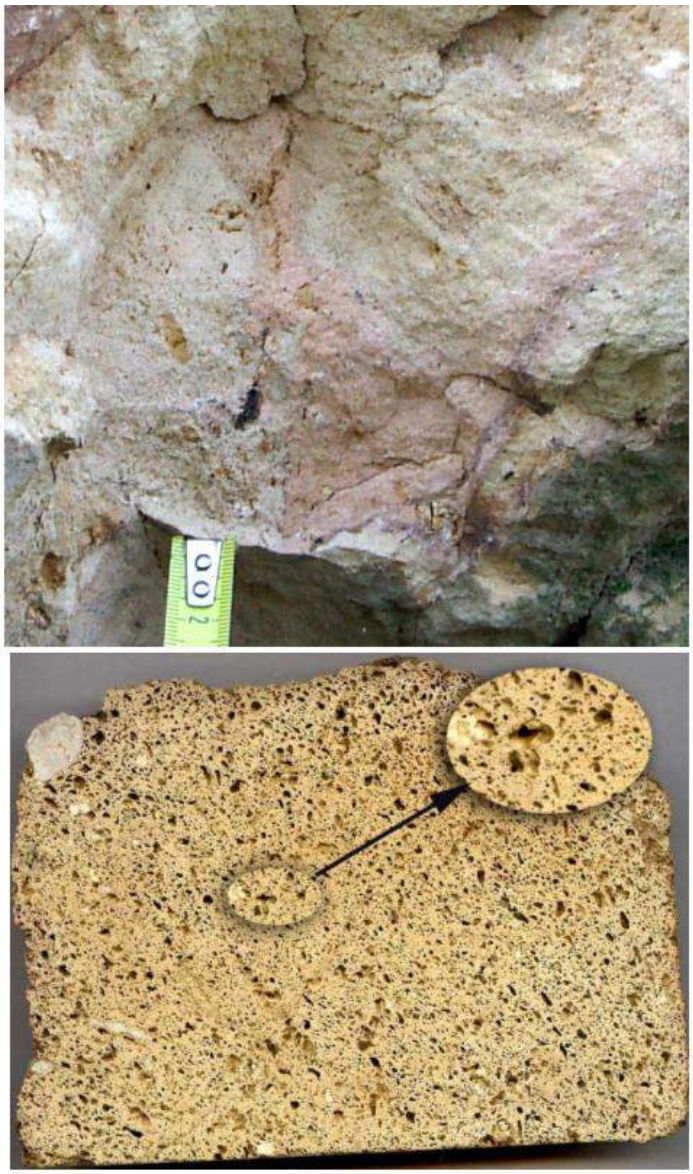

Figure 34: Impact melt rock at Babaudus (1.5 km SE of the center of the structure). Top: "fresh" cut. B: Same material but more weathered (stone from the wall of a farm at Babaudus). Very few lithic clasts. Small spherical vesicles enlarged by weathering (B).

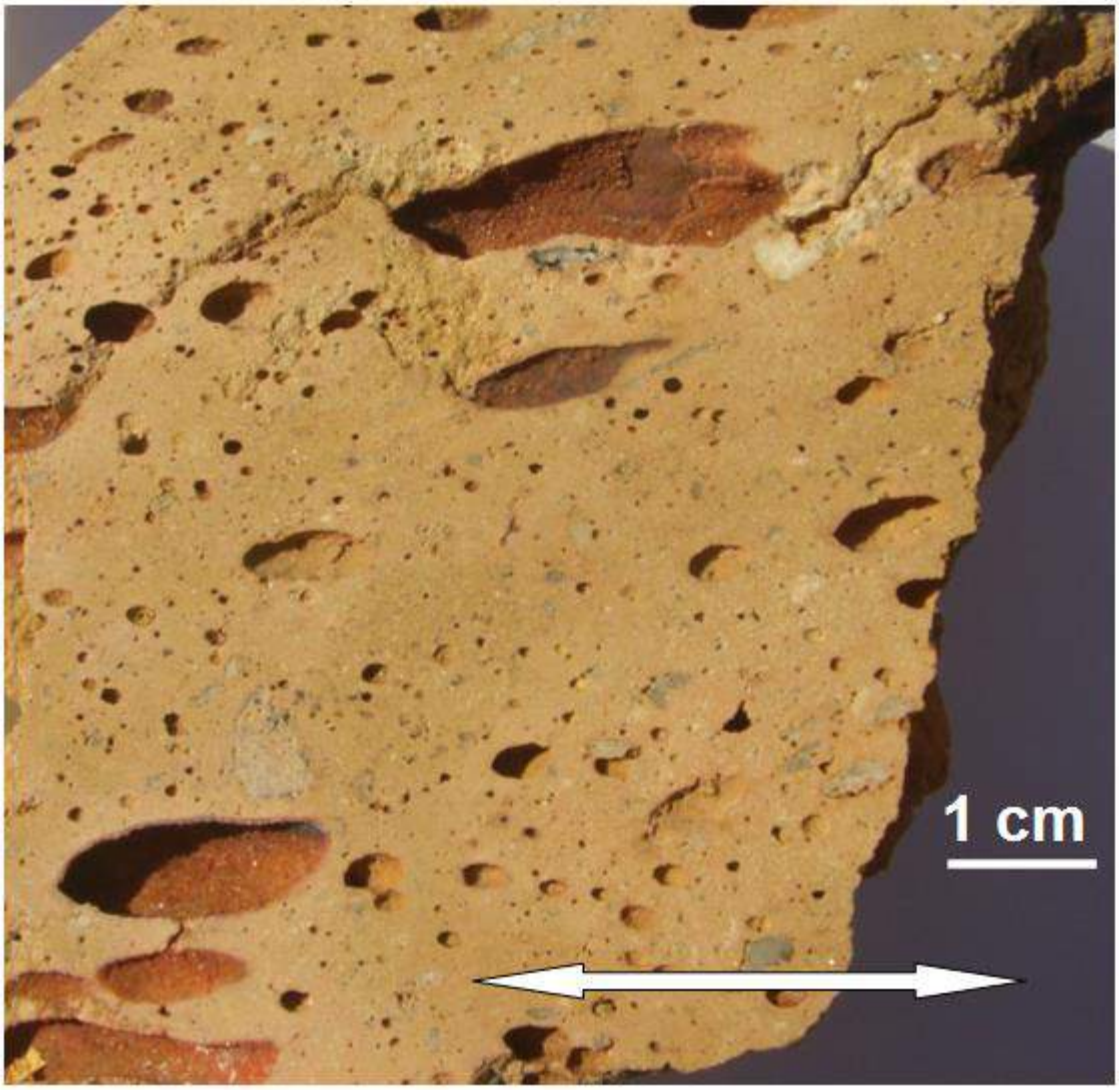

Figure 35: Saw-cut of an impact melt rock sampled near Fontceverane 2 km SW of the center of the structure. Double arrow: Trace of the horizontal plane at the sample locality. Note bubbles elongated in the horizontal plane indicating the melt was still in motion at the time of quenching. It also implies that the crater floor, observed immediately beneath the melt rocks at that particular locality, acquired the horizontal profile as observed today prior to quenching.

The largest exposure of impact melt rock currently known at Rochechouart is a 1.6 km long, 0.7 km wide vesicular body covering 0.3 km^2 between Valette and Fontceverane, ca. 2 km southwest of the center of the structure (Figure 9). It is only a few meters thick and its volume is about 0.007 km^3. Bearing 80 vol% of melt, on average, as measured in thin sections, this unit accounts for ca. 0.005 km^3 of melt representing about half of the total volume of melt residing in the impact melt rocks currently exposed at Rochechouart. The other occurrences form smaller bodies, such as that at Babaudus (Figure 9), which is a few hundred meters wide and one or two meters thick. The smallest bodies such as that near Bel-Air are only a few meters wide and meter thick (Figure 36).

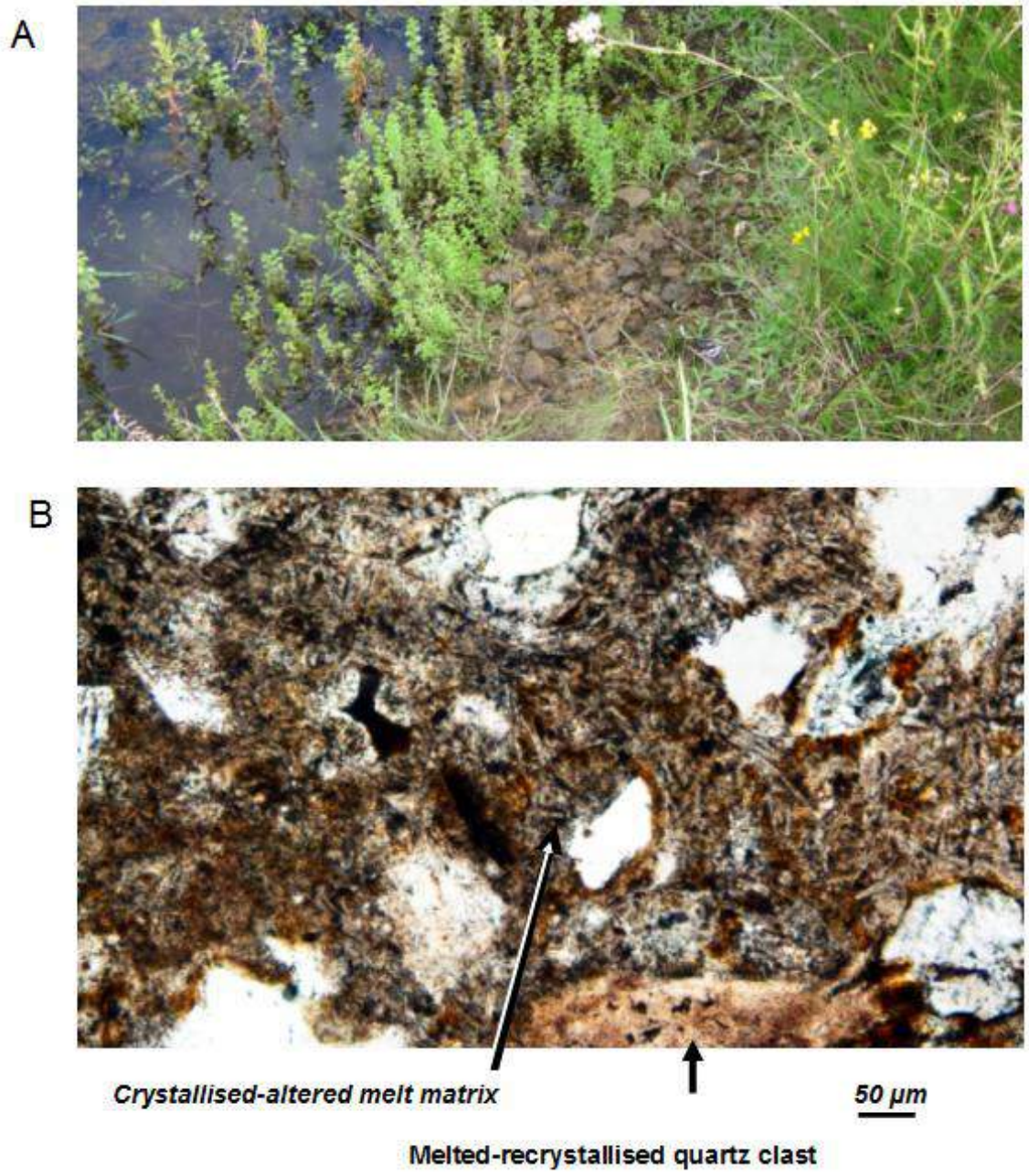

Figure 36: Impact melt rocks at Bel-Air located ca 5.5 km N-NE of the center of the structure. A: Field view ca 3 meters wide) showing the poor conditions of outcropping. B: View under the optical microscope in plane polarized light of a thin section of a typical Bel-Air sample.

The thickest body is also the most remote from the center of the structure (7.5 km). It forms a 900 m long and 600 m wide hill near Mountoume village at the southern edge of the impact deposit zone (Figure 9). The maximum thickness deduced from the intersection with topography is ca 25 m. The contact with underlying granitoid bedrock dips at 2° to the north (Figure 11). This unit was initially distinguished from suevite and from impact melt rocks and described as "Mountoume red welded breccia" (Kraut and French, 1971).

It appears as a suevite on the current 1:50 000 geologic map (Chevremont et al., 1996); however, this material more closely resembles a clast-rich impact melt rock than a suevite and has been referred to and mapped as impact melt rocks in Lambert's works (1977a,b) and more recently by Sapers et al. (2009).

The Montoume breccia is massive structure, lacks vesicles, and displays columnar jointing (Figure 37).

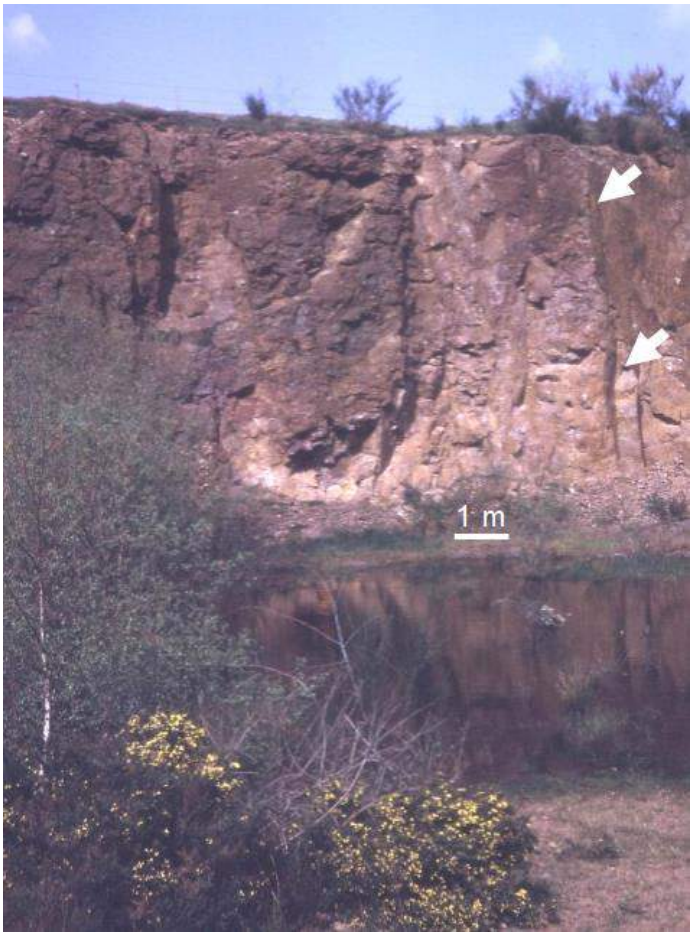

Figure 37: Clast-rich impact melt rock from Montoume 7.5 km S of the center of the structure. Old view (1970's) of the Mountoume quarry displaying large columnar joints (arrows).

Its texture is complex and variable at the meter scale (Figure 38). The proportion of lithic clasts >0.5 mm varies between ca. 25 and 40 vol% as measured by Lambert (1977a). The proportion of undoubtedly lithic clasts <0.5 mm in the matrix varies between 3 and 12 vol% and the proportion of matrix thus varies between 50 and 70 vol%.

The matrix is crystalline; it locally displays flow features. Flow features are seemingly related to local sorting of small lithic clasts and to elongation of partially digested schlierig clasts (as demonstrated for instance by the wavy contour of the periphery of the lithic clasts on Figure 38B). There is no preferred orientation of these flows at the scale of the unit. From the geological setting and the relative proportion of clasts measured in the melt it is deduced that the total amount of melt contained in the Montoume area comprises between 0.002 and 0.004 km^3.

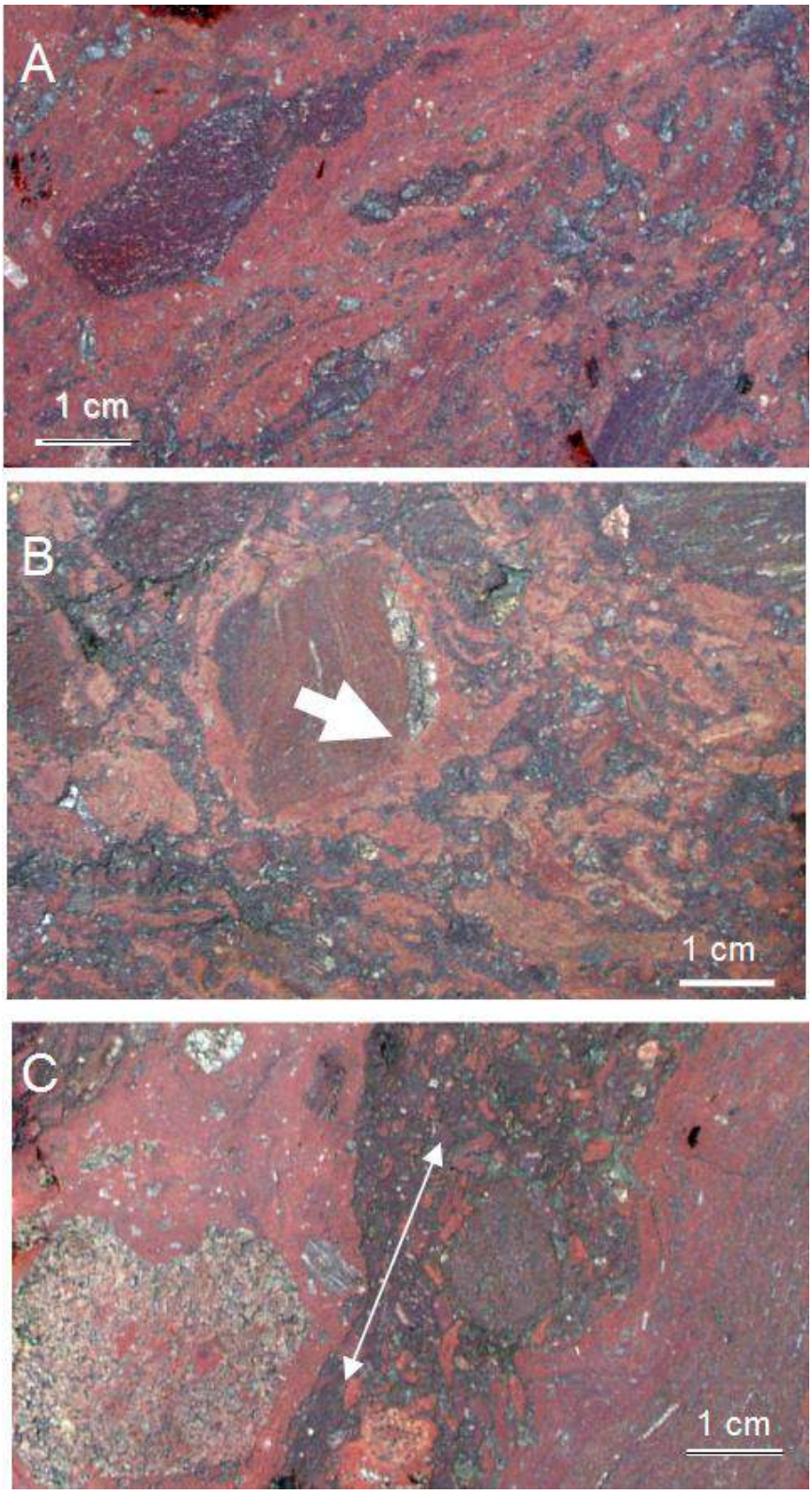

Figure 38: Polished slabs of clast-rich impact melt rock from Montoume 6 km S of the center of the structure. A: Highly fluidal melt with partially digested clasts elongated in the direction of the flow (arrow). B: Oriented and schlierig fluidal felsic melt clasts with more or less diffuse edges locally coating a lithic clast (arrow) embedded in a darker melt matrix. C: Assemblage of 3 distinct clast rich schlierig melts displaying different types, proportion and size of lithic clasts. Arrow: direction of the flow features.

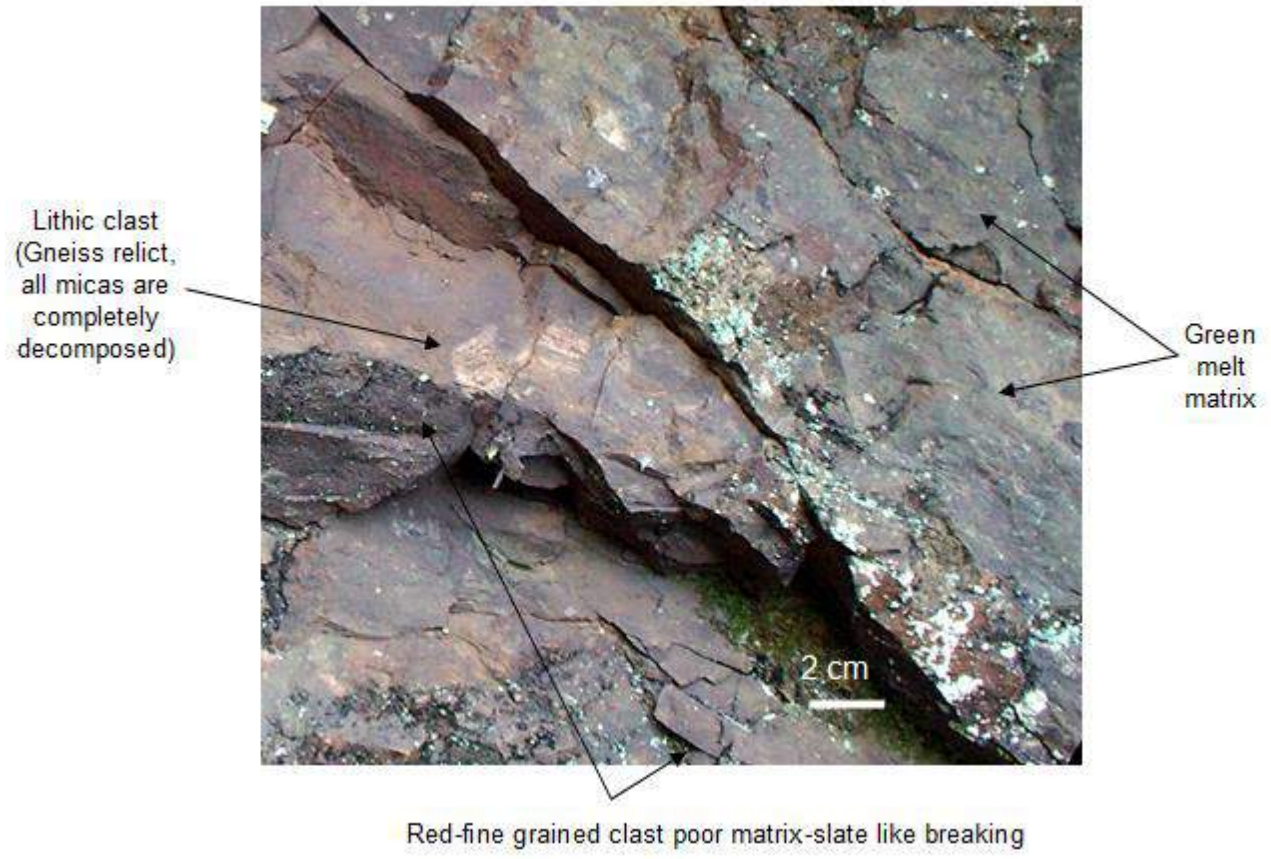

Figure 39: Wall of the Montoume quarry, 6 km S of the center of the structure showing variations of color in the massive impact melt rock. At this particular spot the melt is quasi free of clast.

Although the Montoume impact melt rocks are essentially all deep red in color, limited occurrence of gray-green matrix material resembling (in color only) to Chassenon suevite is observed locally in the red breccias (Figure 39). The contact with the red matrix material is gradual. Local occurrences of clast poor fined grained matrix material are also encountered (Figure 39). All this to conclude that despite of an apparent homogeneity of the Montoume formation, the texture is complex and the relationships between the different textural declinations remain unexplored.

The occurrence of deformed and schleric clasts of melts and melt matrix breccia clasts in the Mountoume impact melt rocks may explain why this formation can be confused with a suevite. It seems worthwhile alerting the community to these textures that do not necessarily fit in with the nomenclature.

In addition to distinct melting mechanisms (shock melting and post-depositional melting) the occurrence of impact melt breccia as clast in basal suevite as well as in melt poor impact melt rocks (such as at Montoume) imply multiple discrete source of impact melt breccia that become mixed at a latter stage. A minimum time gap that remains to be constrained is indeed required between the generation of the early impact melt breccia and the formation of the suevite or the impact melt rock in which the first generation melt breccia is occurring as clast. It also implies the first generation melt breccia has acquired a minimum strength and cohesion at the time it is processed by the second mechanism leading to the observed suevite or impact melt rock.

Non homogenized melt clasts in impact melt rocks are also constraining time and temperature conditions of cooling and mixing. The composition factor is also involved. One notes the melt clasts in impact melt rocks at Rochechouart are typically quartz rich in composition (such as those illustrated at Figure 11). This has certainly to do with the refractory character of quartz when compared to granite and gneiss.

All this will require further and more detailed investigation in order to provide full understanding and quantitative estimates of the various parameters involved.

Eventually Rochechouart impact melt rocks displays all the intermediate stages of clasts fabrics between that of a typical lithic clast and that of a completely molten, yet non digested melt clast that has lost essentially the memory of its lithic origin, but which maintains its chemical signature. This raise the open question of where to set the boundary between clast and melt and how does this interfere with the evaluation of melt content in impactites.

The geochemical record of melt at Rochechouart.

Geochemical analysis shows that all the Rochechouart impact melt rocks bear a common granitic composition as seen in the Fe-alkali element-Mg ternary diagram (Figure 5A). Compared to the target composition, the composition of this material displays a prominent shift towards the orthoclase pole on the quartz-orthoclase-albite ternary diagram (Figure 5B).

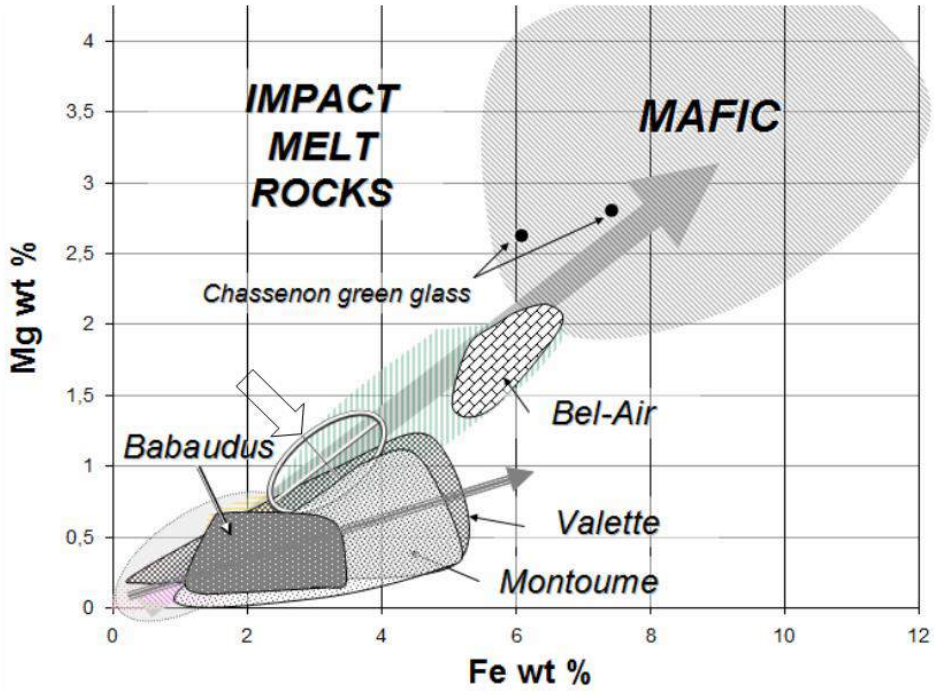

Figure 40: Correlation plots for the impact melt rocks at Bel-Air, Babaudus, Valette and Montoume. Note the same symmetry axis for the correlation fields of Montoume, Babaudus and Valette melt rocks (open arrow), which is shifted toward the Fe axis compared to that of the target formations (black solid arrow). Background: plots of the granite (lower left) and gneiss (Figure 6B). Ellipsoïd (open arrow):"average" target composition field mixes the composition of the various basement rocks according to their relative proportion of exposure in the Rochechouart area (ca 50% granite + leptynite and 50% gneiss).

The same shift is observed for the lithic clasts in the impact melt rocks (Figure 5B). This shift is associated with a relative increase in K_2O and relative depletion of both Na_2O and CaO (Table 2). The K/Na ratio for impact melt rocks is ca. 15 times that of the target rocks, whereas the K/Na ratio in lithic clasts in the impact melt rocks is ca. 10 times that of the target rocks. The K/Ca ratio in impact melt rocks is ca. 10 times that of the target rocks.

Beyond the common granitic signature and the pronounced change in the K/Na ratio, the various impact melt rocks show small but significant differences in composition. They plot separately in the Fe-Mg diagram (Figure 40). The Babaudus impact melt rock plots into a narrow field that is much more felsic than the average target composition (based on presently exposed country rocks). It matches the compositional field of the leptynites. Conversely, the Bel-Air melt rock is much more mafic than the average target and plots between the most mafic gneisses and the diorite-amphibolite field (Figure 40).

The Valette melt rock compositions fall into the broadest field, which covers the granitic compositions and extends to the lower half of the gneissic field (Figure 40). Despite the specific red color of this deposit, the Montoume breccia has the same composition as the yellow Valette impact melt rocks. As seen on the Fe-Mg diagram, Montoume and Valette melt rock compositions are almost identical. Both melt rock data sets fully cover the granitic compositions and extend to the lower half of the gneissic field (Figure 40).

The relative inefficiency in homogenizing and mixing of melt at Rochechouart.

The abundance of "multi-melt breccia" textures and melt clasts in suevite and in impact melt rocks at Rochechouart reflects a relative inefficiency in homogenizing and mixing at the scale of a hand specimen. The geochemical data suggest that this may also be true at the kilometer scale. The Mountoume impact melt rocks reflect the composition of nearby granitoids, leptynite and gneiss.

The Valette and other southwestern (bottom) suevites are characterized by a granitic composition which is consistent with the local target composition dominated by granites. The composition of the Bel-Air (bottom) suevite matches that of the local gneiss. The very small Bel-Air impact melt rock patch is significantly more mafic than local suevite and local gneiss (Figure 40). It is suggested that it incorporates some contribution from a mafic lithology, which is common in this region (see Figure 4).

Such a local source of melt is also advocated for the two green glass clasts extracted from the upper suevite at Chassenon (Figure 29). Their Fe-Mg composition is completely different from that of the host suevite and corresponds to that of the diorites and microdiorite dykes which are both developed in this part of the target. These two clasts are definitely not representative of the overall melt component in the Chassenon suevite as the Fe-Mg correlation field for these rocks would otherwise expand toward the green glass plots on Figure 29. It is not the case. Instead, such a distinct chemical signature of these glass clasts compared to that of the bulk host rocks demonstrates a very local and discrete origin for the glasses in the Chassenon suevite. More generally it suggests melts in the top suevite are not derived from a unique and homogenized melt source.

The Babaudus impact melt rock has a granitic composition, suggesting a major contribution from the nearby leptynites with a minor contribution from the local gneiss. All this suggests a relatively local origin for most impactites in the Rochechouart structure, and especially but not exclusively for the melt-rich

impactites (impact melt rocks and bottom suevite). This further implies that the excavation and readjustment did not mix/or homogenize ejecta at the scale of the Rochechouart crater, a feature that is also observed at other craters such as Bosumtwi (Coney et al., 2010).

The Rochechouart Impactoclastic Deposit

An approximately 1 m thick and few meters wide outcrop of very fine-grained, horizontally multilayered gray rock occurs above suevite in the quarry of Chassenon (Lambert, 1974, 1977b). Contrasting in both color and texture with the local suevite, it superficially resembles an ignimbrite. The material is compact, despite having a tuff-like aspect (Figure 41). The contact between the fine-grained deposit and the underlying suevite is gradational over a several-centimeter-wide transition zone in which centimeter-sized clasts of the suevite are mixed into the fine-grained deposit, which then looses its regular sorting.

The fine-grained horizontal deposit at the top of the Rochechouart impactite sequence strictly complies with the definition of an impactoclastite deposit recently introduced in the impactite nomenclature (Stoffler and Grieve, 2007). The shocked minerals cast no doubt about the relationship of this material to impact. The prominence of mineral debris and the granitic composition of the debris indicate an origin by comminution of the same basement rocks from which suevite and the other impactites at Rochechouart were formed.

Data regarding the original extent and thickness of the impactoclastic deposit are extremely scarce. It is possible that it may have had a 2 to 3 m thickness in the Chassenon quarry before complete extraction. As seen on ancient photographs (Figure 28), the top of the historic Chassenon quarry at the beginning of the 20th century displayed a ca. 2 m thick formation that is seemingly distinct from the underlying suevite and that displays a faint horizontal stratification. It appears massive and apparently shows curved bedding seemingly intersecting the underlying suevite with a low-angle unconformity (Figure 28).

This fine-grained rock was considered waste and discarded by both the Roman and latter generations of builders in the area who preferred the colorful and textured aspect of suevite for construction.

Individual components of the fine-grained deposit are not recognizable with the naked eye (Figure 41). Image analysis of photomicrographs indicates that 83 vol% of the material comprise unresolved matrix and clasts less than 25 µm in size; only 8 vol% is 50 µm in size or larger (Table 3). Particles identifiable with the optical microscope are mostly mineral debris with a small proportion (< 5 vol%) of lithic debris (Figure 43).

Unlike in suevite, no individual melt clasts could be observed macroscopically, nor among the finest particles (25-50 µm). Rounded glass particles similar to “lapilli” or “microtectites” were also not observed. There is no trace of sediment, and no evidence of diagenesis, in the matrix. The overall porosity is ca 5 %, as measured by image analysis on backscattered electron images. Clasts are mostly angular and consist of quartz, feldspars and micas, corresponding to the main mineralogical components of the target (Figures 43-49).

The matrix is made of the same detrital and porous assembly of microscopic and submicroscopic debris, including extremely thin mica laths (50-200 nm thick and a few micrometers long). Long and very thin mica laths are also common among the largest clasts. The mica clasts commonly display partial delaminating along cleavage and edges perpendicular to the cleavage may be splayed (Figure 17).

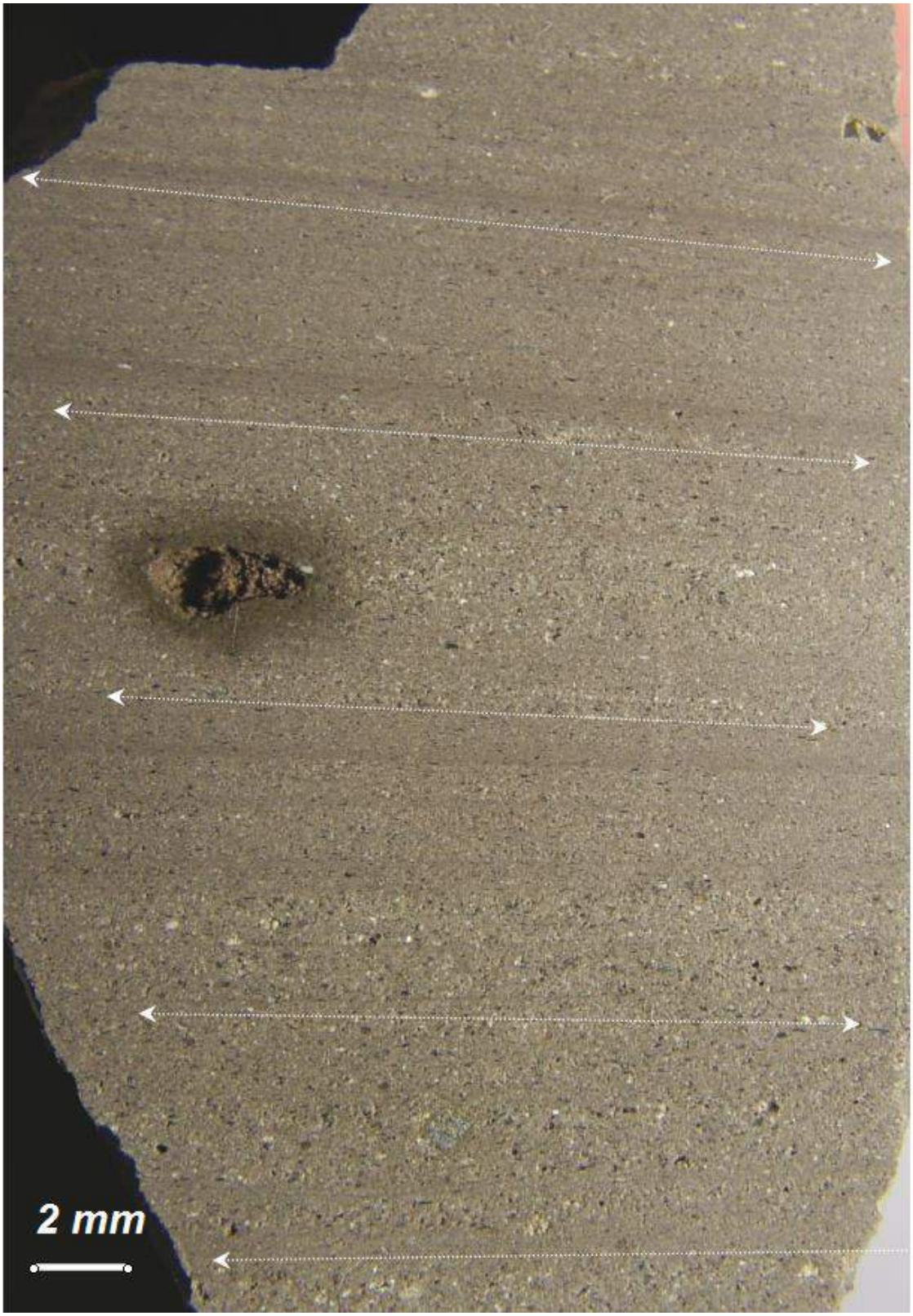

Figure 41: Impactoclastic deposit. The Chassenon fine-grained horizontal deposit sampled at the Arenes quarry at ca 4km of the center of the structure. The material is characterized by a relatively dense and massive texture and extremely regular bedding.

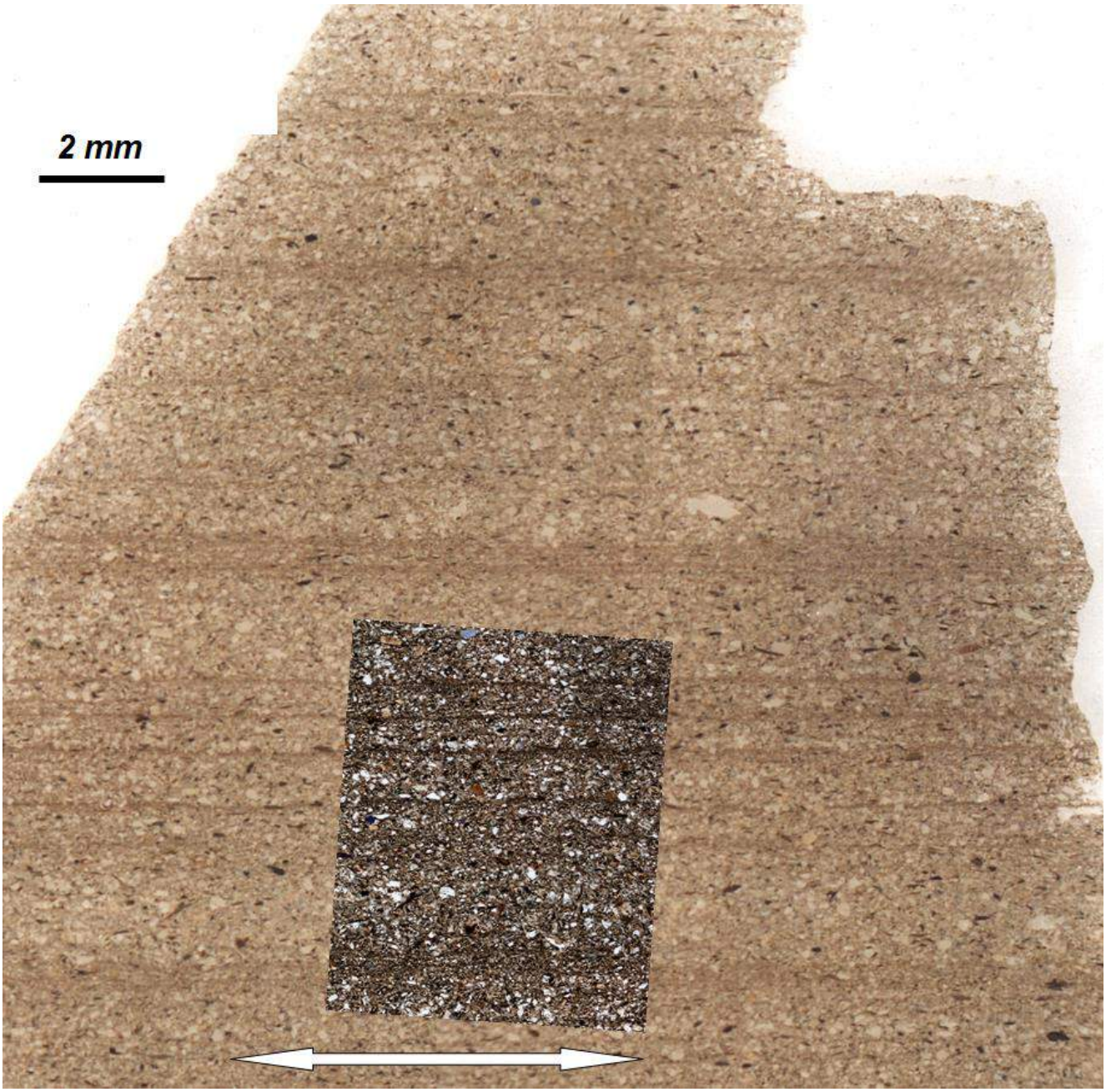

Figure 42: Impactoclastic deposit near Chassenon, 4 km of the center of the structure. Optical view of a thin section under plane polarized light of the sample of the Chassenon fine-grained horizontal deposit seen at Figure 41. Double arrow: Trace of the local horizontal plane at the sampling locality. Insert: crossed polars (see Figure 43). The material is characterized by a relatively dense and massive texture and extremely regular bedding. The stratified aspect is due to slight variation in grain size, porosity and composition (see Figures 43 and 44).

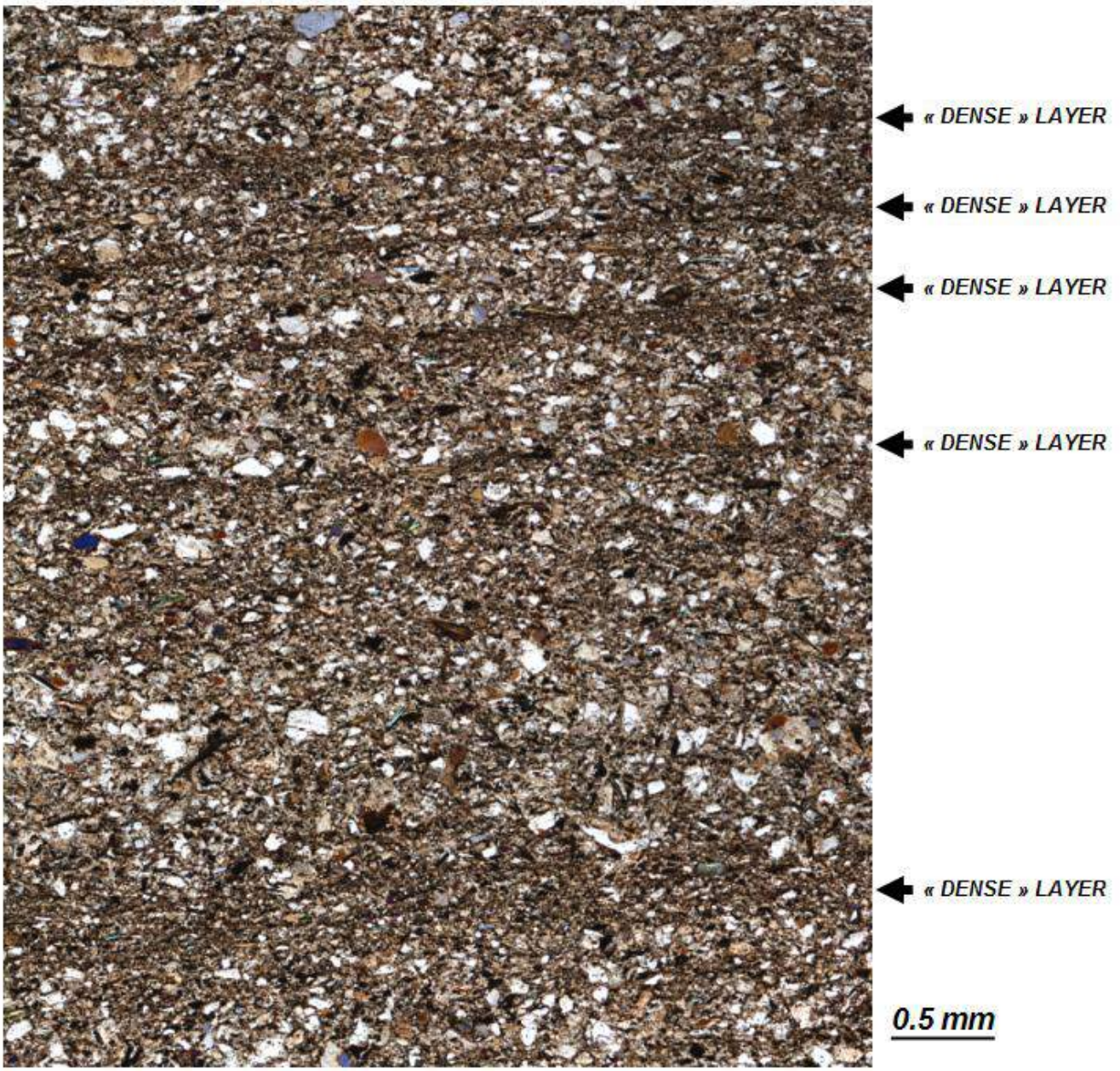

Figure 43: Impactoclastic deposit near Chassenon, 4 km of the center of the structure. Optical view of a thin section under polarized light (crossed polars) of the framed field at Figure 42.

The stratified aspect of the unit reflects slight variations in grain size and composition, and differences in porosity between the layers. The thinnest and darkest layers visible macroscopically have higher proportions of phyllosilicates and a significantly reduced porosity, both in terms of pore size and pore volume (Figures 42-45). These bands are 10 µm to a few tens of micrometers thick. The layering is extremely planar at the micro-scale; however, it curves slightly and branches at the decimeter to meter scale (Figure 41). On average, it is horizontal.

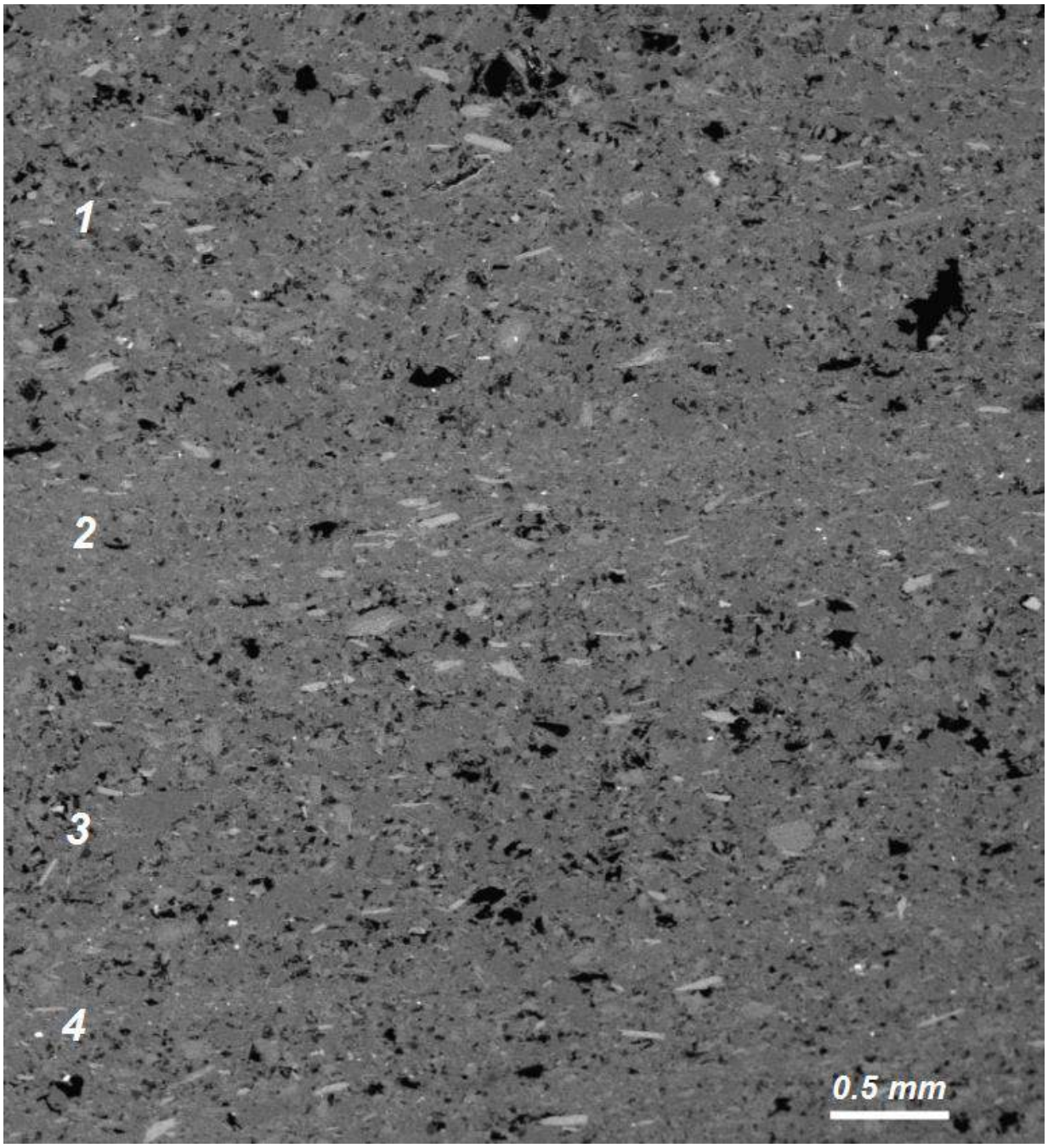

Figure 44: Impactoclastic deposit near Chassenon, 4 km of the center of the structure. SEM view (back scattered electron image) of the double polished thin section seen under polarized light at Figures 42-43 (same orientation). Note the preferred orientation of mica (lighter mineral). 1-4 sequence of alternating dense and porous layers (see detail at Figure 45).

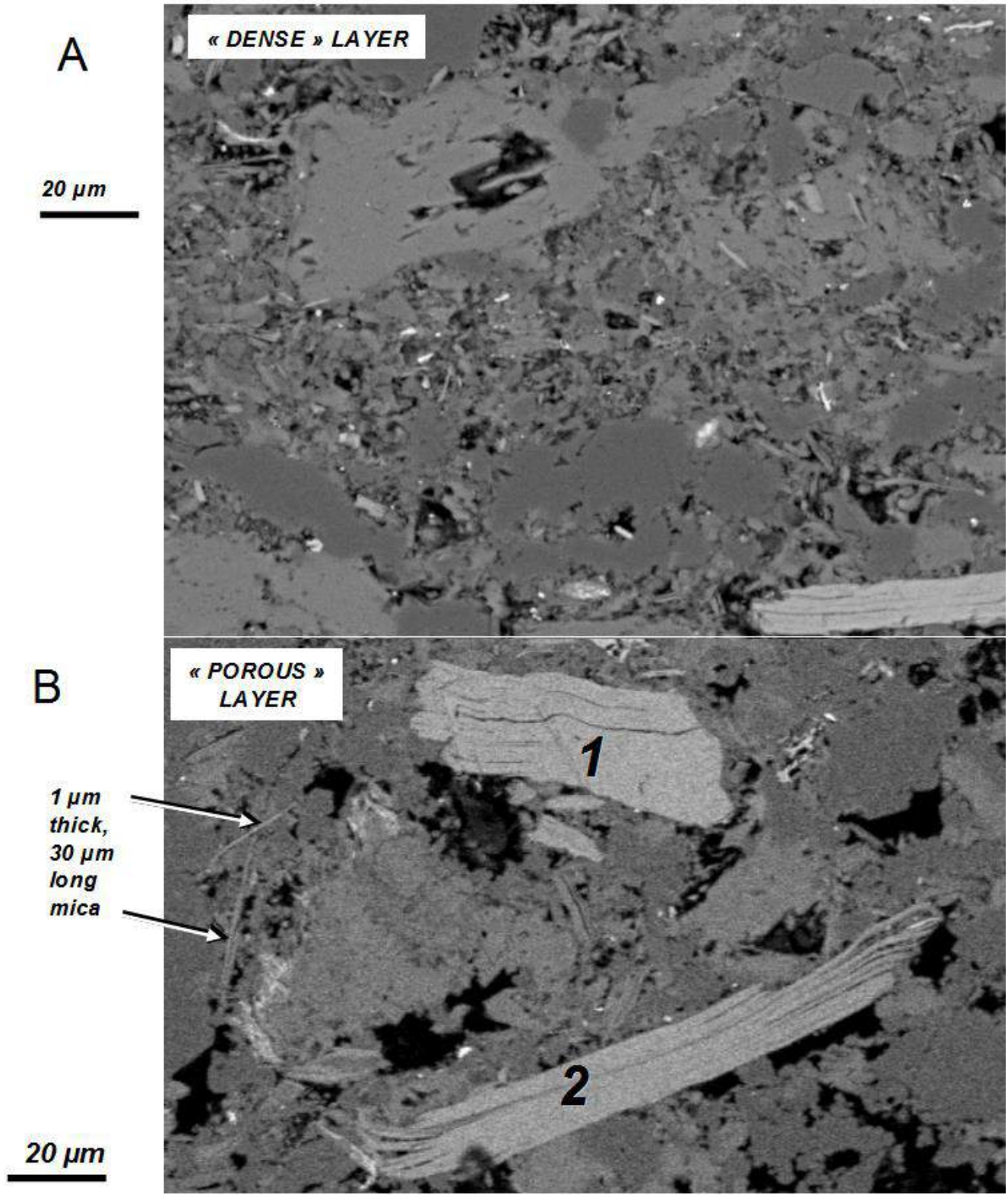

Figure 45: Impactoclastic deposit near Chassenon, 4 km of the center of the structure. Detail of the double polished section of a sample of the Chassenon fine-grained horizontal deposit seen under the SEM (back scattered electron image). A: Dense and fine particle layer (denoted 2 and 4 in Figure 43); B: Coarser layer (denoted 1 and 3 in Figure 44). Note the deformation (kinking (1)) and the splays at the end of large mica flakes (2).

The microscopic mineral debris and rock clasts display a wide range of shock metamorphic grades. Decorated planar microdeformation features in quartz and feldspars (Figures 46-47) and partial melting and decomposition lithic debris are observed (Figures 48). Tiny automorphous crystals of quartz and feldpars 5-20 µm wide are common and decorate the pore spaces (Figures 48-49).

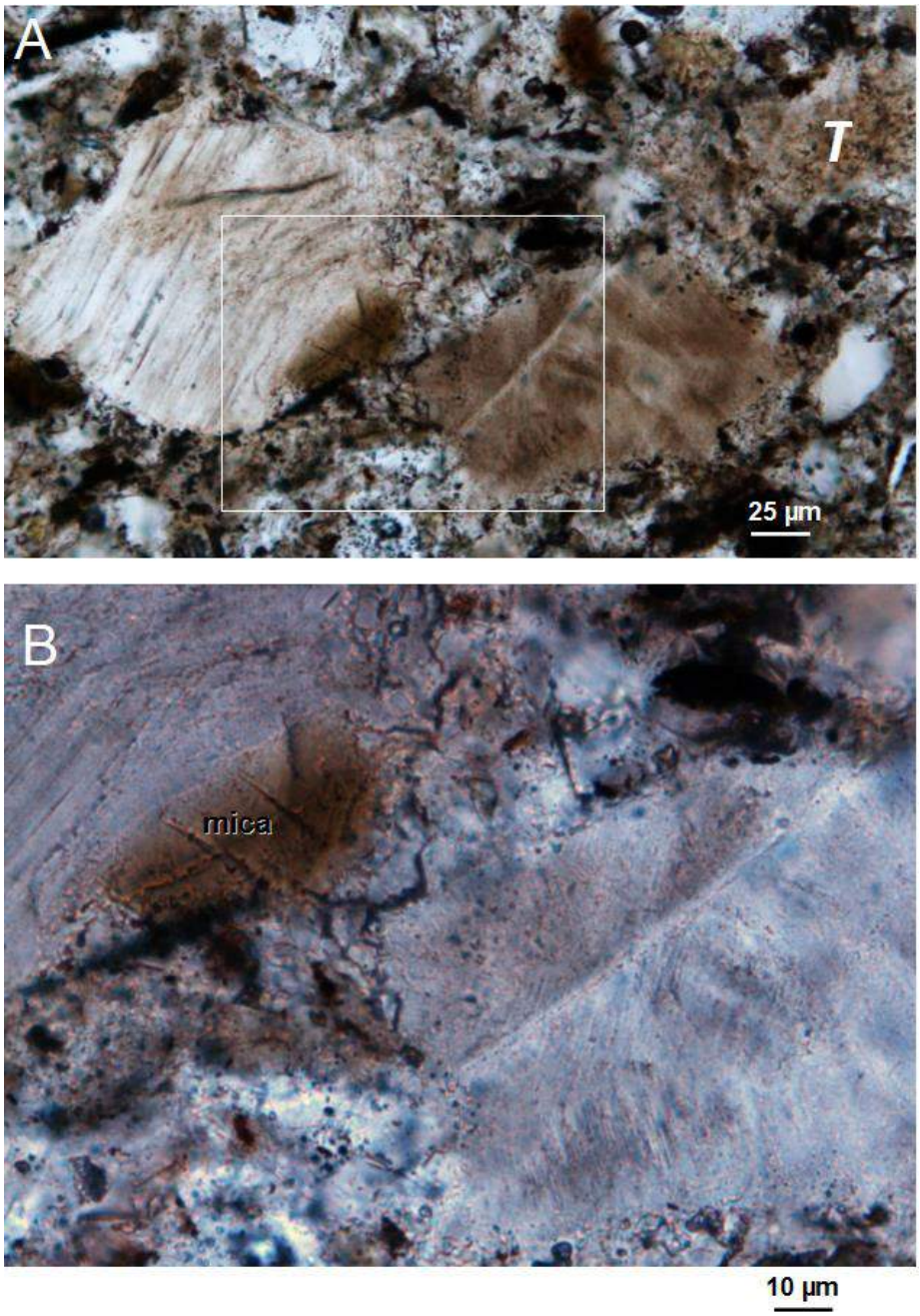

Figure 46: Petrographic details seen by optical microscope in plane polarized light of a double-polished thin section of a sample of the Chassenon impactoclastic deposit. Quartz clasts displaying a high density of planar deformation features. T: toasted quartz. Rectangle in A: field of view B.

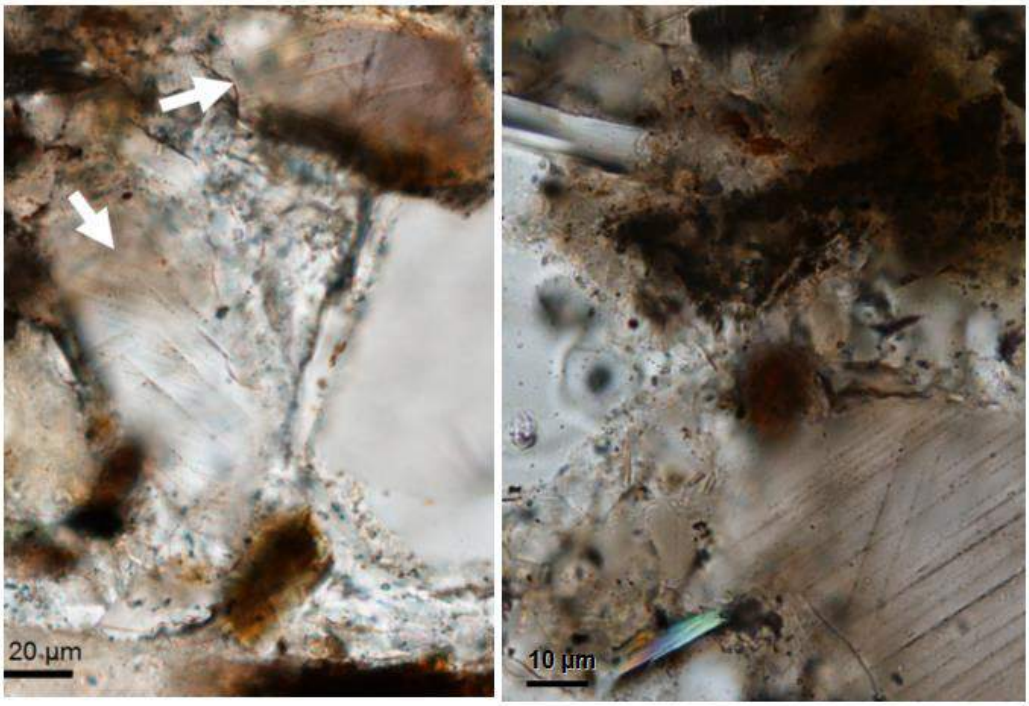

Figure 47: ***Petrographic details seen by optical microscope in plane polarized light of a double-polished thin section of a sample of the Chassenon impactoclastic deposit. Quartz clasts displaying decorated planar deformation features.***

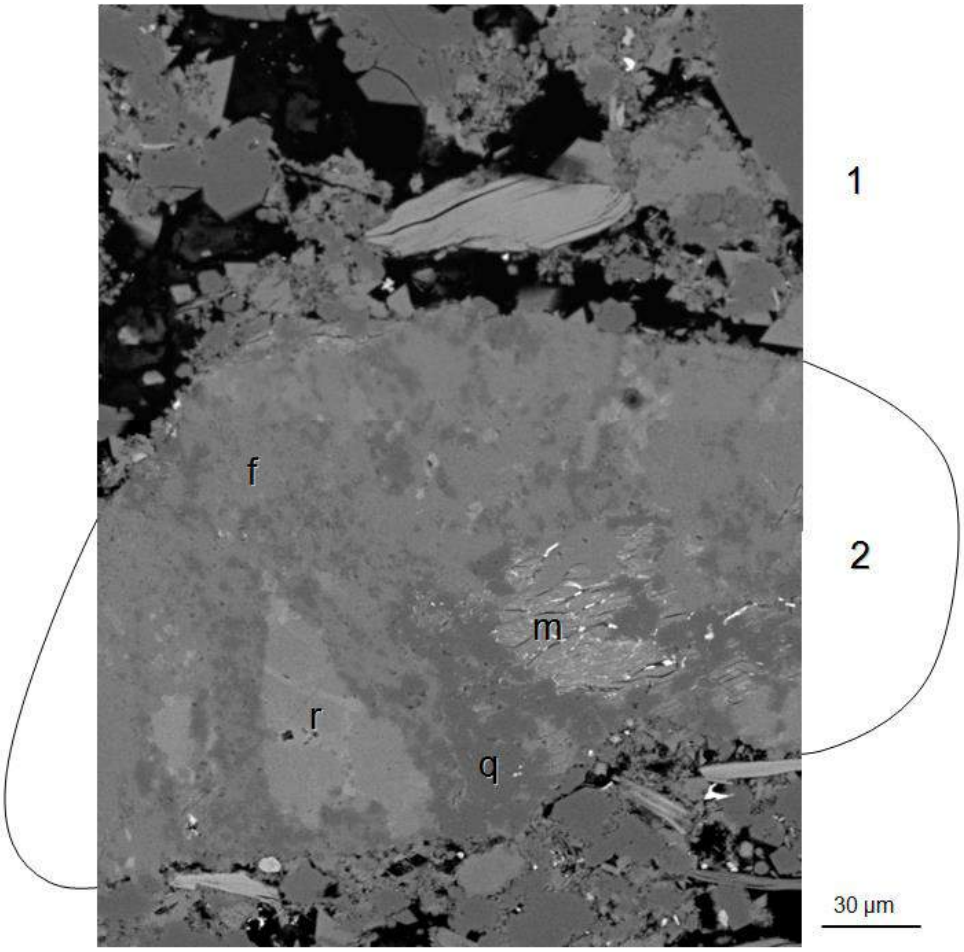

Figure 48: ***Impactoclastic deposit. Detail of the double polished section of a sample of the Chassenon fine-grained horizontal deposit seen under the SEM (back scattered electron image). 1-Highly porous zone with abundant new born tectosilicate cristalites characterized bywell developped crystal faces. 2- Lithic clast of granitic composition almost completely molten but not homogenized, with relicts of the original lithic material (r), relict of mica (m) in a matrix made of a diffuse assembly of quartz and feldspar (q and f).***

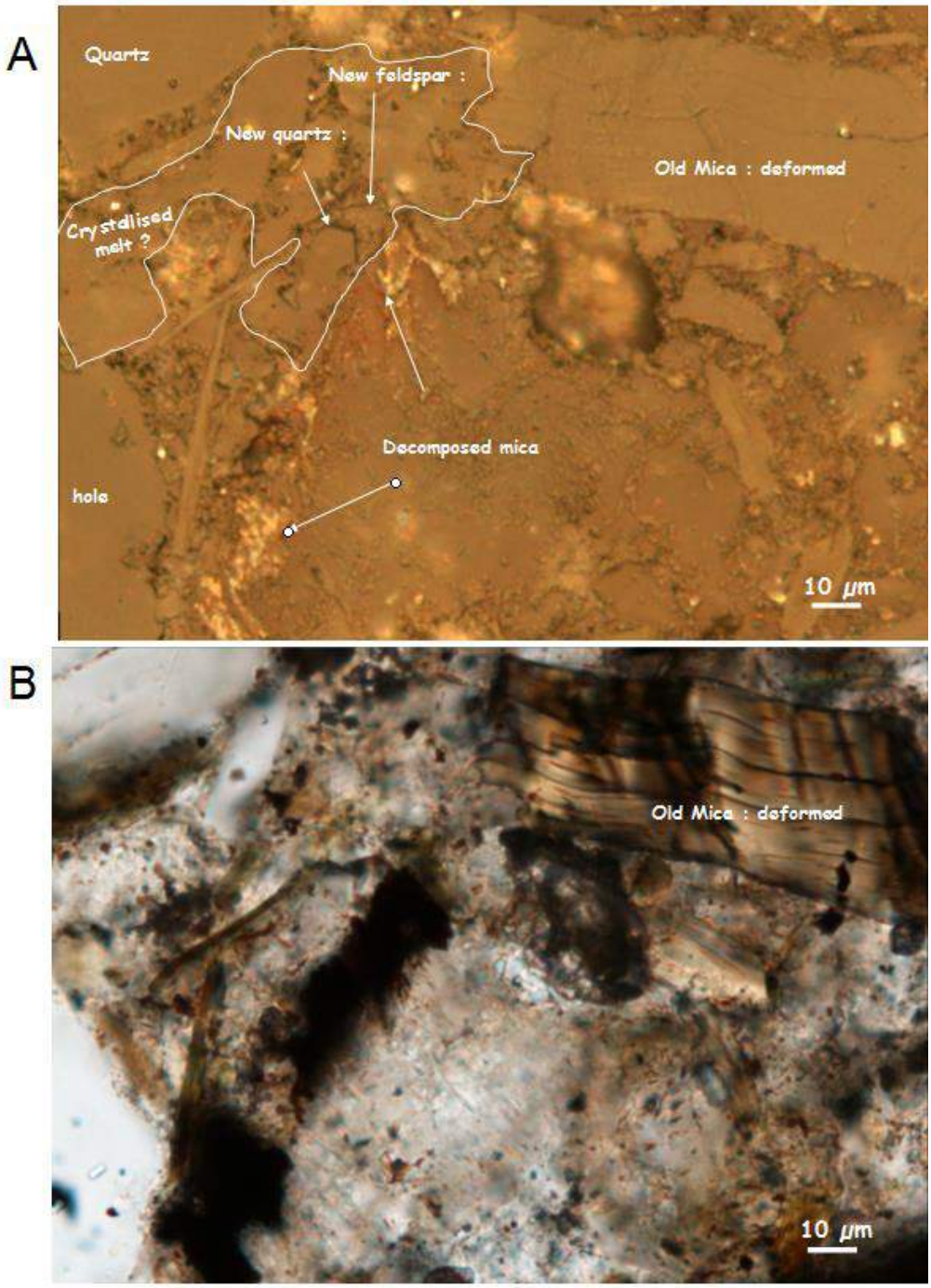

Figure 49: Petrographic details of the same field seen by optical microscope in reflected light (A) and in transmitted light (B- crossed polars) of a double-polished thin section of a sample of the Chassenon impactoclastic deposit. The framed area in A is mainly formed of a new generation of tiny crystals as deduced by clean extinction and automophous crystal shapes.

Both thermal decomposition (Figure 49) and congruent melting of mica are observed. The later results in a highly vesicular opaque froth invading local porespace and intragranular fractures in neighbouring tectosilicates (Figure 50). A significant proportion (20-40 %) of micas is affected by these thermal effects.

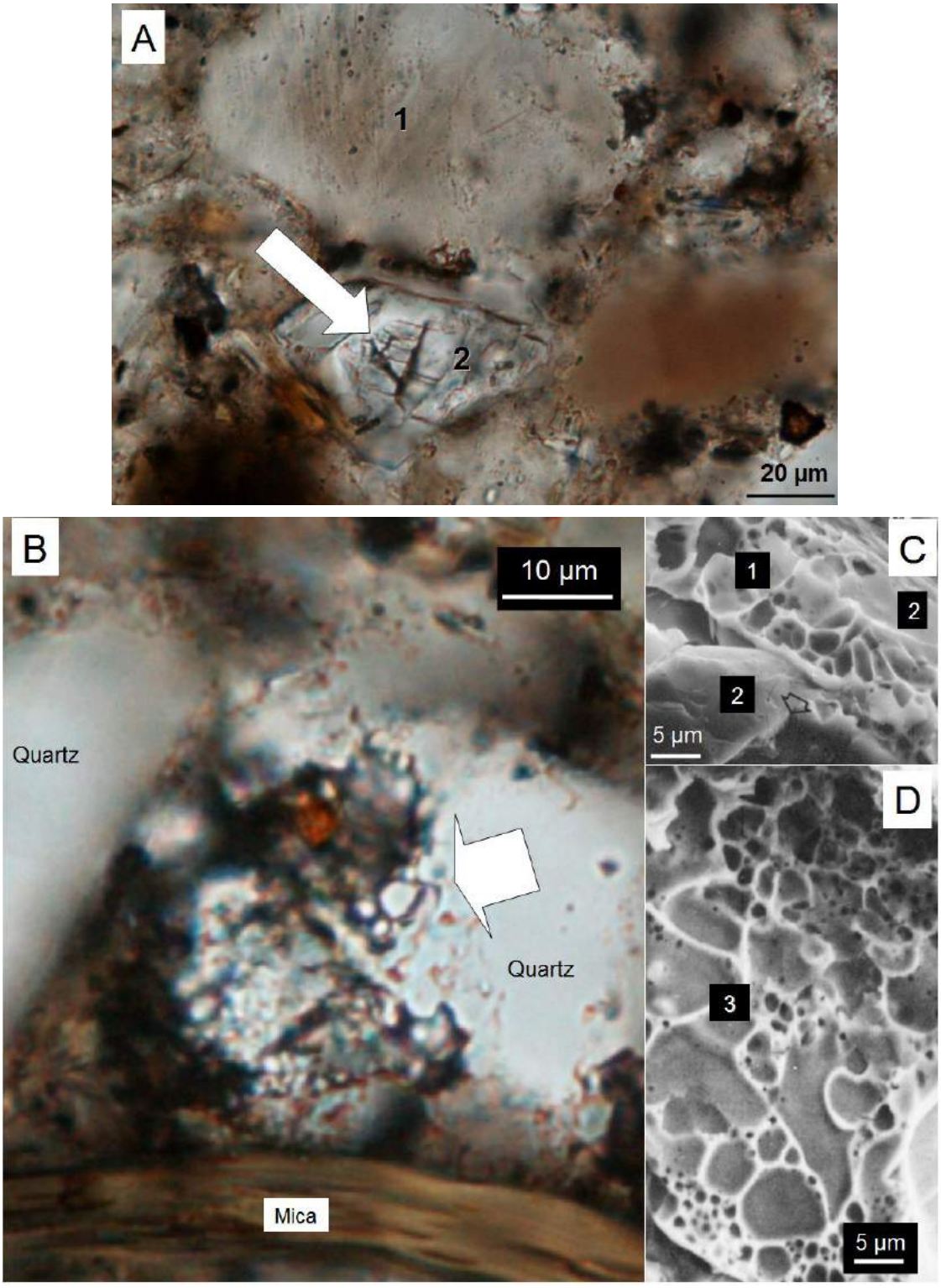

Figure 50: A-B: Detail, in the optical microscope, partially crossed polarizers, of a double-polished thin section of a sample of the Chassenon impactoclastic deposit. Arrow: black glass decorating intragranular fractures in quartz displaying flat vesicles when the fracture is seen in the plane of focus of the microscope; C-D: SEM view of a Rochechouart gneiss experimentally shocked at 35 GPa displaying highly vesicular devolatilized mica glass (1), diaplectic quartz (2) and froth of devolatilized mica glass (3) decorating the surface of a joint and an intragranular fracture in quartz after congruent melting of mica, flow and injection of the melt into local porespace driven by the expansions of volatile in the mica liquid upon pressure release (Lambert and Mackinnon, 1984).

Despite evidence for strong shock deformation in some clasts, most show no shock damage and the average shock level is relatively low (shock stage 0 and 1b).

No evidence of carbonate crystal is observed.

The major element composition of the fine-grained clastic deposit is intermediate between that of the granite and the gneiss. On the Fe-Mg diagram, it matches the composition of the average target (Figure 29). Like the other impact formations, the K_2O/Na_2O and the K_2O/CaO ratios of the fine-grained deposits are significantly increased compared to that of the target rocks. The values are similar to those of the impact melt rocks (Table 2).

Physical evidence for a fine-grained impact fallback layer at other impact structures remains rare. Such a layer has only been reported to date from drilling (core LB-5B) at the interface between impact breccia and post-impact sediments in the 10.5 km, 1.07 Ma old Bosumtwi crater (Ghana) (Koeberl et al., 2007b) and from the post-impact resurge sediment at Chesapeake Bay (Reimold et al., 2009, in press). The Bosumtwi layer comprises a large proportion of melted and highly shocked material, whereas the Chesapeake Bay layer comprises a very large proportion of sedimentary material mixed with a subordinate amount of impact-related debris during the post-impact tsunami stage of this shallow-marine impact. Unlike the reported 30 cm thick fine-grained layer in Bosumtwi core LB-5B containing accretionary lapilli and microtectite-like spherules, there is no evidence of such features in the Rochechouart impactoclastic deposit.

Interpretation and implications: Any mechanism proposed for the origin of the Rochechouart impactoclastic deposit must thus explain the comminuted nature of the impactoclastites, the prominence of overall relative weak shock levels, the absence of melt clasts and the welding.

The welding and the relative abundance of thermal alteration of micas suggest the impactoclastic deposit is not cold despite the absence of melt particles and was possibly emplaced at a relatively high temperature near thermal decomposition of micas.

The remarkable thinness and regularity of the stratification of the Rochechouart impactoclastic deposit constrain the conditions of final deposition to a calm environment. This and the horizontal setting indicate it took place after the crater adjustment had been completed, and turbulent mixing in the underlying impactites had ceased. The texture and the fragility of the extremely small and thin mica laths (as seen in Figure 45) compares to that of glass shards in pyroclastic deposits. With the exception of a lack of a glass mesostasis, all the textural characteristics of the impactoclastic deposit match those of ignimbrite supporting the interpretation it is depositing in the atmosphere. The discontinuity between the impactoclastic deposit and the suevite indicates the fine debris forming the impactoclastic deposit travelled in suspension significantly longer than the coarser glass and lithic debris forming the underlying suevite and, thus, that they were deposited separately. Yet the time hiatus must have been extremely brief compared to the time needed to erode the underlying impactites, implying the underlying sequence of deposits is complete at this particular location (Chassenon).

Impactoclastic Intercalations (dikes) in suevite

In addition to the stratified though massive impactoclastic deposit, distinct dikes occur that intersect, or are intercalated within, the uppermost section of the massive suevite deposit. The fine structure, better resolved under the optical microscope, appears more complex and multilayered than that of the material described in the previous section, and

there are some layers that contain small glass particles.

A steeply-dipping dike, tapering from ca. 1 m wide at the top of a ca. 1.5 m high wall in the historical Chassenon suevite quarry to ca. 0.5 m at the base merges into the fine-grained horizontal deposit overlying the suevite before over a transition zone of about 10 centimeters width (Lambert, 1974).

A similar dike is exposed 800 m from Chassenon at Longeas in the active archaeological excavation next to the Roman Baths. The irregular dike of ca. 50 cm width cuts through suevite (Figure 51) with a vertical to steep dip, but the attitude below the current level of exposure requires further attention (providing digging is permitted).

Figure 51: Field view of a 50 centimeter wide multi-layer impactoclastic dike in suevite near Longeas near the top of the Chassenon suevite deposit, at ca 4km of the center of the structure .

Another site is located ca 400 meters south in the remnant of opposite walls of two ancient quarries abandoned since the 4th century. Several 10 to 30 cm wide, subparallel and apparently low-angle intercalations appear there interbedded with faintly layered suevite.

The intercalations and dikes display similar characteristic features. The fine-grained texture contrasts with the breccia texture of the host suevite, and the multi-layered texture is distinct from that of the horizontal deposit described before. The characteristics are illustrated in Figure 52, which shows the macroscopic view of a cross-section cut from one of these intercalations. The cross-section is perpendicular to the contact with the suevite. The texture is significantly different from that of the host suevite deposit. Three main "layers" are visible that are each a few centimeters wide (Figure 52).

Layer 1 at the contact with the suevite is characterized by a fine-grained flow-banded texture. It is not a breccia. It is similar in color, texture and grain size variation to the fine-grained horizontal deposit described before. This material is formed from the same mineral

debris that displays the same range of shock features as that forming the fine-grained horizontal deposit described before. Only a single glass clast was observed in layer 1 (Figure 52). The morphometric characteristics of particles as measured by image analysis (top left at Figure 52) compare to those of the particles observed in the fine-grained horizontal deposit (Table 3). The population of objects 50 µm long and larger accounts again for 12 vol% of the material. The average diameter of particles is less than 50 µm. Particles > 0.3 mm form 0.4 vol% and no particle larger than ca. 500 µm was observed (Table 3).

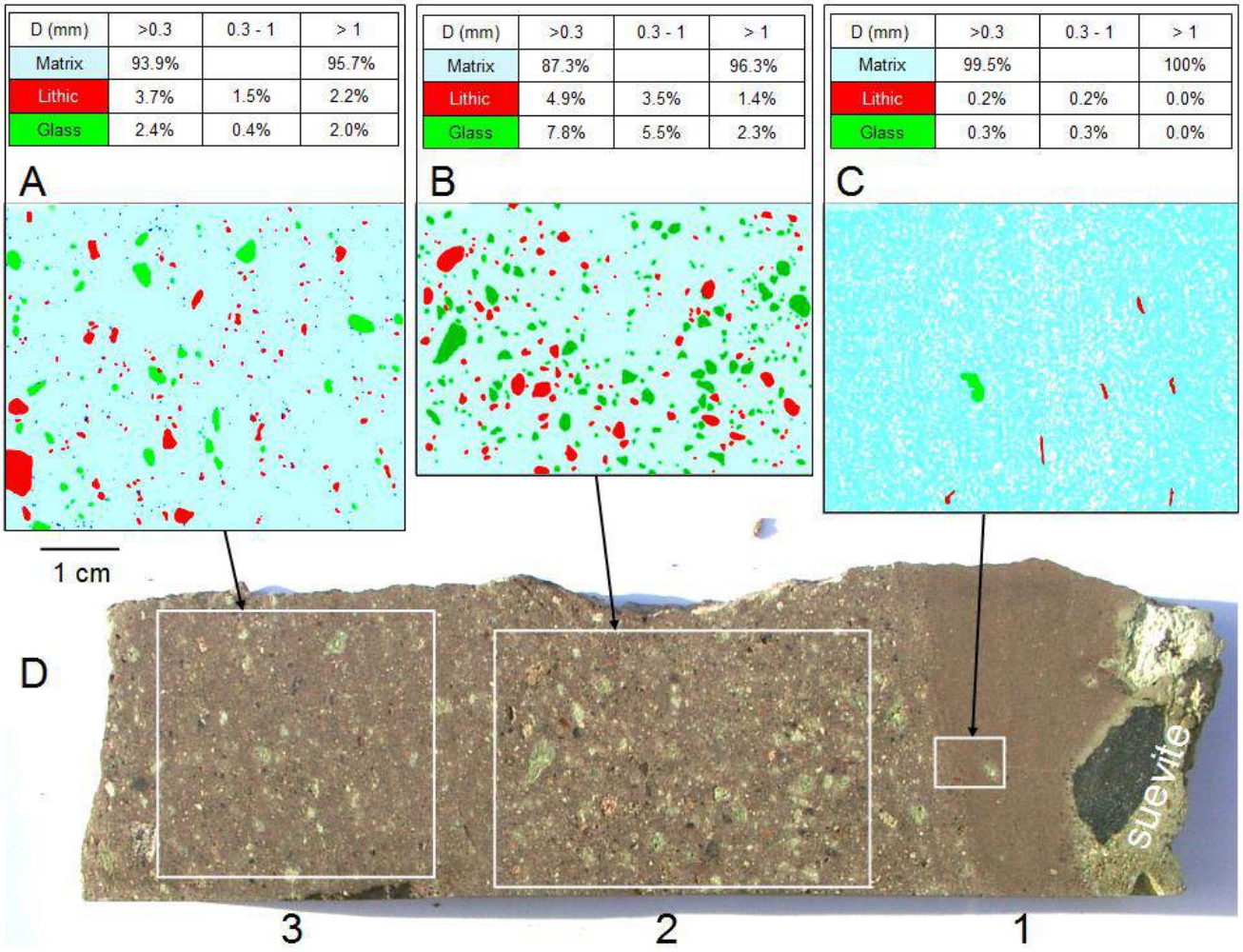

Figure 52: Impactoclastic dike. Fine-grained intercalation at the top of the Chassenon suevite deposit, at ca 4km of the center of the structure. A-C: Segmented false color images distinguishing different phases of the framed areas on a polished slab (D) and related tabulated values of relative proportions of the phases according to modal and granulometric measurements by image analysis. Red phases: Lithic clasts. Green phases: Glass. Light bleus: Matrix. White phases (view C): Clasts < 0.3 mm in diameter. D: Macroscopic view of half section cut perpendicular to the wall of one of the 25 cm thick multi-layer impactoclastic intercalations in suevite near Longeas. Layer 1 is characterized by a fine-grained and flow-banded texture. It is similar in color, texture and granulometry to the fine-grained horizontal deposit. Only one glass particle was observed in this layer. Layer 2: Bearing green glass clasts, it resembles the surrounding suevite except for the grains sizes which are much smaller. Layer 3: Same texture as layer 2 but with a smaller proportion of glass clasts. Note the gradual transition between the 3 layers and suevite (on the right).

As observed for the fine-grained horizontal deposit, layer 1 is characterized by a microscopic layering related to sorting and preferred orientation of mineral debris; however, the layering is neither regular nor planar - it displays undulations and vortex-like features (Figure 53). The contact between layer 1 and the suevite is characterized by a 10 mm wide transition zone with clear evidence of turbulent flow, as shown by the loss of the regular banded texture that characterize layer 1 and by the deformation of centimeter-sized melt clasts in the neighboring suevite (Figure 53).

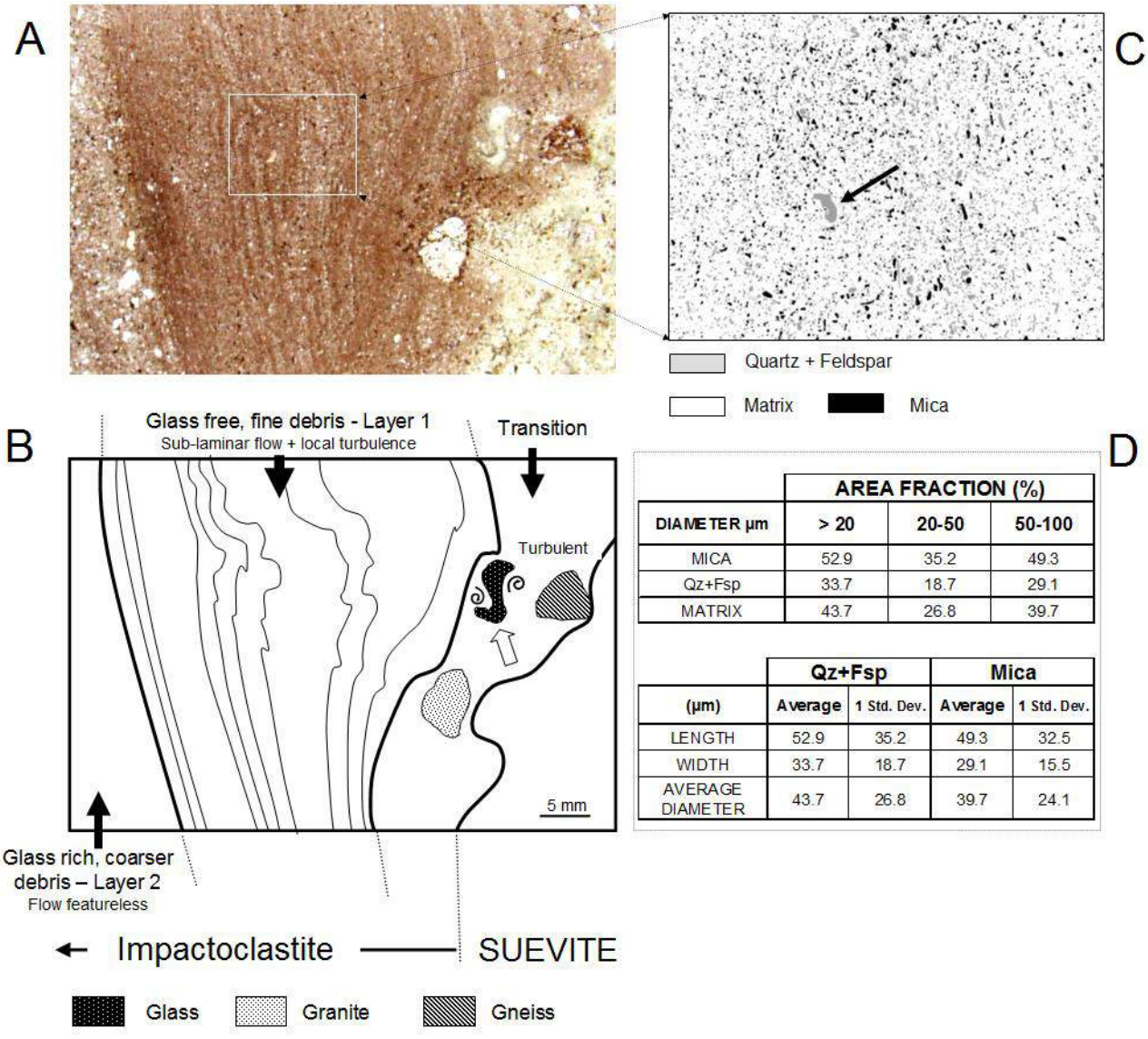

	AREA FRACTION (%)		
DIAMETER µm	> 20	20-50	50-100
MICA	52.9	35.2	49.3
Qz+Fsp	33.7	18.7	29.1
MATRIX	43.7	26.8	39.7

	Qz+Fsp		Mica	
(µm)	Average	1 Std. Dev.	Average	1 Std. Dev.
LENGTH	52.9	35.2	49.3	32.5
WIDTH	33.7	18.7	29.1	15.5
AVERAGE DIAMETER	43.7	26.8	39.7	24.1

Figure 53: Impactoclastite dike at the top of the Chassenon suevite deposit, at ca 4km of the center of the structure. Detail of Layer 1 in Figure 52. A: Macroscopic view showing a transitional zone with evidence of turbulent flow at the contact with suevite (curving of the fine mica layers of the fine-grained material and deformation of the centimeter sized glass clasts in the neighboring suevite (open arrow: "S" shaped double vortex). B: Detail of the framed area in A. Undulations of the fine grained layer signify flow perturbation. C: Segmented false color image distinguishing different phases of the framed area on view A. Arrow: "large" elongated and contorted clast of green vesicular glass. D: Morphometric data and volume % of the various phases according to modal analysis and granulometric measurements by image analysis, for the population of clasts > 15 µm long.

This fine-grained layer 1 grades into layer 2, which is characterized by a distinct granulometry and texture (Figure 52). Unlike layer 1, there is no or little banding in layer 2. Approximately 13 vol% is made of particles > 0.3 mm, i.e., 40 times more than in layer 1 (Figure 52). Unlike layer 1, this layer meets the textural characteristics of a breccia (more specifically a micro-breccia owing to the granulometry). It is constituted of clasts embedded in the same fine-grained material as that constituting layer 1. Bearing granitic lithic clasts and green glass clasts (altered), it resembles the surrounding suevite except for the clast granulometry. In both Rochechouart suevite and polymict lithic impact breccias, the particles 1 mm in diameter and larger represent, on average, 50 vol% or more (Table 3). In layer 2 they account for only 4 vol% and no particles larger than 5 mm are present, whereas they represent about 30 vol% in the suevite and other impact breccias in the Rochechoaurt structure (Table 3).

Green glass clasts account for two-thirds of the particles larger than 0.3 mm in layer 2. Besides color, these melt particles display the same petrographic characteristics and the same composition as those observed in the surrounding suevite. The lithic clasts in layer 2 display the same type and the same variety of shock metamorphic features as the lithic clasts in the surrounding suevite.

Layer 2 grades into the layer 3 which, like layer 2, shows little evidence of flow banding. It also has a micro-breccia texture and shares the same clastic matrix with layer 2. The proportion of clasts > 1 mm is the same as in layer 2 (4 vol%) (Table 3). The proportion of clasts > 5 mm is about half that measured in layer 2 (6 vol%) (Table 3). The glass clasts in layer 3 are significantly less abundant than in layer 2 as seen in Figure 52. Glass clasts over 0.3 mm in size represent only 2.4 vol% of the material in layer 3, whereas they account for 7.8 vol% of layer 2 (Figure 52).

Interpretation and implications: The similarities in texture and composition between the impactoclastic deposit and the glass-free layer 1 in the fine-grained multilayered dikes and intercalations with the Chassenon suevite indicate that they are genetically related. The glass-bearing layers 2 and 3 are texturally intermediate between suevite and the sediment-like impactoclastic deposit. The main difference is that the grain size values are an order of magnitude smaller in the glass-bearing layers compared to suevite. This feature is common to both the fine-grained horizontal deposit and the multilayered fine-grained intercalations, which supports the proposal that they are members of a single family where the dominant characteristic is the prominence of comminuted target debris and the fine grain size (Lambert and Reimold, 2009), with two members, the impactoclastic deposit and the impactoclastic dikes (and other intercalations of melt-bearing impactoclastic material).

The undulation of the fine bedding in the fine-grained, glass-free layers in the impactoclastic dikes and the disturbances along the contact with the host suevite suggest the material in the dike flowed very rapidly (sublaminar flow).

Owing to the highly turbulent and energetic conditions of deposition of the allochthonous breccia formations and to the large concentration of solid debris that acts like abrasives, it could be argued that the dikes and the fine-grained character of the impactoclastites relate to mechanical grinding within the suevite at the time of deposition. This might happen rather deep inside the deposit, possibly toward or at the bottom of the suevite as confinement is required to produce the grinding.

Indeed, deep and close to the center of the crater, the deposits remaining in the crater may have experienced a complex history starting with outward and turbulent high-velocity flow during the latter stage of transient cavity

growth, followed by a further impetus either in the same direction (toward the rim) because of the central uplifting of the bottom of the crater, or in the opposite direction because of the collapse of the rim.

These complex movements amount to mega-landslides which could be responsible for major shearing, grinding and compaction leading to the observed fine-grained material in the Rochechouart suevite. The undulating and striated surfaces at the interface between Bunte Breccia and suevite in the Ries crater reflect such an abrasive character. If such a scenario appears consistent with i) the observed field setting (dike and low-angle intercalations of impactoclastites in the suevite) and ii) the fine-grained character of the rocks, it seems incompatible with: a) the fine and regular layering of the ignimbrite-like deposit at the top of the sequence, which rather suggests an aerial deposit, b) a setting at the top of the deposit sequence (see ensuing discussion), and c) the shape of the debris particles which display an increased aspect ratio (elongation) and an increased sharpness of edges compared to the debris in the host suevite. Whilst confined grinding and shearing could considerably reduce the size of the clasts, it would also significantly reduce angularity. This is the inverse of what is observed in the impactoclastic deposits at Rochechouart.

Morphometrical characteristics of the Rochechouart crater and of its deposits

Crater floor morphology.

The wide access to the crater floor at Rochechouart clearly establishes that Rochechoaurt belongs to the category of flat floored readjusted crater. The most distinctive feature of the crater floor is the irregularity at the decameter scale and regularity at larger scales. Variations in elevation of the crater floor over the 15 km wide central zone are limited to +/-50 m relative to the horizontal when corrected for the 0.6° dip. In that context the faint 50 m high central raise only observed along a specific N-S traverse **is definitely not a conclusive signature of a central uplift.** The Rochechouart crater is definitely characterized by a large flat foored central cavity at least 15 km in diameter.

	El'gygytgyn		Ries	
Feature	Obs.	Model	Obs.	Model
Sediment thickness (m)	0	0	470–750	660
Rim-to-rim diameter (km)	18[1]	19	?	20
Pre-impact surface diameter (km)	~15	16.8	?	17
Diameter of largest-offset concentric fault (km)	?	16	~22[2]	17.5
Apparent diameter (km)	31–32[4]	–	26[5]	–
Transient crater diameter (km)	–	11	–	11.3
Rim height (m)	142[1]	175	?	176
Apparent depth[6] (m)	650	800	480–530	800
Gravity anomaly diameter (km)	18[7]	–	20–22[8]	–

Table 5: Summary of comparative dimensions of El'gygytgyn, Ries given by Collins et al., 2008.

[1]At current level of erosion.

[2]Estimate based on depression of basement and major fault at Thalmühle (Collins et al. 2008).

[4]Diameter of outer rim: semi-continuous ring with ~14 m topographic relief (Gurov et al. 2007).

[6]Depth from current surface to top of syn-impact crater fill.

[7]Dabija and Feldman (1982).

[8]Pohl et al. (1977).

Such a flat central zone is not unique to Rochechouart; it is also observed at other craters of similar size developed in crystalline basement or mixed sedimentary-crystalline basement targets. The interpretative cross-section of El'gygytgyn based on geologic observation and seismic survey given by Collins et al. (2008) and reported in Table 5, shows a flat 8 km diameter central zone where the relative variations of the crater floor are the same order as at Rochechouart, followed by a by a 5 km wide 650 m high wall (depth from current surface to top on syn-impact crater fill given in Collins et al., 2008) before reaching the position of the current erosional rim that possibly correspond the peak ring. A "weakly expressed" outer concentric ring with an average relief of 14 m is present at a radial distance of 15.5–16 km, although it is not clear what this represents and if this is a primary impact-generated feature (Gurov et al. 2007).

Similarly, the central part of the Ries crater seems to be characterized by a flat contact between the impactite deposits and the basement rocks. The cross sections based on geologic observations, drilling and geophysical surveys at Ries (see references in Collins et al., 2008) suggest an inner 6 km diameter central zone where the contact elevation remains within a +/-50 m bracket, followed by the 3-3.5 km wide 480-530 m high wall before reaching the position of the inner crystalline rim.

Size of the original Rochechouart crater

As seen Figure 9, the outer limit of possible impact effects occurs at ca 15 km west of the center of the structure (Lambert, 1977a). Although the field evidence at this site is not unequivocally impact-related and could be related to pre-impact tectonics of Variscan age, it also matches the limited and preliminary geophysical data available on the Rochechouart structure, which place the outer limit of a small negative gravity anomaly at the position of these cataclastic rocks (Pohl et al., 1978). The 23-24 km diameter value for the Rochechouart impact reported in the literature and in the terrestrial impact crater data bases corresponds to this outer limit and relates to the size of the structure as exposed today; it does not necessarily constrain the size of the initial crater immediately after impact.

The best available field data set for estimating the original size of the Rochechouart final crater is the profile of the crater floor in the 15 km diameter inner zone and the fact that the flat central depression of the crater extends as far as the position of the Cheronnac drilling, 10 km from the center of the crater. To get to the position of the rim (and thus to the estimate of the original crater size), one must add to the diameter of the flat central depression, the lateral width of the wall of the depression. Crater profile data such as at the 9.5 km Deep Bay, which is one of the deepest and steepest readjusted craters on Earth, indicate 2 km is the strict minimum for the radial width of the wall of crater. This sets at 24 km the most conservative value for the estimate of the diameter of the final crater at Rochechouart immediately after impact.

More likely the wall of the original crater at Rochechouart was not as steep as at Deep Bay and comparison with larger structures also developed (or mainly developed) in basement rocks, such as Ries and El'gygytgyn, are more appropriate (Figure 54). Providing that the profile of the crater floors at Ries and Elgygytgyn are reliable, the comparison with Rochechouart implies that the final crater diameter at Rochechouart was in the **40-50 km** range rather than 20-25 km. This is because the diameter of the central flat floored cavity at Rochechouart is approximately twice larger than at Ries and El'gygytgyn.

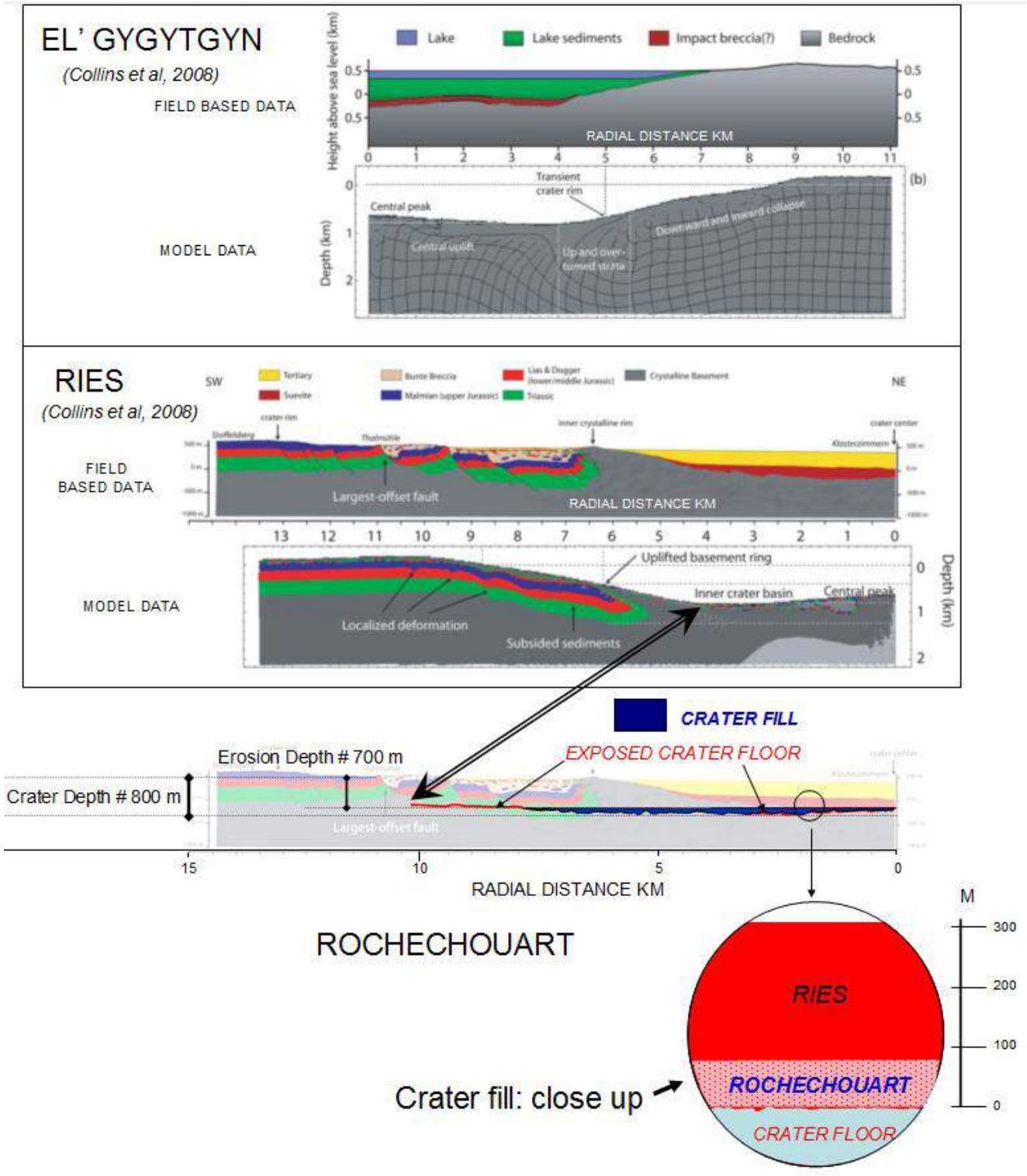

Figure 54: Comparative crossections of El'gygytgyn, Ries and Rochechouart (data from Collins et al., 2008, Lambert, 1977a, 2010)

Target Composition

Although one clast of carbonate has been reported in a polymict lithic breccia from Rochechouart (Sapers et al. 2009), a significant contribution to the Rochechouart impactites from sedimentary rocks, especially from carbonates, seems unlikely, as:

1) The late Triasic-early Jurassic sediments occurring in the vicinity of the Rochechouart impact site at the presumed time of impact (Figure 1) are only a few meters to a few decameters thick and are composed of silicate rocks.

2) The geochemical record shows no positive anomaly in either Si or Ca in the impact melts compared to the granitic basement. A contribution from quartz-bearing sediment would shift the impact melt compositions toward the quartz apex in Figure 3b, which is not observed. A contribution from carbonates would shift the impact melt rock compositions toward the alkali element and/or the Mg poles in Figure 5A, which is not observed either.

Thus, if there is a contribution from sedimentary rocks to the Rochechouart impactites, it is very small compared to the contribution from granitic basement rocks; however, a small contribution from quartz or quartzo-feldspathic sedimentary rocks in the impact melted rocks cannot be excluded. It could account for part of the observed quartz-rich melt clasts and remnants of quartz-rich lithic clasts that occur abundantly in melt-rich impact melt rocks (Figures 32-33). The most likely source for the quartz-rich clasts are pegmatites or quartzo-feldpathic augen in gneiss, but it cannot be excluded that some may derive from quartz-bearing formations such as those forming the late Triassic to early Jurassic sediments known at the margin of the impact site (Figure 3).

In conclusion, the bedrock currently exposed in the Rochechouart structure appears to be an accurate reflection of the target composition at the time of impact; a minor proportion of sedimentary material cannot be excluded but would be limited to a component in the impact melt.

Stratigraphy of impact deposits

Field data and the petrological and geochemical record suggest the impact fill of the Rochechouart crater structure is essentially composed of two major units deposited separately - the polymict lithic breccia unit at the base, and the upper suevite unit.

It appears unlikely that the impact melt rocks originally formed a continuous sheet at the Rochechouart structure: a continuous melt body would likely have had a homogeneous composition (see review by Dressler and Reimold, 2001) whereas in Rochechouart the geochemical data base indicates significant heterogeneity. Impact melt rocks at Rochechouart are encountered at the bottom of the impactite deposits directly above bedrock. Textures and setting prove these melts were essentially flowing laterally over an already-settled crater floor. The hottest, the most vesicular and, thus, the most fluid melts were restricted to the center of the crater, whilst more massive and cooler melts settled toward the periphery, such as around Mountoume.

Initial volume of deposits and the relative inefficiency of cratering at Rochechouart

The morphological and morphometrical considerations discussed above and the horizontal impactoclastic deposits on top of the suevite provide constraints on the volume of material deposited within the Rochechouart crater. Located in the faint “low” of the crater floor, the Chassenon sequence gives an “upper limit” for the thickness of the impactite deposit over the whole structure, namely 50-70 m at most.

This is extremely thin for a crater of its size developed in a crystalline target, even if we consider the lowest estimate for the initial crater diameter (20 km) and even if we compare it to craters developed in sedimentary or mixed sedimentary-crystalline rocks, such as Ries. The 1973 Nördlingen deep drilling, located ca. 3 km from the center of Ries crater (similar to the Chassenon radial distance) revealed a ca 300 m thick impactite sequence (Stöffler et al., 1977).

The complete impactite sequence is thus 5 times thinner at Rochechouart compared to Ries. This clearly establishes that the initial impact deposit at the Rochechouart crater is significantly depleted, the deficit factor lying between c.a. 5 and 10 depending on the value taken for the size of original final crater (20-50 km). Possible reasons for this could be:

1) The initial impact crater is much smaller than thought: A reduction by 5 times of the impactite and melt volumes implies a comparable reduction of the parameters such as the energy released on impact and the volume of the transient cavity. First-order simple model calculations based on the online tool of Collins et al. (2005) show that a 12 km final diameter crater would produce a volume of impact breccia matching the Rochechouart estimates. This value is less than the diameter of the zone covered by the deposits today and arguments have already been put forward that indicate that the crater must originally have been larger than 15 km.

2) Low-angle trajectory: Low-angle impacts have significantly reduced cratering efficiency (Melosh, 1989); however, as the constraint on impactite volume estimates relies on a crater diameter value, the low-angle argument does not apply. A low-angle impact at Rochechouart would only imply the size of the projectile was larger than expected.

3) Sedimentary cover: It was widely reported that the volume of impact melt rocks recognized in predominantly sedimentary and in mixed (sedimentary–crystalline) targets is on the order of two magnitudes less that for crystalline targets in comparably sized impact structures (Grieve and Cintala, 1992). More recently it has been suggested that this inconsistency is due to the challenges in recognizing impact melt products derived from sedimentary-rich target rocks, rather than different processes and products occurring at impacts into different target lithologies (Osinski et al., 2008). In the case of Rochechouart, there is no impact formation or material that could have been misinterpreted. It is thus very unlikely that the explanation of the relative depletion in impactites at Rochechouart comes from the presence of a sedimentary cover at the time of the impact.

4) Sea cover: Despite the likely absence of sedimentary rock in the target area, the proximity of the impact site to the erosional Late Triassic-early Jurassic sea shore (Figure 3) indicates that the sea was at least very near to, if not covering, the Rochechouart site at the time of the event (either the new T-J boundary age - Schmieder et al., 2009a - or the Late Triassic age - Kelley et al., 1997). However, even if the sea reduced the efficiency of melting and excavation, this cannot account for the apparent deficit, for the same reason as for the low-angle trajectory hypothesis discussed above. The constraint on impactite volume estimates relies on a crater diameter value and a sea cover at Rochechouart at the time of impact would only imply the size of the projectile was larger than expected. Nonetheless, a marine impact is of potential importance for interpreting the characteristics of the Rochechouart structure and is further discussed in the next section dealing with the paleoenvironmental interpretations of the field data presented in the paper.

Projectile contamination

We will not enter in the debate of the Rochechouart projectile identification (see introduction). If the nature of the projectile can still be debated, the chemical contamination is beyond doubt and the “meteorite signal” at

Rochechouart is intense owing to the felsic composition of the target. In that context it is possible to look at the projectile signal distribution. The PGE data indicate an Ir content in melt rich impactites in the 0.1-2 ppb range, ten thousand time above the basement values (Janssens et al, 1977, Tagle et al, 2010). Yet, as of today, PGE measurement remains a heavy exercise and it is not yet appropriate for systematic tracking and mapping the meteorite signal at impact craters. Ni is more readily accessible. It has been measured in a large series of rocks sampling all the lithologies of impactites and basement rocks in Rochechouart (Lambert, 1975, 1977a, 1977c). The results show an exogenic Ni component in all impactites, with the highest values in melt bearing rocks (typically in the 100 ppm range, up to 700-800 ppm for Bel-air impact melt rocks (ca 100-1000 times the target values) (Lambert, 1977cn Tagle et al., 2010)). The results also demonstrate the mobility of the meteorite signal as the clasts in the breccias and the highly shocked basement below the crater floor also display a positive Ni anomaly (Lambert, 1975, 1977c). Figure 55gives a schematic and interpretative map of the Ni contamination based on above mentioned Ni studies. This data set will be completed by field measurement, planed during the field trip (see section 2 and see Roald and Lambert, 2009).

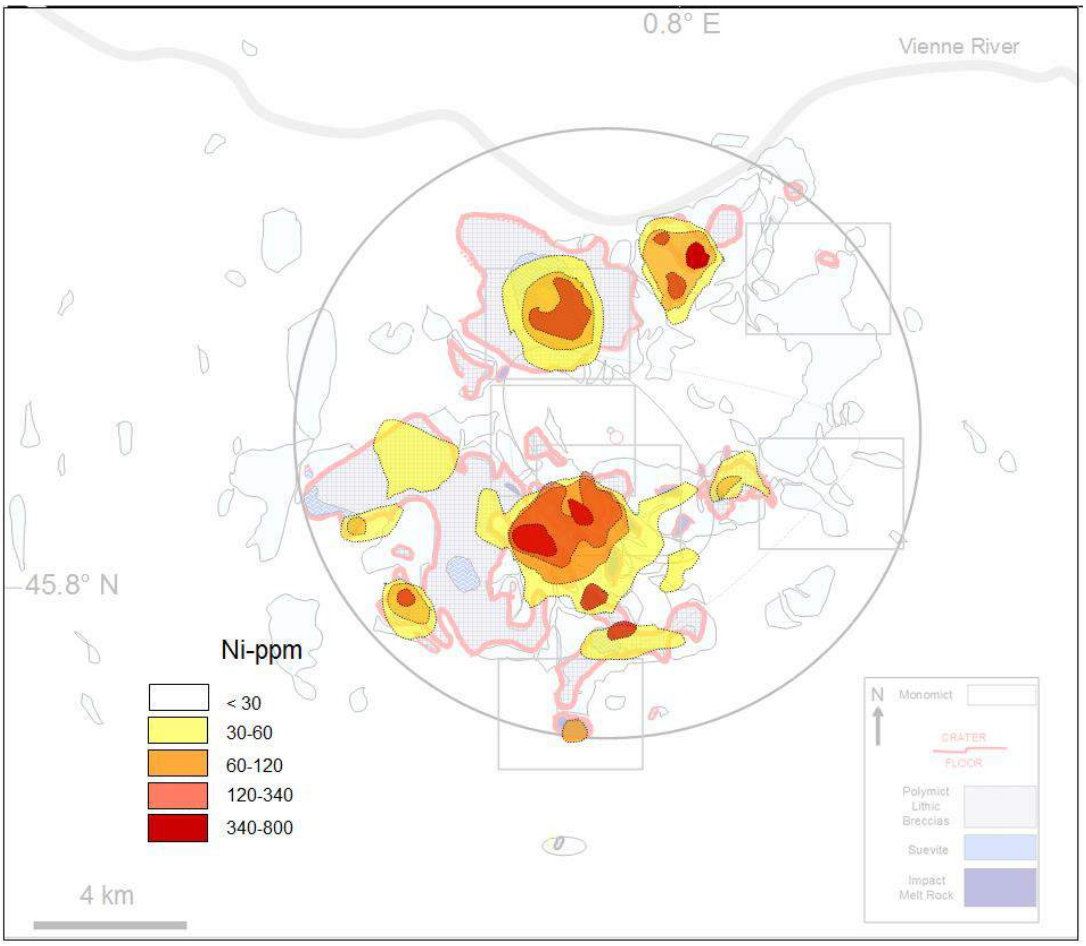

Figure 55. Schematic representation of "intensity" of the meteoritic contamination at Rochechouart based on the measurement of the Ni content (after data from Lambert, 1977a, c)

Paleoenvironmental considerations: Impact and postimpact regional implications

Ground zero

The Rochechouart impactites provide direct constraints on the altimetry position of the paleotopographic surface at the time of impact (ground zero). Ground zero can be inferred from the actual position of the crater bottom and from the estimation of the initial depth of the crater. As seen earlier, the altitude of the bottom of the crater is well established from field data. It oscillates between ca. 200 and 300 m.

The initial depth of the crater is more difficult to assess as it is not directly accessible in the field. However, it can be estimated by considering modeling and geological studies at other craters of similar size developed in crystalline rocks and mixed crystalline-sedimentary targets (e.g., Collins et al., 2008). From comparison with other terrestrial craters and model based estimate a final crater depth of ca 600-900 m is expected for craters between 20 and 50 km in diameter seems. It is thus deduced that ground zero at the time and location of the Rochechouart impact was at 700 to 1000 m above today's sea level (adding to the observed elevation of the crater floor at the center of crater the height of the rim taken as the value of depth minus the relative elevation of rim to ground zero.

Depth of the nearby sea

The level of the bottom of the nearby sea at the time of impact is directly accessible as it corresponds to the altimetry of the bottom of the late Triasic-early Jurassic sediments outcropping west and southwest of the impact site. As seen in the result section, this contact stands at ca 250 m in the southwestern outcrops (Montbron region) and at ca 170 m in the western area (Mazières) (Figure 3). From this, the bottom of the nearby sea at the time of impact was at precisely the same level or only a few tens of meters below that of the bottom of the final cavity.

The paleo-sea level is more difficult to assess, but it can be constrained indirectly by the presence of the aerially-deposited impactoclastic deposit in the cavity which indicates that the sea did not flood the cavity after the impact. Consequently, sea level at the time must have been at least below the level of ground zero and the water depth could not have exceeded 500-700 meters.

Tsunamite

Owing to the immediate vicinity of the sea at the time of impact, the collision is very likely to have produced significant effects and possibly triggered a tsunami. It has been tentatively proposed that the Rochechouart impact could be responsible for the puzzling ~2-4 m thick 'seismite' of about 250,000 km² extent partially overlain by 'tsunamite' in the uppermost Triassic of the British Islands (Schmieder et al., 2009b).

Post-impact sedimentary shielding of the crater

The fine-grained impactoclastic deposit at the top of the Chassenon sequence also constrains the paleoenvironmental and post-impact history of the impact crater. Owing to its position, this deposit would have been the first exposed to erosion unless it was rapidly shielded. It is thus inferred that the whole area was rapidly protected from erosion after impact.

The most likely protection is to be found in post-impact sediments, although there is no trace of such a sedimentary record anywhere in this part of the French Central Massif. But it appears to be generally accepted (Curnelle and

Dubois, 1997; Dercourt, 2002) that the region was indeed covered by a sea until the early Tertiary. Furthermore, because of the long exposure to erosion since the early Tertiary, the "ghost" protective sedimentary cover deposited during the Jurassic and Cretaceous must have been very thick to allow shielding of the 50-70 m Rochechouart impactite deposit until the present day.

Post-impact erosion

The present data constrain the minimum thickness of material eroded since the crater was formed and then filled. This value is ca 700 meters. It is deduced from the final depth of the Rochechouart crater ca 800 m (deduced from model estimates and observational data from other craters in the same size range, see Figure 54) minored from the thickness of the crater fill deposits (estimated 100 m or less according to the Chassenon complete sequence).

Post-impact hydrothermal alteration

The pervasiveness of post-impact hydrothermal alteration of the Rochechouart impactites is striking. It has been noticed by all authors having worked in the area (Kraut and French, 1972; Lambert, 1977a, b; Reimold et al., 1987; Sapers et al., 2009). Although hydrothermal alteration of melt-bearing impactites has been reported at many other terrestrial impact structures (see for instance Wittmann et al., 2008 and references therein), the importance of these effects appears as a distinctive and unusual characteristic of the Rochechouart impact.

The mineralogy of the Rochechouart impactites is strongly affected by the hydrothermal alteration as it appears responsible for complete or quasi-complete alteration of glass, for the wide argillisation of melt-bearing impactites and for the systematic occurrence of neoblastic quartz and K-feldpar in the pore space of all impactites, including the impactoclastites. The composition of Rochechouart impactites is also strongly affected by the hydrothermal alteration, as shown by the systematic positive K_2O/Na_2O-K_2O/CaO anomaly (Table 2).

As the same anomaly is observed in the lithic clasts of the impact melt rocks, it is clearly established that this characteristic is not restricted to the melt phase alone. As the effects extend to all the impactites, including the monomict lithic breccias beneath the crater floor and the impactoclastic deposit at the top of the sequence, it implies a system of hot circulating fluids pervading the entire deposit for a significant duration.

This raises the question of the heat source and of the source of fluid. If the primary heat source available for this hydrothermal activity is obviously the melt and the hot clasts contained in the various deposits, the question is raised whether the limited amount of melt and highly shocked, hot material remaining in the crater allow the production of such a large hydrothermal cell or not.

The answer will require further study. At this stage it can be noted that despite the large deficit of hot material and melt inferred from the discussion above, the cooling conditions of the impact deposit at Rochechouart are not necessarily much different from those in other craters as the entire deposit (defining the size of the cell) is reduced in the same proportion as are the impact melt rocks in the Rochechouart crater.

The source and the amount of fluid required for establishing such a large, pervasive and prominent hydrothermal system can certainly not be related to the crystalline bedrocks. Granite and gneiss are known as amongst the driest rocks in the upper crust. Shock is not responsible either. If high shock is proven to mobilize water by decomposition and melting of hydrous silicates in crystalline rocks (Figure 16 and Lambert and McKinnon, 1984) it is